Improving the Availability of Wind Turbine Generator Systems

Shipurkar, Udai

DOI
10.4233/uuid:6002c1a0-b19f-4a2b-b42d-bffcd914dd6b

Publication date
2019

Document Version
Final published version

Citation (APA)
Shipurkar, U. (2019). *Improving the Availability of Wind Turbine Generator Systems*. [Dissertation (TU Delft), Delft University of Technology]. https://doi.org/10.4233/uuid:6002c1a0-b19f-4a2b-b42d-bffcd914dd6b

Improving the Availability of Wind Turbine Generator Systems

Dissertation

for the purpose of obtaining the degree of doctor
at Delft University of Technology
by the authority of the Rector Magnificus, prof. dr.ir. T.H.J.J. van der Hagen,
chair of the Board for Doctorates
to be defended publicly on
Wednesday 09 January 2019 at 1500 hrs

by

Udai SHIPURKAR

Master of Science in Electrical Engineering, Delft University of Technology, the Netherlands,
born in New Delhi, India

This dissertation has been approved by the promotors:
Prof. dr. eng. J.A. Ferreira and Dr. ir. H. Polinder

Composition of the doctoral committee:

Rector Magnificus,	chairperson
Prof. dr. eng. J.A. Ferreira	Delft University of Technology, promotor
Dr. ir. H. Polinder	Delft University of Technology, promotor

Independent members:

Dr. H. Wang	Aalborg Universitet
Prof. ir. C.G.E. Wijnands	Eindhoven University of Technology
Prof. dr. S.J. Watson	Delft University of Technology
Prof. dr. ir. J.W. van Wingerden	Delft University of Technology
Prof. dr. ir. P. Bauer	Delft University of Technology

D4REL

The research leading to these results was performed within the project – Design for Reliable Power Performance (D4REL) – sponsored by the Dutch R&D program TKI Wind op Zee under grant TKIWO2007.

Printed by: Ridderprint BV

ISBN: 978-94-6384-001-9

Contents

Summary

Wind energy is becoming an important contributor in the world's energy needs. An important trend in wind turbine design is the focus on reliability and increased availability of wind turbines. This is the aim of the study. It focusses its attention on the generator and power electronic converter due to the susceptibility of the generator system to failure.

The first step is identifying the problem. This is achieved by a review of existing studies in failure rates and failure mechanisms to identify critical failures, their probabilities and their failure mechanisms. This is followed by the identification of approaches that can be used to increase the availability of wind turbine generator systems, focussing on – component reliability, active control, and fault tolerance. It identifies three aspects that are analysed in detail.

Converter Topologies for Improved Semiconductor Lifetimes

In this study, multilevel converters are investigated from the viewpoint of reliability. The approach followed uses stress and strength modelling to map the loads that drive the failure mechanisms in the considered components. The assessment is based on the power losses of each converter, the distribution of these losses, and their impact on the thermal behaviour of the power electronic components.

With a focus on developing converters with extended reliability which would result in increased energy yields and reduced costs, the current practice is to use over-rated components. However, another solution could be the use of over-rating in terms of topology - i.e., the designing of more complex topologies or control strategies that offer a more evenly distributed loading of the power converter or even topologies that can sustain faults and preserve their functioning ability. This study examined such over-rated topologies, as well the use of over-rated components.

The study finds that the use of over-rating – be it in the form of overrated topologies (like the ANPC and the T2C), or the use of over-rated components – is successful in improving the lifetime performance of power semiconductors in converters. However, the improvement offered by overrated topologies over and above the use of over-rated components is not significant and it is unlikely to replace the current practice of using over-rated components.

Adaptive Cooling in Wind Turbine Converters

While the lifetime of power semiconductors depends on both – the mean junction temperature, and the amplitude of temperature cycles – an analysis of the empirical lifetime equations show that it is more sensitive to temperature cycling amplitude than the mean temperature. Therefore, this study investigates adaptive cooling for improving reliability. It uses developed analytical

models to analyse the performance of such systems and quantify the improvement in lifetimes. In the simulation involving a yearly wind profile, the gradient based control showed an increase in lifetime by an order of magnitude for the grid side converter. Further, it demonstrates the effectiveness of this concept using a scaled-down experimental setup.

Modularity in Generator Systems

As the generator system has a sizeable contribution to the overall failure rates of turbines, it is important to consider methods of reducing the effects of these failures on the availability of turbines. This study examines modular concepts for wind turbine generator systems from the viewpoint of increasing the availability of wind turbines. It explores the modularities possible in wind turbine generator systems at different layers, i.e. the functional and the physical layer.

The study analyses the effect of functional and physical modularity on the availability of the converter in a wind turbine. Furthermore, it focussed on extreme modularity - i.e., designs where the number of modules is much larger than what is used at present (in the industry). It concluded that extreme modularity for converter systems where failure rates are constant do not hold merit as they do not offer significant improvements in availability. However, if the failure rates can be reduced by introducing extreme modularity, the increase in availability can be significant. Therefore, extreme modularity can be a powerful tool, but only when it is accompanied by a reduction in failure rates, for example through other manufacturing techniques.

Samenvatting

Wind energie begint een belangrijke bijdrage te leveren aan de energieproductie van de wereld. Een belangrijke trend in wind turbine ontwerp is de focus op betrouwbaarheid en beschikbaarheid van windturbines. Dit is het doel van dit onderzoek. Dit onderzoek besteet vooral aandacht aan de generator en vermogenselektronica door de vatbaarheid van het generatorsysteem voor falen.

De eerste stap is om het probleem te identificeren. Dit wordt bereikt door een overzicht te maken van bestaande onderzoeken naar faalpercentages en faalmechanismen om kritieke storingen te identificeren. Dit wordt opgevolgd door de identificatie van benaderingen die gebruikt kunnen worden om de beschikbaarheid van windturbines te verbeteren, met een focus op – betrouwbaarheid van componenten, actieve aansturing, en tolerantie voor falen. Het identificeert drie aspecten die in detail onderzocht worden.

Topologieën van vermogenselektronica voor verbeterde levensduur van halfgeleiders

In dit onderzoek wordt multi-level vermogenselektronica onderzocht vanuit het oogpunt van levensduur. De aanpak gebruikt modellen voor de stress en krachten om de belastingen die leiden tot falen in kaart te brengen voor de overwogen componenten. De beoordeling is gebaseerd op de verliezen van elke omzetter, de verdeling van deze verliezen, en de impact op het thermische gedrag van de vermogenselektronica.

Met een focus op het ontwikkelen van vermogenselektronica met verbeterde levensduur, en daarmee betere energieopbrengst en lagere kosten, is de huidige praktijk om overgedimensioneerde componenten te gebruiken. Echter, een andere oplossing is om een overgedimensioneerde topologie te gebruiken – in andere woorden, het ontwerp van complexere topologieën of aansturingsstrategieën die de belasting evenrediger distribueren of topologieën die tijdens falen kunnen blijven opereren. Dit onderzoek onderzocht zulke overgedimensioneerde topologieën evenals overgedimensioneerde componenten.

Het onderzoek laat zien dat het gebruik van overdimensionering, zij het in vorm van topologieën (zoals ANPC en T2C) of componenten, succesvol is in het verbeteren van de levensduur van halfgeleiders in vermogenselektronica. Echter is de verbetering die overgedimensioneerde topologieën bieden over overgedimensioneerde componenten niet significant en zal daarom de de huidige praktijk waarschijnlijk niet vervangen.

Adaptieve koeling in de vermogenselektronica van windturbines

Ondanks dat de levensduur van halfgeleiders afhankelijk is van de gemiddelde junctie temperatuur en de amplitude van de temperatuur cycli, laat een analyse van empirische levensduur formules zien dat het meer afhankelijk is van thermische cycli dan de gemiddelde temperatuur. Daarom wordt er in dit onderzoek een adaptieve koeling onderzocht voor het verbeteren van de betrouwbaarheid. Er worden analytische modellen gebruikt om de prestatie van zulke systemen

te onderzoeken en om de verbetering in termen van levensduren te kwantificeren. In een simulatie, die gebruik maakt van een jaarlijks windprofiel, toont de op gradiënt gebaseerde aansturing een levensduurverbetering met een orde van grootte. Verder demonstreert het de effectiviteit van dit concept met een experimentele opstelling op kleine schaal.

Modulariteit in generatorsystemen

Omdat het generatorsysteem een belangrijke bijdrage levert aan de totale faalpercentages van wind turbines, is het belangrijk om methoden te overwegen om de effecten van deze storingen op beschikbaarheid van windturbines te minimaliseren. Deze studie onderzoekt modulaire concepten voor wind turbine generator systemen vanuit het oogpunt van de beschikbaarheid. Het verkent de mogelijke modulariteit in wind turbine generatoren op verschillende lagen, zoals de functionele en fysieke laag.

Dit onderzoek analyseert het effect van functionele en fysieke modulariteit op de beschikbaarheid van de vermogenselektronica in een windturbine. Verder besteedt het aandacht aan extreme modulariteit – bijvoorbeeld ontwerpen waar het aantal modules groter is dan wat momenteel in de industrie gebruikt wordt. Er wordt geconcludeerd dat extreme modulariteit voor omzettersystemen waar faalpercentages constant zijn geen verdienste houden omdat de verbeteringen op beschikbaarheid marginaal zijn. Echter, als de faalpercentages verminderd kunnen worden door extreme modulariteit te introduceren kan de verbetering van beschikbaarheid significant zijn. Daarom kan extreme modulariteit een krachtig hulpmiddel zijn, maar alleen als het gepaard gaat met een vermindering van faalpercentages, bijvoorbeeld door andere fabricage techniek.

CHAPTER 1

Introduction

1.1 Wind Energy

Wind energy has a major contribution in the transition from fossil-fuel-based to renewable energy. The growth of wind energy generation justifies this statement: in 2016, wind energy overtook coal as the second largest form of power generation capacity [1]; and in 2017, wind energy covered an average 11.6% of the EU's electricity demand [1]. Wind energy shows strong annual growth as seen from the cumulative installed capacity figures shown in Fig. 1.1. Offshore wind has seen a sharp rise in installed capacity too (Fig. 1.2). Still, offshore wind farms are limited largely to Europe (accounting for about 84% of all offshore installations) with the remaining 16% are in East Asia and the United States of America. Therefore, there is large untapped potential worldwide for offshore wind energy.

Offshore wind farms offer a number of advantages over onshore farms: the availability of larger

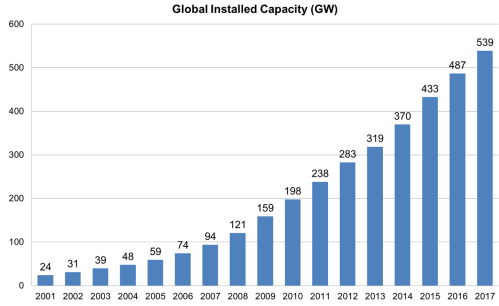

Figure 1.1 Global cumulative installed wind capacity. With data from [2].

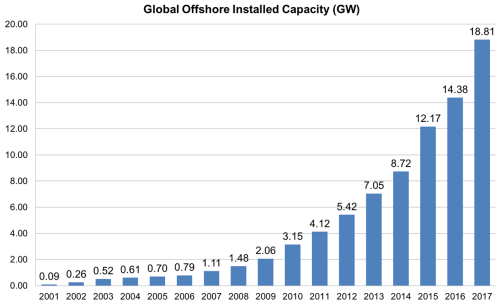

Figure 1.2 Global cumulative installed offshore wind capacity. With data from [2].

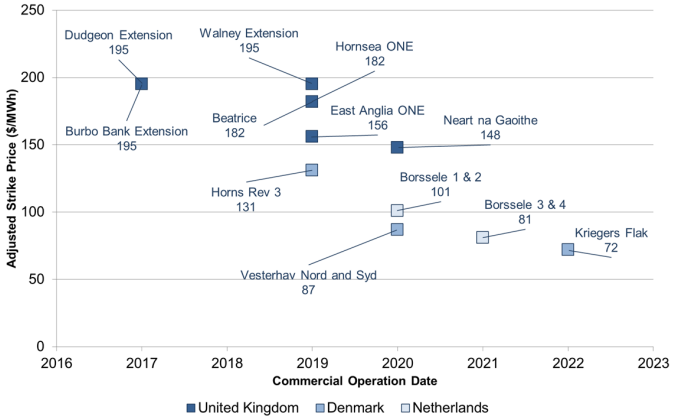

Figure 1.3 Recent strike prices of offshore wind tenders. With data from [3].

areas for large wind farms; lower visual impacts; and, most importantly, the higher wind velocities with lower turbulence at offshore sites [4, 5]. Still, the Levelised Cost of Energy (LCoE) has been an issue. However, the LCoE of offshore wind projects has significantly reduced over time. Fig. 1.3 shows this trend in recent strike prices in Europe. A large part of this reduction comes from lower financing costs due to a reduction in perceived risk. An example of the distribution of different components of the LCoE for an offshore wind farm commissioned in 2015 is shown in Fig. 1.4.

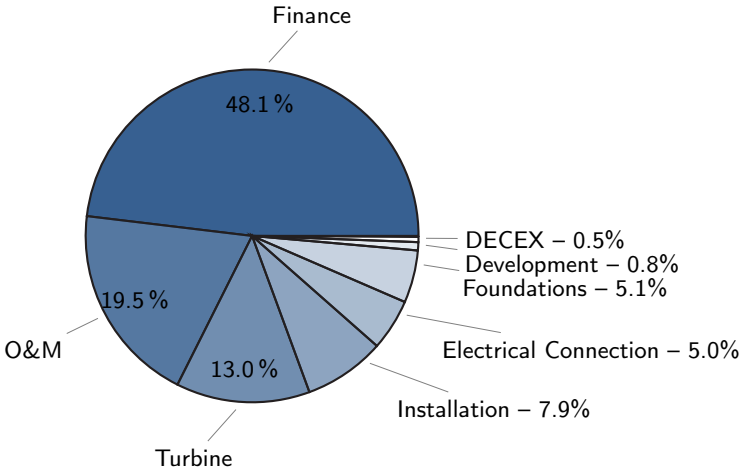

Figure 1.4 LCoE for an offshore farm commissioned in 2015. With data from [6].

While about 50% of the LCoE was attributed to the financing costs, the Operation and Maintenance (O&M) costs also contribute a major share to the cost of energy. This becomes more critical with

reducing financing costs. Further, maintenance accounts for between 50–80 % of these O&M costs [7,8], which makes addressing maintenance costs of prime importance for offshore wind turbines. Therefore, reliability of power performance is a critical factor for cost of wind energy and forms the basis of this thesis.

1.2 Motivation

TheWindStats and LandwirtschaftKammer data highlighted the problem of high failure rates in wind turbines. Fig. 1.5 shown the results are from the survey spanning 10 years and covering approximately 7000 wind turbines of varying power ratings and configurations. Recent studies, for example the one by Carroll *et al.* [9] and the SPARTA project [10], show that the failure rates still remain a problem to be solved.

The study by Carroll *et al.* analysed about 350 offshore turbines and found notably higher failure rates [9] as shown in Fig. 1.6 and failure distribution according to Fig. 1.7. Futhermore, the SPARTA study [10] found a mean annual repair rate of 15.8 repairs per turbine per year for their offshore population. These values are significantly higher than those reported for onshore turbines.

This increased failure rate in offshore wind turbines could be due to a number of reasons:

- offshore turbines experience a higher average wind speed which could result in higher stresses on the components,
- the harsher offshore environment,
- better maintenance in onshore turbines due to easier access,
- and, the maturity of onshore wind turbine technology.

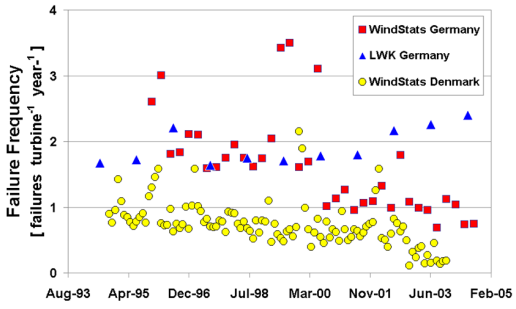

Figure 1.5 Average failure rates of onshore German and Danish wind turbines over about 10 years (1994–2004). From [**?**].

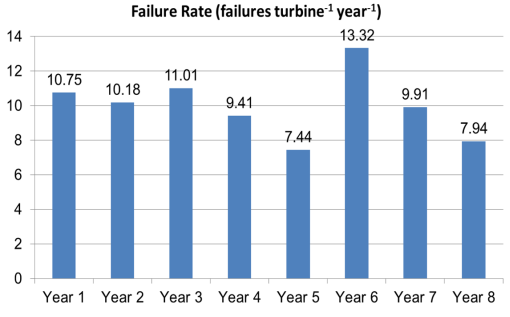

Figure 1.6 Offshore turbine failure rates. With data from [9]

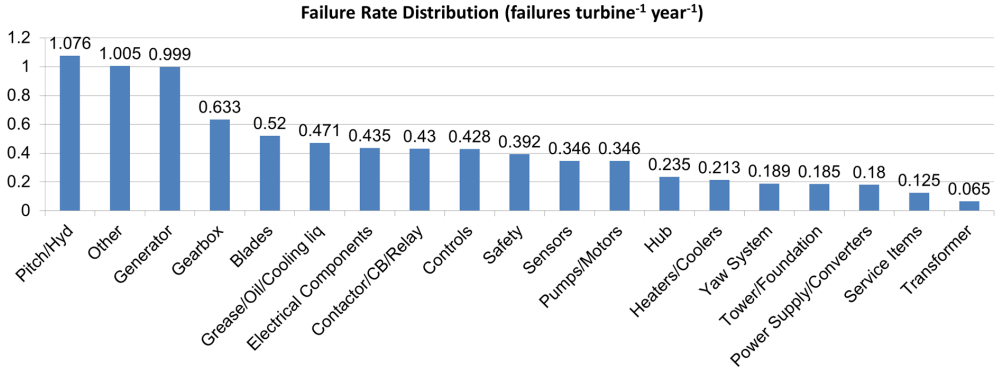

Figure 1.7 Distribution of failures in offshore wind turbines. With data from [9].

Of these failures, the drivetrain (comprising the gearbox, the generator, and the power converter) is a major contributor. It demands attention as a large portion of the failures are concentrated in this part of the system (≈22% according to [9], ≈30% according to [12], ≈26% according to [13], and ≈28% according to [10]).

The motivation behind this thesis is to improve the reliability and availability of offshore turbines because this affects the cost of offshore wind energy. It focusses its attention on the generator and power electronic converter due to the susceptibility of the generator system to failures. A direct comparison of generator system failure rates for onshore and offshore turbines was presented by Carroll *et al.* [9] and the SPARTA database [10], as seen in Fig. 1.8. It can be seen that offshore turbine failure rates are significantly higher. At this point, it is important to note that while the motivation of this study is offshore wind, the approaches discussed in this thesis are valid for onshore wind turbines as well.

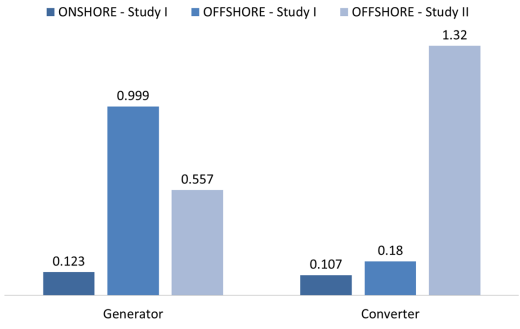

Figure 1.8 Failures in the generator system for onshore and offshore turbines. Study 1 is [9], and Study 2 is [10].

The importance of such an aim is further strengthened when the future scenario for offshore wind is considered. It is estimated that the installed offshore wind capacity, in Europe alone, would be between 45–100 GW by 2030 [14]. This would result in about 10 000 offshore turbines that need to be serviced and maintained (considering 100 GW installed capacity and 10 MW turbines). This would mean ≈100 000 failures per year according to the data presented in Fig. 1.6. The need for improved reliability is evident.

This aim of improving reliability and availability of turbines has clear technical challenges. However, there are other challenges as well - such as the availability of supporting data. Offshore wind installed capacity is only ≈ 3% of net wind installed capacity which means that this technology has not reached maturity yet. Furthermore, most data is held confidentially by wind farm operators and turbine manufacturers. Therefore, there is less data on failure and failure mechanisms for offshore wind turbine generator systems making it a challenge to study failures and propose improvements.

Before addressing the objectives and research questions for this thesis, the next section first details a number of key definitions. These are terms that are often used in common parlance and therefore, a clear technical definition is provided to avoid ambiguity.

1.3 Key Definitions

A number of key terms are highlighted and discussed in this section. This is to put them into proper context and so that their meaning is clear and unambiguous. These definitions are based on [15] and [16].

1.3.1 Reliability

Reliability is the probability that the system (or component) performs the specified function under specified operational and environmental conditions at and throughout the specified time. It can be expressed as the probability (P[T>t]) that the time to failure (T) is greater than the specified time interval (t), or

$$R(t) = P[T > t]. \tag{1.1}$$

Often, the reliability is expressed as Mean Time Between Failure (MTBF) where

$$MTBF = \int_0^\infty R(t)dt. \tag{1.2}$$

1.3.2 Maintainability

Maintainability is the ability of an item, under stated conditions of use, to be restored to a state in which it can perform its required function, when maintenance is performed under stated conditions and using prescribed procedures and resources. In other words, maintainability measures the ease and speed with which a system can be restored to operational status after a failure occurs.

The measure of the maintainability of a system can be quantified as the Mean Time To Repair (MTTR). Apart from the actual repair time, it includes the logistics, lead, and access times which may be considerable for offshore turbines.

1.3.3 Fault Tolerance

Fault-tolerance is defined as the ability of a system to continue operation after a fault in one of the system components. Therefore, in a fault-tolerant system, a single fault in the system does not lead to a system failure.

Fault-tolerant systems may either use redundant/overrated components to maintain rated power after failures, or reduce the output depending on the extent of failure. As wind turbines are not critical systems, the fault-tolerance considered in this thesis considers operation with a reduced output after failure occurs.

1.3.4 Availability

Availability is the probability that a system is available for use at a given time. It is a function of the reliability and maintainability and expressed as

$$A = \frac{MTBF}{MTBF + MTTR}. \tag{1.3}$$

However, this definition is incomplete for the case where fault-tolerant systems are used. In such systems, the system does not fail with a failure in a component but the power output may be reduced. Therefore, the concept of equivalent availability [17] is used in this thesis. This is given by

$$A_{eq} = \frac{P_h p_h + P_f p_f}{P_h}, \tag{1.4}$$

where P_h and P_f are the power outputs of the system when they are healthy and with the failed component, p_h and p_f are the probabilities of being in the healthy or failed state. Equivalent Availability (A_{eq}) is the ratio of the power that is produced, divided by the power that would be produced if there were no failures.

1.4 Objectives

The primary objective of this thesis is to:

'Improve the availability of wind turbine generator systems.'

It targets availability rather than reliability. This is because addressing the availability is a comprehensive approach that incorporates reliability, fault tolerance, and maintainability.

To address this broad objective, first, the following key question is considered:

- *What are the approaches to improve the availability of wind turbine generator systems?*

Further, three case studies are analysed in detail and the following sub-questions are examined:

- *How does over-rating – in terms of over-rated topologies and over-rated components – influence the lifetime of the power semiconductors?*
- *Can the power semiconductor lifetime be extended by controlling the thermal management of the converter?*
- *How can modularity improve the availability of a wind turbine generator system? What are the limits of increasing modularity?*

1.5 Contributions

The following are the principal contributions of this thesis:

- Analysis of three-level topologies from the perspective of lifetime using configurations built into complete drivetrain models and evaluated on wind distribution over an annual cycle.
- Development of an adaptive thermal management strategy to improve lifetime of power semiconductors in wind turbine converters.
- Investigation of extreme modularity for improved availability of the generator system with insight into factors that come into play with such extreme modularity.

1.6 Outline and Approach

On the basis of the outlined objectives, the thesis is organised into chapters such that each chapter address one of the objectives. Fig. 1.9 schematically shows the different topics (in the form of different chapters) that have been covered in this thesis and their relation to each other. Each of these chapters is based on published research articles, athough they appear here with minor changes to maintain the flow of the thesis.

The first step is identifying the problem. This is tackled in Chapter 2 through a study of failures and failure mechanisms in the generator system. Based on the findings, Chapter 3 identifies and analyses different methods to increase the availability of the generator system in a wind turbine. It also identifies a number of promising solutions, three of which are selected for further investigation in this thesis. Chapters 4, 5, and 6 detail the investigation of these selected cases. The following is a description of the chapters:

- **Failures - Probabilities and Mechanisms** To address failures and improve reliability, it is important to develop an understanding of failures and failure mechanisms occurring in the generator system. This chapter addresses this issue by looking at failures in wind turbine generators and their power electronic converters, their probabilities and their failure mechanisms. This is based on a review of existing studies in failure rates and failure mechanisms and combines these studies to form a holistic view of failures in generator systems.
- **Increasing Availability** Increasing the availability of wind turbine generator system is based on five pillars. These include the design for component reliability, active control for reliability, design for fault tolerance, prognostics, and design for maintainability. This chapter focusses on the first three, i.e. component reliability, active control, and fault tolerance. This is based on a literature review that identifies existing technologies and mechanisms that can be used to increase the availability of wind turbine generator systems. On the basis

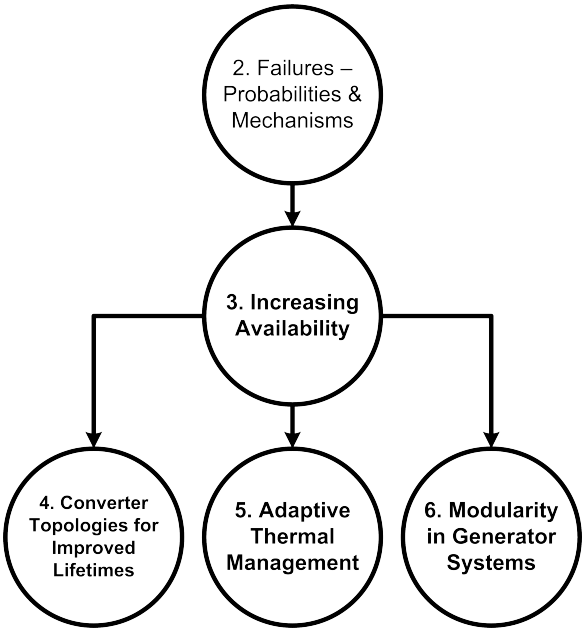

Figure 1.9 Thesis outline.

of this chapter, three case studies are selected for detailed analysis.

- **Converter Topologies for Improved Lifetimes** Conventional control schemes for wind turbines are based on the extraction of maximum energy from the wind. However, considering the cost of maintenance for far offshore wind turbines, it is important to look at reliability oriented design and control strategies that look to maximise the availability of the wind turbines rather than maximise the power production at each instant. This chapter compares existing topologies like the NPC, A-NPC, H bridge, T type from the point of view of reliability based on developed drivetrain, power semiconductor loss and thermal models. It further analyses the factors affecting the result of such a comparison. It also analyses modulation and control strategies such as a controlled ALD modulation strategy for the A-NPC to increase lifetime of the most stressed switches in a converter.
- **Adaptive Thermal Management** While the lifetime depends on both the mean junction temperature and the amplitude of temperature cycles, an analysis of the empirical equations show that the lifetime is more sensitive to temperature cycling amplitude than the mean temperature. This chapter investigates adaptive thermal management for improving reliability. The chapter further uses developed analytical models to analyse the performance of such systems and quantify the improvement in lifetimes. A scaled-down experimental setup is used to demonstrate the proposed system.
- **Modularity in Generator Systems** As the generator system has a sizeable contribution to the overall failure rates of turbines, it is important to consider methods of reducing the effects of these failures on the availability of turbines. This chapter examines modular concepts for wind turbine generator systems from the point of view of increasing the availability of wind turbines. It explores the modularities possible in wind turbine generator systems at different layers, i.e. the functional and the physical layer, and explores the use of extremely modular generators and converters.

Bibliography

[1] I. Pineda and P. Tardieu, "Wind in Power 2017," WindEurope, Tech. Rep., 2018.

[2] L. Fried, L. Qiao, and S. Sawyer, "Global Wind Report – Annual Market Update 2017," Global Wind Energy Council, Tech. Rep., 2018.

[3] P. Beiter, W. Musial, L. Kilcher, M. Maness, and A. Smith, "An Assessment of the Economic Potential of Offshore Wind in the United States from 2015 to 2030," National Renewable Energy Laboratory (NREL), Tech. Rep., 03 2017.

[4] P. Weis-Taylor, L. Bevard, and A. Taylor, "Wind Energy – Annual Report," IEA, Tech. Rep., 2006.

[5] G. Failla and F. Arena, "New perspectives in offshore wind energy," *Philosophical Transactions of the Royal Society of London A: Mathematical, Physical and Engineering Sciences*, vol. 373, no. 2035, 2015.

[6] IRENA (2016), "Innovation Outlook: Off shore Wind," International Renewable Energy Agency, Abu Dhabi, Tech. Rep., 2016.

[7] C. Moné, M. Hand, M. Bolinger, J. Rand, D. Heimiller, and J. Ho, "2015 Cost of Wind Energy Review," National Renewable Energy Laboratory (NREL), Tech. Rep., 2017.

[8] WEC, "World Energy Resources – Wind," World Energy Council, Tech. Rep., 2016.

[9] J. Carroll, A. McDonald, and D. McMillan, "Failure rate, repair time and unscheduled o&m cost analysis of offshore wind turbines," *Wind Energy*, vol. 19, no. 6, pp. 1107–1119, 2016.

[10] "System Performance, Availability and Reliability Trend Analysis: Portfolio Review 2016," SPARTA, Tech. Rep., March 2017.

[11] P. Tavner, J. Xiang, and F. Spinato, "Reliability analysis for wind turbines," *Wind Energy*, vol. 10, no. 1, pp. 1–18, 2007.

[12] G. van Bussel and M. Zaayer, "Reliability, availability and maintenance aspects of large-scale offshore wind farms, a concepts study," in *MAREC 2011: Proceedings of the 2-day International Conference on Marine Renewable Energies, Newcastle, UK, 27-28 March 2001*, 2001.

[13] F. Spinato, "The reliability of wind turbines," Ph.D. dissertation, Durham University, 2008.

[14] G. Corbetta, A. Ho, and I. Pineda, "Wind energy scenarios for 2030," European Wind Energy Association, Tech. Rep., 2015.

[15] A. K. Verma, D. Ajit, and D. R. Karanki, *Reliability and Safety Engineering*, 1st ed. Springer-Verlag London, 2010.

[16] A. P. Teixeira and C. Guedes Soares, "Fundamentals of reliability," in *Thermal Power Plant Performance Analysis*, G. F. M. de Souza, Ed. Springer-Verlag London, 2012, ch. 6, pp. 91–122.

[17] A. McDonald and G. Jimmy, "Parallel wind turbine powertrains and their design for high availability," *IEEE Transactions on Sustainable Energy*, vol. 8, no. 2, pp. 880–890, April 2017.

CHAPTER 2

Failures – Probabilities and Mechanisms

Reliability is a critical consideration for wind turbine generator systems as failures contribute directly to operation and maintenance costs and hence the cost of energy. Improving reliability hinges on understanding the mechanisms of failures that occur. This chapter addresses three questions –

- *What components fail in a wind turbine generator system?*
- *How often do they fail?*
- *Why do they fail?*

This is based on a review of existing studies in failure rates and failure mechanisms and combines these studies to form a integrated view of failures in generator systems.

Based on:
U. Shipurkar, K. Ma, H. Polinder, F. Blaabjerg, and J.A. Ferreira, "A review of failure mechanisms in wind turbine generator systems," in *European Conference on Power Electronics and Applications (EPE'15 ECCE-Europe)*, 2015, pp. 1-10.
This chapter is an extension of the above paper with updated failure statistics based on recent publications.

2.1 Introduction

A challenge faced by offshore wind turbines is achieving Levelised Cost of Energy (LCoE) comparable to that of conventional sources of electrical energy. Of this LCoE, the cost of Operations and Maintenance (O&M) is a major component [1]. In such a scenario, improved reliability of wind turbines can be a major factor in lowering the O&M costs and therefore, the CoE, especially when they are installed offshore or in remote locations.

Improving reliability hinges on understanding the mechanisms of failures that occur. The challenge is that there is limited data on failures and failure mechanisms for wind turbine generator systems. This chapter addresses three questions about failures in wind turbine generator systems–

- What components fail?
- How often do they fail?
- Why do they fail?

A number of papers in literature focus on failure mechanisms of power semiconductors and electrical machines. However, they either focus on a single component, such as the power semiconductor in [2], or on a part of the drivetrain, as in [3]. This chapter collates and reviews existing literature on failures and failure mechanisms in wind turbine generator systems.

The WindStats and LandwirtschaftKammer data highlighted the problem of high failure rates in wind turbines. Fig. 1.5 shows the average failure rates for the German and Danish wind turbine population from 1994 to 2004. Recent studies, for example the one by Carroll *et al.* [4] and the SPARTA project [5], show that the failure rates still remain a problem to be solved.

Fig. 2.1 shows the distribution of failures of a wind turbine from four different studies: the WindStats data for Germany (WS-D) and Denmark (WS-DK); the LandwirtschaftKammer data for Germany (LWK-D); and the Swedish data from the Elforsk report (E-S). The more recent studies have also analysed failure rates. For example, Carroll *et al.* analysed the failures for a population of approximately 350 offshore wind turbines with nominal power between 2–4 MW. The resulting failure distribution of this study is shown in Fig. 2.2. Another example is the SPARTA initiative in the UK that monitors approximately 1400 offshore wind turbines. Fig. 2.3 shows the top 10 wind farm components that require the most intervention from this study.

Is is evident that offshore wind turbines have high failure rates. Furthermore, these studies demonstrate that the generator and converter are two major sources of failures. However, they diverge in the failure rates for generators and converters. This can be explained by the difference in drivetrain topologies. The SPARTA project uses data from UK offshore wind farms where the majority of turbines use full scale converters with either permanent magnet generators, or squirrel cage induction generators (more than 80% of the installed capacity). The use of these topologies reduces the failure mechanisms (and hence failure rates) in the generator by avoiding the use of slip rings, but uses full scale power converters which see a higher failure rate. On the other hand, the study by Carroll *et al.* have a large number of doubly fed induction machines fed by partially

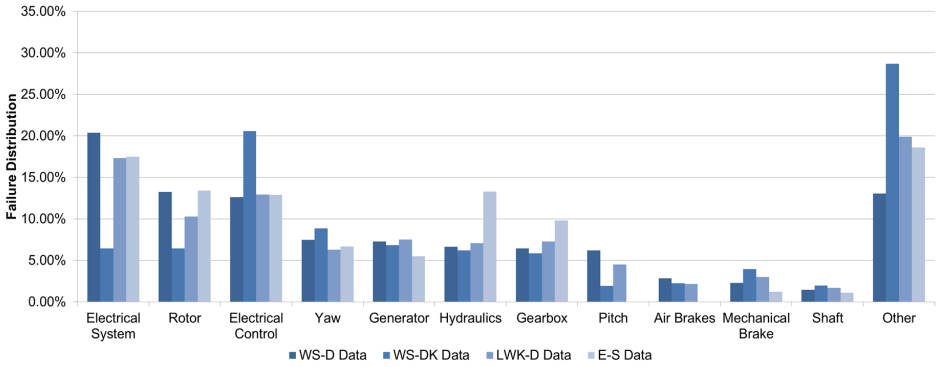

Figure 2.1 Overview of failure distribution in wind turbines. The results from different studies show good agreement. The WS-D, WS-DK, and LWK-D are distributions over about 10 years (1994–2004) with 1291–4285, 851–2345, and 158–643 turbines respectively. The data has been taken from [6]. The data from the Swedish wind turbines (from [7]) is for 527–723 turbines during the years 2000–2004.

rated converters in the analysed population (based on slip ring issues being the major cause of generator failures) leading to a larger generator failure rate.

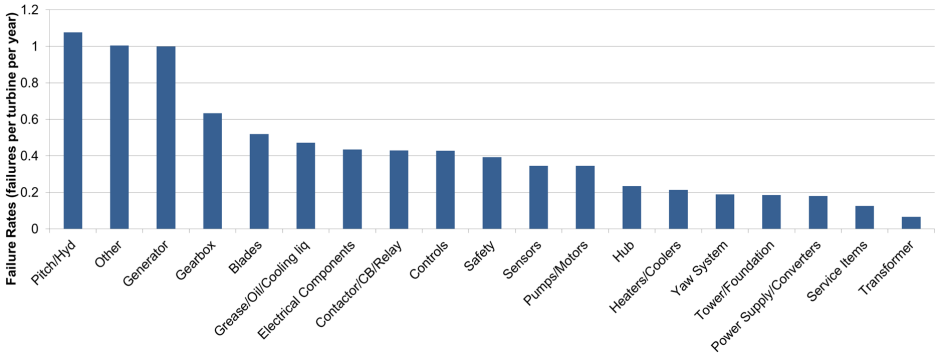

Figure 2.2 Failures in offshore wind turbines. The results are from an analysis of ~350 offshore turbines by Carroll *et al.* The data has been taken from [4].

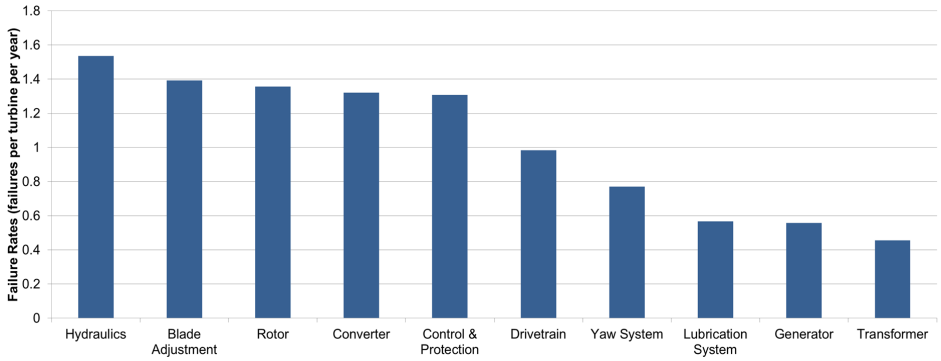

Figure 2.3 Failures in offshore wind turbines. The results are from an analysis of ~1400 offshore turbines by the SPARTA project. The data has been taken from [5].

2.2 Failures in Converters and Generators

There has been little published data on failures in wind turbines at a sub-component level. Lyding *et al.* [8] have studied failure rates of power electronic converters at a sub-component level with data from the WMEP database which is a monitoring programme that ran between 1989–2006. Fig. 2.4 shows the distribution of failures amongst converter sub-components based on this study.

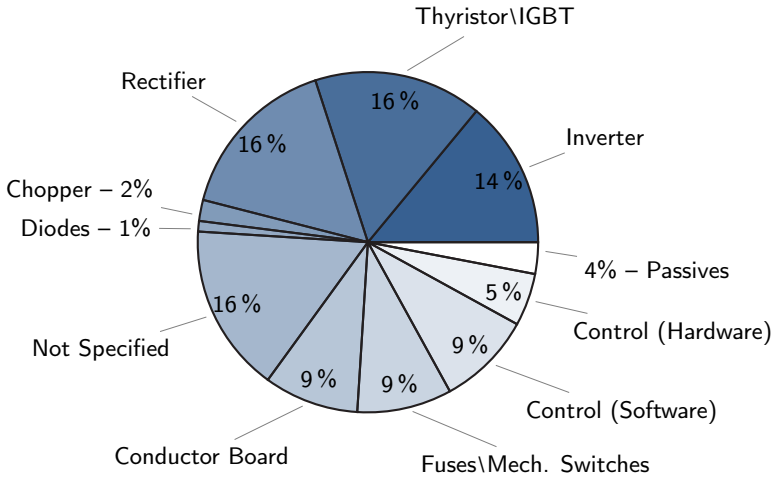

Figure 2.4 Sub-component level failure distribution in power electronic converters. From [8]

This shows that the majority of failures involve the power semiconductors. An industry based survey by Bryant *et al.* gave similar results with maximum respondents selecting semiconductor

power devices as the most fragile component in converters [9].

Another study by Carroll *et al.* analysed failures in drivetrains of 2222 onshore wind turbines between 1.5–2.5 MW. The wind turbine population consists of doubly fed induction generators (DFIG) with a partially rated converters and permanent magnet generators (PMG) with fully rated converters. The population of the DFIG configuration builds upto 1822 turbines over five years and the PMG population builds to 400 turbines over three years. Fig. 2.5 and Fig. 2.6 show the distribution of failures in converters from this study.

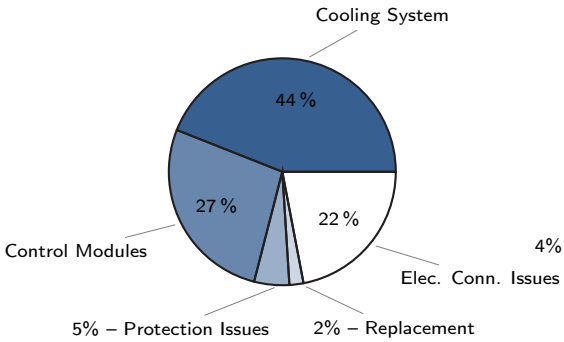

Figure 2.5 Sub-component level failure distribution of fully rated converters. The data has been taken from [10]

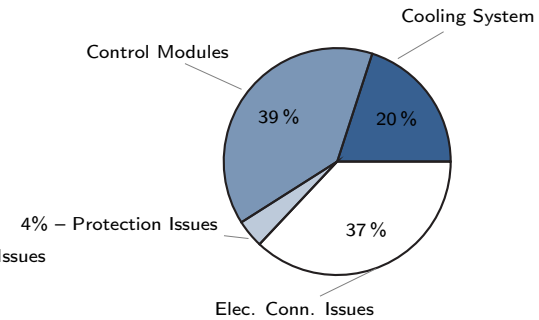

Figure 2.6 Sub-component level failure distribution of partially rated converters. The data has been taken from [10]

The study finds that the fully rated converter fails approximately 5.5 times as much as the partially rated converter. The higher failure rate is due to the higher losses that could cause cooling issues as well as greater stresses on the converter. In both these converters, the cooling system, the control modules, and the electrical connection issues are the main contributors. In this analysis, the gate driver and the IGBT are included in the electrical connection issues.

Failures in wind turbine generators were studied by Alewine *et al.* [3]. They studied over 1200 generators from a wide variety of manufacturers and the resulting failure distribution is shown in Fig. 2.7. This distribution is for generators rated above 2 MW.

The bulk of failures originate in the bearings, but the stator insulation and wedges also have a large share of the failures. The study by Carroll *et al.* resulted in the failure distributions shown in Fig. 2.8 and Fig. 2.9 for the DFIG and PMG configurations.

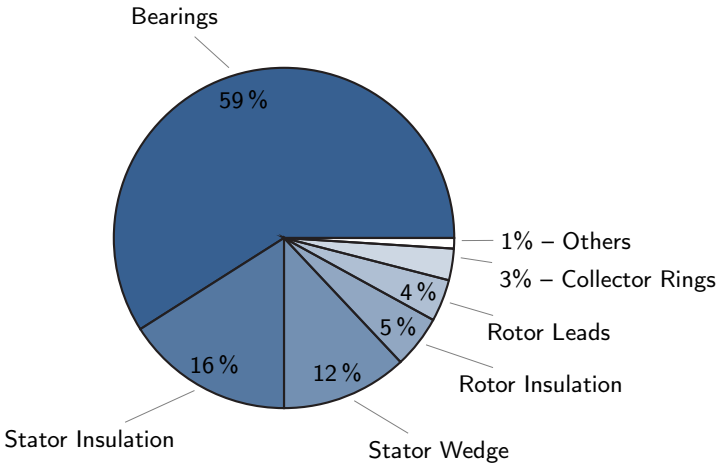

Figure 2.7 Sub-component level failure distribution in generators. The data is from [3]

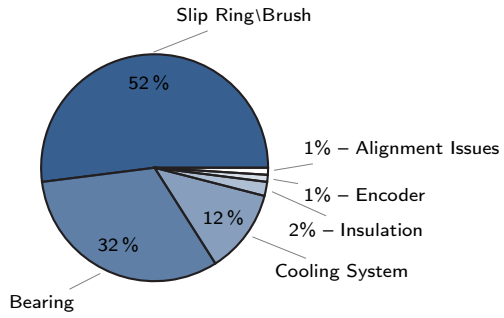

Figure 2.8 Sub-component level failure distribution of doubly fed induction generators (DFIG). The data has been taken from [10]

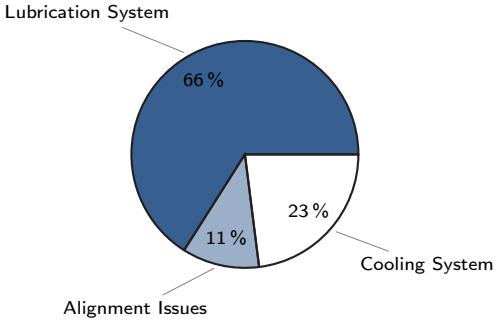

Figure 2.9 Sub-component level failure distribution of permanent magnet generators (PMG). The data has been taken from [10]

The PMG had a lower failure rate than the DFIG (0.076 failures per turbine per year for the PMG and 0.123 failures per turbine per year for the DFIG [10]) due to the fewer possible failure modes in the PMG. For the DFIG, the slip ring/brush system followed by the bearings had the highest contribution to failures. For the PMG, the majority of failures are related to auxiliary systems. One reason for the difference in failure distributions between the studies by Alewine *et al.* and Carroll *et al.* could be the length of operational data available. The study by Carroll *et al.* analyses failures for the first five years of operation for the DFIG and the first three years for the PMG.

2.3 Failure Mechanisms in Power Electronic Converters

Fig. 2.10 gives an overview of failure mechanisms in Power Electronic Converters. Published work has shown that power semiconductors are most likely to fail in power electronic converters; therefore, this section starts by looking at the failure mechanisms of power semiconductors.

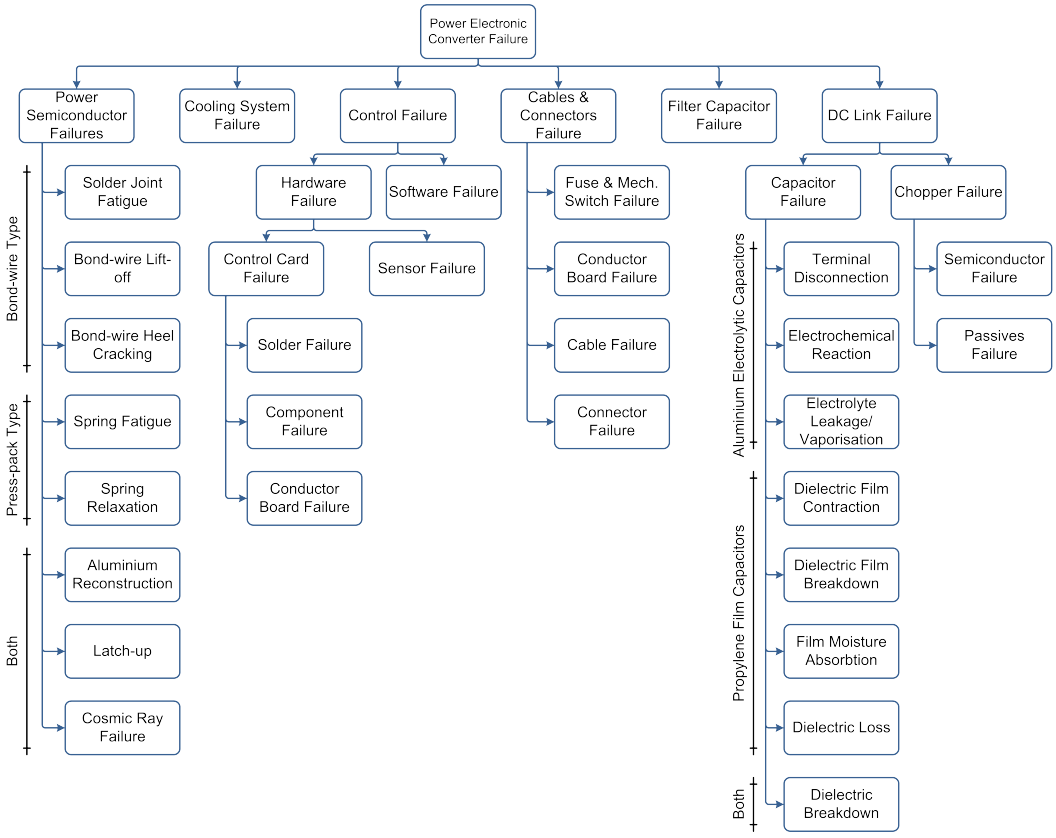

Figure 2.10 Failure Tree for Power Electronic Converters

2.3.1 Semiconductors

Semiconductor switches suffer from a number of failures such as - bond wire lift-off, bond wire heel cracking, aluminium reconstruction, corrosion of interconnections, solder fatigue and voids, latch-up and cosmic ray failures among others [2]. These failure mechanisms are discussed in the following sections. Fig. 2.11 gives an overview of the driving parameters for failures in

semiconductor switches.

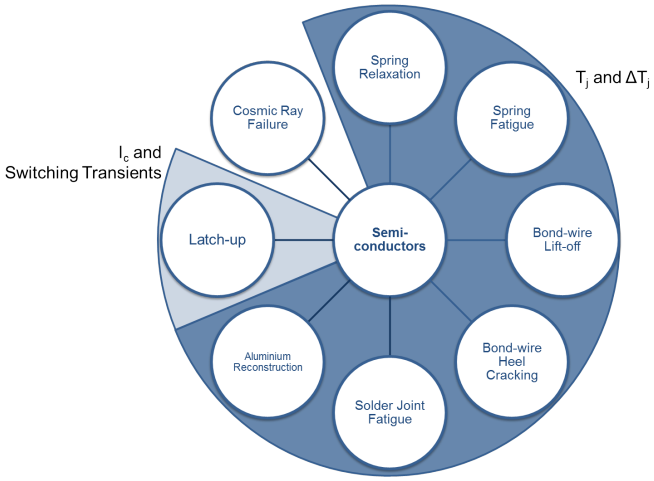

Figure 2.11 Driving parameters for failures in semiconductor switches.

Solder Joint Fatigue

Solder joint fatigue is considered a major failure mechanism in power electronic components [11]. This failure occurs because the solder layer is subjected to mechanical stresses under temperature cycling, because of the difference in the Coefficient of Thermal Expansions (CTEs) of the two materials between which the solder is present.

IGBTs have two such joints - silicon chip and ceramic substrate, and ceramic substrate and base plate. Of these, the ceramic substrate–base plate solder joint is especially prone to failure due to a greater mismatch between the CTEs of the two materials resulting in shear stress in the solder layer and eventually cracks and voids [12]. Solder fatigue cracks are generally found close to the DCB ceramic due to higher temperatures. These cracks lead to a reduction in the heat conduction capability of the solder layer causing an increase in the temperature of the junction with further exacerbates the problem [2].

These effects may be a result of external heating (thermal cycling) or by internal heating due to losses in the IGBT (power cycling) [13].

Bond Wire Lift-off

Bond wire lift-off has been considered as one of the principal forms of failures in IGBTs and diodes. Failure of wire bonds occur as a result of fatigue caused either by shear stresses generated

between the chip and wire, or due to repeated flexure of the wire [2]. These develop as cracks propagating along the bond wire-chip interface due to thermo-mechanical stresses caused by temperature cycling and the fact that aluminium (bond wire material) and silicon (chip material) have very different Coefficient of Thermal Expansion (CTE) [14].

However the use of improved bonding methods, protection layers [13] and molybdenum-aluminium strain buffers [2] have reduced these failures to such an extent that they do not seem to pose any particular threat to IGBT reliability.

Bond Wire Heel Cracking

This failure, also, is due to the thermo-mechanical effect of the wire subjected to temperature cycling. Under such a cycling, the wire undergoes flexure fatigue. However, this failure mechanism is a slow process and rarely occurs in modern IGBTs [2].

Latch-up

Latch-up is a failure inherent in the IGBT and occurs when the collector current cannot be controlled by the gate. It occurs when the parasitic thyristor in the IGBT is turned on by the parasitic transistor. This makes the IGBT lose control through the gate [15]. Latch-up is of two types, static and dynamic. Static latch-up happens at high collector currents which turn on the parasitic transistors. Dynamic latch-up occurs due to switching transients especially during turn off. This is done by the displacement currents of the parasitic capacitance between the p region of the pnp transistor and the n region of the parasitic transistor [16].

Cosmic Ray Failure

Burnout in semiconductor devices can be initiated through self-sustaining discharges in the silicon by recoil nuclei [2]. Energetic neutrons create ionizing recoils within the substrate. Originally, this failure mechanism was attributed to high voltage devices only. However, studies show that cosmic radiation-induced breakdown cannot be disregarded for power devices of voltage classes as low as 500V [17].This makes cosmic ray failure mechanism of interest for wind turbine power electronics as well.

Press-pack Technology

Press-pack semiconductors eliminate the dominant failure mechanisms of standard wire bonded semiconductors like bond wire lift-off and solder joint failure. However, they suffer from other failures such as fretting, spring fatigue and spring relaxation.

When press-pack IGBT's are subjected to temperature cycling and the variation in Coefficient of Thermal Expansions (CTE) of the layers will lead to reciprocating sliding causing fretting damage. This results in a deterioration of thermal and electrical properties [12].

Spring fatigue and spring relaxation occur due to the compression and relaxation cycles caused by power cycling. These failures lead to an increase in contact resistance [12]. Latch-up and Cosmic Ray Failure can occur in press-pack semiconductors as well.

2.3.2 Control

According to Birk *et al.* the Converter Control Unit (CCU) is one of the components with the lowest reliability. As with the semiconductors, the failures in the CCU are related to thermal cycling [18].

In this document the gate driver is considered to be part of the control hardware. Apart from failures due to thermal cycling issues, failures may also occur due to conditions of the IGBT. Continued narrow overvoltage spikes between collector and emitter may open the gate emitter resistance [16]. This would result in a loss in the driving signal and misfiring of the IGBT and could result in thermal breakdown or steady-state power dissipation [19]. Also, modern IGBT's can work at much higher temperatures than the gate drive circuit components, in the event that such a scenario is experienced, the driver circuit could suffer from these thermal effects [16].

2.3.3 Passive Components

Industry experience shows that failures in resistors and inductors are rare [9]. Therefore this section deals primarily with the failures in capacitors. Two types of capacitors are used in wind turbine power electronic converters - aluminium electrolytic capacitors and metallised polypropylene film capacitors. The electrolytic capacitor offers high power density at a lower cost but suffers from reliability issues while the film capacitor offers higher reliability but a lower power density [20].

Failures in electrolytic capacitors include degradation of parameters, short circuits, open circuits and electrolyte leakage. Breakdown failures may be dielectric breakdown or thermal breakdowns. Dielectric breakdowns are primarily due to defects in the device itself while thermal breakdowns occur due to a rise in temperature of the device. This is a common short circuit failure in electrolytic capacitors [21]. Open circuit failures occur either due to electrochemical corrosion leading to lead fractures or the drying of capacitor cores when they are subjected to high working temperatures [21].

Even though polypropylene film capacitors are self-healing, when the energy passing though the localized discharge path created by local breakdowns is larger than the energy required for self-healing, then the capacitor fails in the short circuit mode [22]. The contact between the ends of electrode edges and the spray ends are irregular. Under the combined effect of mechanical stress, electro-dynamic force, thermal stress, as well as the electric spark effect caused by the

potential difference between electrode edge and sprayed end, the contact degrades gradually and eventually leads to the detachment of the sprayed ends and an open circuit fault [22]. Another short circuit mechanism is the absorption of moisture under humid conditions by the dielectric film [23].

Both Aluminium Electrolytic Capacitors and Metallised Polypropylene Film Capacitors have wear out or parameter degradation as a dominant failure mode. Capacitor Voltage stress and Temperature stress are two major causes of this failure mode. Humidity also plays a role, especially for polypropylene film capacitors. Fig. 2.12 gives an overview of the driving parameters for failures.

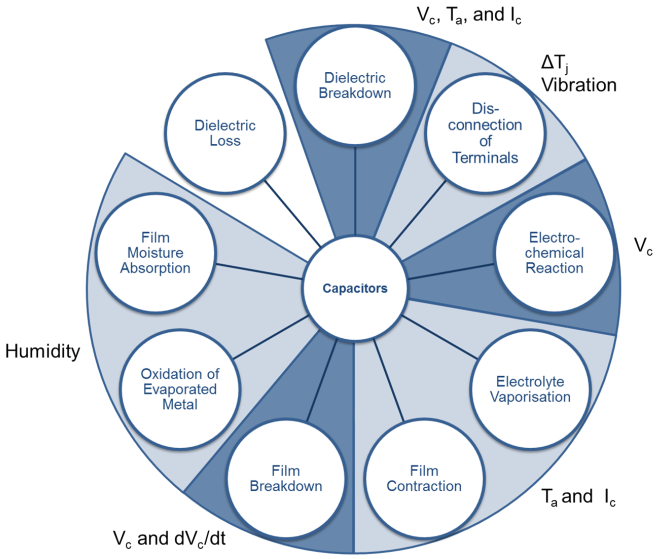

Figure 2.12 Driving parameters for failures in capacitors.

2.4 Failure Mechanisms in Generators

This section looks at the mechanisms of failures occurring in the generators of wind turbines. The overview of these failure mechanisms is shown in Fig. 2.13. These are discussed in the following sections.

2.4.1 Stator and Rotor Windings

Although electrical breakdown causes the final failure in an insulation system, it is not the dominant ageing factor. It is believed that ageing is dominated by thermal degradation, mechanical

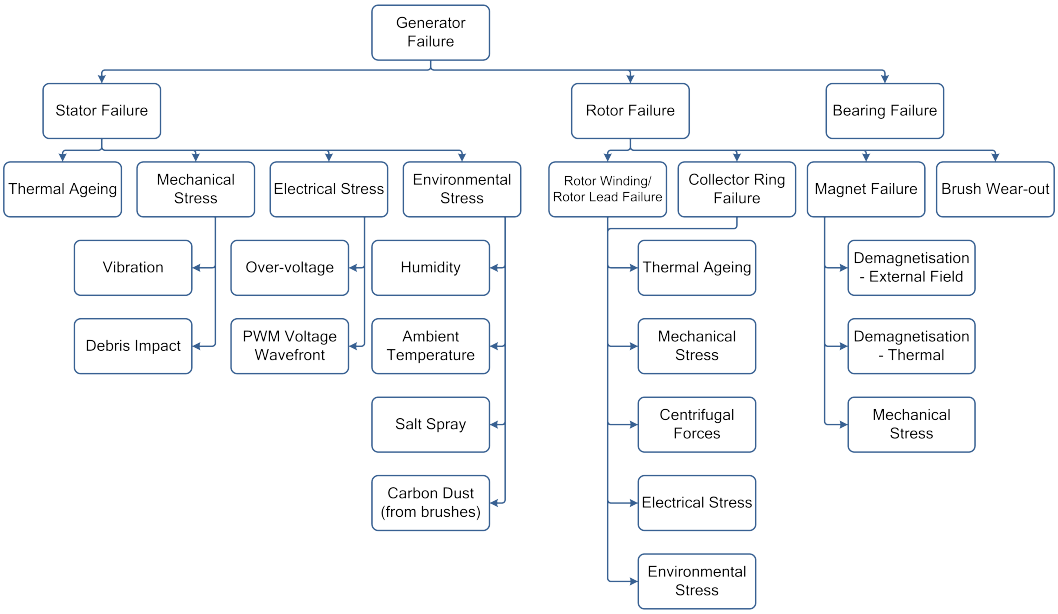

Figure 2.13 Failure Tree for Generators

stress due to vibration and switching pulses, and stress caused by different thermal expansion coefficient of the materials [24].

Lifetime models of generator insulations based on thermal degradation are well established [25][26]. However, like for semiconductor switches, thermal cycling can be a major issue for wind turbine generators due to large variations in their duties. The ageing of hydrogenerator insulation due to thermal cycling which go through start-stop cycles has been investigated [27][28]. Such studies for wind turbine generators could lead to more realistic lifetime models for winding insulation in wind turbines.

The Power Electronic Converter operated using PWM is another reason for the stressing and possible failure of the windings. This is applicable for the rotor winding in the DFIG and the stator winding for the Permanent Magnet Synchronous Machine. The fast travelling voltage wavefront, especially pronounced when PWM is used, generates reflection waves at the cable-generator junction. These reflected waves cause overshoots or spikes at the front of the voltage wave [29]. According to Gao *et al.* these spikes can be in the order of 2.5kV for a system rated at 690V [30]. Another factor that could be an initiator of failures in the windings of wind turbines is the environment. Offshore wind turbines are especially exposed to moisture and corrosive saline water. Moisture may condense on windings and initiate surface tracking in winding insulation.

While life expectancy analysis for windings of high voltage machines have been developed based on the measurement of certain insulation parameters, as most wind turbine generators are low-

medium voltage machines, further research is required to develop such methods for monitoring wind turbine generators.

2.4.2 Stator Wedges

A major failure that has been identified in wind turbine generators is the failure due to the loosening of magnetic stator wedges. This loosening of slot wedges could lead to grounding faults or mechanical damage to the coils.

Magnetic stator wedges are used to reduce the effective stator slot opening and offer some benefits such as smoothing of the airgap flux, improving efficiency and reduce temperature rise [31]. Stator wedges made of magnetic material will vibrate under the effect of rotating fields causing the bonding of the wedges to weaken. Also the ferrous nature of the wedges speeds up corrosion through oxidation [3]. Magnetic Stator Wedge faults could offer an option for fault avoidance.

2.4.3 Rotor Lead Damage

The Doubly Fed Induction Generator (DFIG) requires power to be fed to the rotor through a Power Electronic Converter. This power is transferred though the Rotor Leads. These leads pass through the hollow shaft of the generator. As a consequence, any thermal issues occurring due to the bearings can cause damage to the leads and failure of the generator [3]. Also, the end bearing of the generator has additional thrust forces due to the mounting angle of the generator causing higher temperatures and greater possibility of causing rotor lead failure.

2.4.4 Collector Rings

The slip rings are also affected by the use of power electronic converters. The voltage spikes generated can cause voltage flash-overs between the rings [30]. Another reason for failure in collector rings could be the degradation of insulation between them due to thermal cycling.

2.4.5 Brush Wear-out

This is a common and inevitable result of using a brush-slip ring system. It is a result of two modes – the mechanical wear caused by friction, and the electrical wear caused by the effect of current on the contact material [32].

2.5 Effect of Wind Speed and Weather

The weather can have a major impact on failure rates in wind turbines. Humidity at the location of installation can lead to an increase in failures, especially in the power electronic converters and the generator. Also, in offshore wind turbines the corrosive nature of the salt laden air could also cause problem to subassemblies. However, these can be overcome with suitable nacelle or sub-assembly sealing.

Also, a number of failure mechanisms in the power electronic converter are caused due to temperature cycling effects. Therefore, it can be expected that the external temperature at a location could have an effect on failure rates. It has been shown by Tavner *et al.* that electrical subassemblies are indeed more prone to the deleterious effect of varying temperatures [33]. Further very low temperatures could have a serious effect on the thermal grease, solder and capacitor electrolytes used in converters. Tavner *et al.* also found a periodicity in failure rate data of 6, 8.4 and 12 months [34]. The 12 and 6 month periodicity is attributed to seasonal variation of weather while the 8.4 month periodicity is difficult to explain, and it is hypothesised that it may be due to sub-seasonal effects.

Studies in [33] highlighted the annual seasonal periodic nature of the Wind Energy Index (WEI) which may be used as a measure of wind speeds. This periodic nature introduces power cycling leading to increased fatigue by mechanisms described in previous sections. Months with higher WEIs also saw higher failure rates. In fact, a report by the Renewable Energy Information Systems on Internet (REISI) as quoted in [34] stated that above wind speeds of 12m/s, the frequency of failures is about twice as high as the frequency of wind classes. This could be attributed to high stresses on components that are already fatigued due to long term fluctuating loads.

2.6 Conclusions

Improving reliability hinges on understanding the mechanisms of failures that occur. This chapter has reviewed failures and failure mechanisms in the wind turbine generator systems. It is seen that temperature and temperature cycling are a major driving factor for the failure mechanisms in power electronic converters and the electric failures in generators.

With an understanding of failures and failure mechanisms, the next step is to examine the approaches that can be used to improve the availability of wind turbine generator systems. This is done in the next chapter.

Bibliography

[1] IRENA (2016), "Innovation outlook: Offshore wind," International Renewable Energy Agency, Abu Dhabi, Tech. Rep., 2016.

[2] M. Ciappa, "Selected failure mechanisms of modern power modules," *Microelectronics Reliability*, vol. 42, no. 4-5, pp. 653–667, Apr. 2002.

[3] K. Alewine and W. Chen, "A review of electrical winding failures in wind turbine generators," in *2011 Electrical Insulation Conference (EIC).*, Jun. 2011, pp. 392–397.

[4] J. Carroll, A. McDonald, and D. McMillan, "Failure rate, repair time and unscheduled o&m cost analysis of offshore wind turbines," *Wind Energy*, vol. 19, no. 6, pp. 1107–1119, 2016. [Online]. Available: http://dx.doi.org/10.1002/we.1887

[5] "System Performance, Availability and Reliability Trend Analysis: Portfolio Review 2016," SPARTA, Tech. Rep., March 2017.

[6] F. Spinato, P. Tavner, G. van Bussel, and E. Koutoulakos, "Reliability of wind turbine subassemblies," *IET Renewable Power Generation*, vol. 3, no. 4, pp. 387–401, 2009.

[7] J. Ribrant and L. M. Bertling, "Survey of failures in wind power systems with focus on Swedish wind power plants during 1997–2005," *IEEE Transactions on Energy Conversion*, vol. 1, no. 22, pp. 167–173, 2007.

[8] P. Lyding, S. Faulstich, B. Hahn, and P. Tavner, "Reliability of the electrical parts of wind energy systems - a statistical evaluation of practical experiences," in *EPE Wind Energy Chapter Symposium*, 2010.

[9] A. Bryant, P. Mawby, and P. Tavner, "An industry-based survey of reliability in power electronic converters," *IEEE Transactions on Industry Applications*, vol. 47, no. 3, pp. 1441–1451, May 2011.

[10] J. Carroll, A. McDonald, and D. McMillan, "Reliability comparison of wind turbines with DFIG and PMG drive trains," *IEEE Transactions on Energy Conversion*, vol. 30, no. 2, pp. 663–670, 2015.

[11] K. Fischer, T. Stalin, H. Ramberg, T. Thiringer, J. Wenske, and R. Karlsson, "Investigation of converter failure in wind turbine," Elforsk, Tech. Rep., 2012.

[12] C. Busca, R. Teodorescu, F. Blaabjerg, S. Munk-Nielsen, L. Helle, T. Abeyasekera, and P. Rodriguez, "An overview of the reliability prediction related aspects of high power IGBTs in wind power applications," *Microelectronics Reliability*, vol. 51, no. 9-11, pp. 1903–1907, Sep. 2011.

[13] H. Berg and E. Wolfgang, "Advanced IGBT modules for railway traction applications: Reliability testing," *Microelectronics Reliability*, vol. 38, no. 6-8, pp. 1319–1323, Jun. 1998.

[14] S. Ramminger, P. Türkes, and G. Wachutka, "Crack mechanism in wire bonding joints," *Microelectronics Reliability*, vol. 38, no. 6-8, pp. 1301–1305, Jun. 1998.

[15] N. Mohan, T. M. Undeland, and W. P. Robbins, *Power Electronics: Converters, Applications and Design*, 3rd ed. Wiley, 2002.

[16] R. Wu, F. Blaabjerg, H. Wang, M. Liserre, and F. Iannuzzo, "Catastrophic failure and fault-tolerant design of IGBT power electronic converters - an overview," in *IECON 2013 - 39th Annual Conference of the IEEE Industrial Electronics Society*, Nov 2013, pp. 507–513.

[17] G. Soelkner, W. Kaindl, H.-J. Schulze, and G. Wachutka, "Reliability of power electronic devices against cosmic radiation-induced failure," *Microelectronics Reliability*, vol. 44, no. 9-11, pp. 1399–1406, Sep. 2004.

[18] J. Birk and B. Andresen, "Parallel-connected converters for optimizing efficiency, reliability and grid harmonics in a wind turbine," in *2007 European Conference on Power Electronics and Applications*, Sept 2007, pp. 1–7.

[19] C. Delepaut, S. Siconolfi, O. Mourra, and F. Tonicello, "MOSFET gate open failure analysis in power electronics," in *2013 Twenty-Eighth Annual IEEE Applied Power Electronics Conference and Exposition (APEC)*, Mar. 2013, pp. 189–196.

[20] M. Boettcher and F. W. Fuchs, "Power electronic converters in wind energy systems – considerations of reliability and strategies for increasing availability," in *Proceedings of the 2011 14th European Conference on Power Electronics and Applications*, Aug 2011, pp. 1–10.

[21] W. Lifeng, Z. Shihong, D. Yinyu, G. Yong, and P. Wei, "Research on failure analysis method of the key components in SMPS," in *2011 Prognostics and System Health Managment Conference*, May 2011, pp. 1–6.

[22] L. Fuchang, D. Xin, L. Jin, Y. Zonggan, and W. Nanyan, "On the failure mechanism of metallized polypropylene pulse capacitors," in *2000 Annual Report Conference on Electrical Insulation and Dielectric Phenomena*, vol. 2, 2000, pp. 592–595.

[23] H. Wang and F. Blaabjerg, "Reliability of capacitors for DC-link applications in power electronic converters —- an overview," *IEEE Transactions on Industry Applications*, vol. 50, no. 5, pp. 3569–3578, Sep. 2014.

[24] R. Brutsch, M. Tari, K. Frohlich, T. Weiers, and R. Vogelsang, "Insulation failure mechanisms of power generators," *IEEE Electrical Insulation Magazine*, vol. 24, no. 4, pp. 17–25, Jul. 2008.

[25] G. Stone, I. Culbert, E. Boulter, and H. Dhirani, *Electrical Insulation for Rotating Machines: Design, Evaluation, Aging, Testing, and Repair*, 2nd ed. Wiley-IEEE Press, 2014.

[26] M. M. Botha, "Electrical machine failures, causes and cures," in *1997 Eighth International Conference on Electrical Machines and Drives*, Sep 1997, pp. 114–117.

[27] V. Kokko, "Ageing due to thermal cycling by start and stop cycles in lifetime estimation of hydroelectric generator stator windings," in *2011 IEEE International Electric Machines & Drives Conference (IEMDC)*, May 2011, pp. 318–323.

[28] ——, "Ageing due to thermal cycling by power regulation cycles in lifetime estimation of hydroelectric generator stator windings," in *Proceedings - 2012 20th International Conference on Electrical Machines, ICEM 2012*, 2012, pp. 1559–1564.

[29] W. Yin, "Failure mechanism of winding insulations in inverter-fed motors," *IEEE Electrical Insulation Magazine*, vol. 13, no. 6, pp. 18–23, Nov. 1997.

[30] G. Gao and W. Chen, "Design challenges of wind turbine generators," in *2009 IEEE Electrical Insulation Conference*, May 2009, pp. 146–152.

[31] R. Curiac and H. Li, "Improvements in energy efficiency of induction motors by the use of magnetic wedges," in *2011 Record of Conference Papers Industry Applications Society 58th Annual IEEE Petroleum and Chemical Industry Conference (PCIC)*, Sep. 2011, pp. 1–6.

[32] M. Braunovic, N. K. Myshkin, and V. V. Konchits, *Electrical contacts: fundamentals, applications and technology*. CRC press, 2006.

[33] P. Tavner, D. M. Greenwood, M. W. G. Whittle, R. Gindele, S. Faulstich, and B. Hahn, "Study of weather and location effects on wind turbine failure rates," *Wind Energy*, vol. 16, no. 2, pp. 175–187, Mar. 2013. [Online]. Available: http://doi.wiley.com/10.1002/we.538

[34] P. Tavner, C. Edwards, A. Brinkman, and F. Spinato, "Influence of wind speed on wind turbine reliability," *Wind Engineering*, vol. 30, no. 1, pp. 55–72, Jan. 2006.

CHAPTER 3

Increasing the Availability of Wind Turbine Generator Systems

Availability is an important factor to be considered when designing wind turbine generator systems. The quest for increased availability is based on the following five design approaches - design for component reliability, active control for reliability, design for fault tolerance, prognostics, and design for maintainability. This chapter reviews approaches focussing on the first three, i.e. component reliability, active control, and fault tolerance. The chapter further identifies some promising directions for further research which form the basis of the subsequent chapters in this thesis.

Based on:
U. Shipurkar, H. Polinder and J. A. Ferreira, "A review of methods to increase the availability of wind turbine generator systems," in *CPSS Transactions on Power Electronics and Applications*, vol. 1, no. 1, pp. 66-82, Dec. 2016.
This chapter is created from the paper by removing parts that have been covered in previous chapters.

3.1 Introduction

This thesis has discussed the problem facing wind turbines with respect to the cost of maintenance. It has also highlighted that addressing availability is the focus of the study. This chapter uses a review of literature to develop a catalogue of methods that can be used to increase the availability of the generator and power electronic converter of a wind turbine.

Increasing the availability of wind turbine generator systems is based on five pillars or approaches as shown in Fig. 3.1. These include the design for component reliability, active control for reliability, design for fault tolerance, prognostics, and design for maintainability.

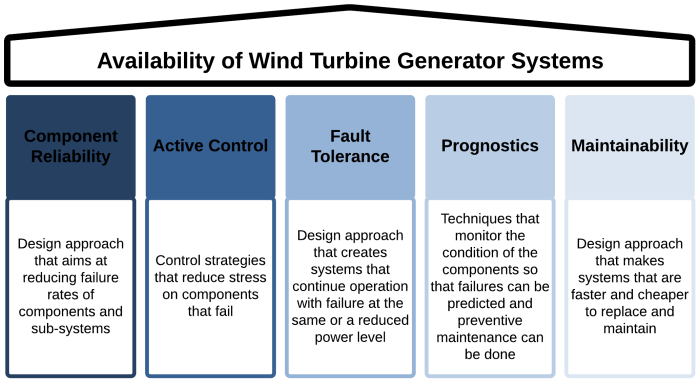

Figure 3.1 How can availability in wind turbine generator systems be increased?

For this chapter, the framework focusses on three pillars or approaches:

- **Component Reliability -** the first approach takes into account steps that can be realised at the design stage. The design aim of increasing the reliability can be achieved by:
  - ▷ Eliminating components that fail.
  - ▷ Increasing the strength of components/materials so that they can sustain larger stresses.
  - ▷ Reducing the stress on failure prone components.
- **Active Control -** the second approach utilises active control strategies that reduce the stress on components. Again, the focus is on increasing lifetimes of the components.
- **Fault Tolerance -** even with the above two approaches being employed there is the chance of failure in the system. Therefore, including fault tolerance will allow the system to continue operation under fault till maintenance/repair can be done, further increasing availability.

The remainder of this chapter is organised in the following sections; Section 3.2 and 3.3 review the methods for improving availability for the converter and generator. Finally, Section 3.4 identifies some promising research directions and Section 3.5 discusses some conclusions from the review.

3.2 Addressing Converter Availability

The framework for improving converter availability with the three approaches is shown in Fig. 3.2. The focus in this section remains with the power semiconductors and improving their lifetimes.

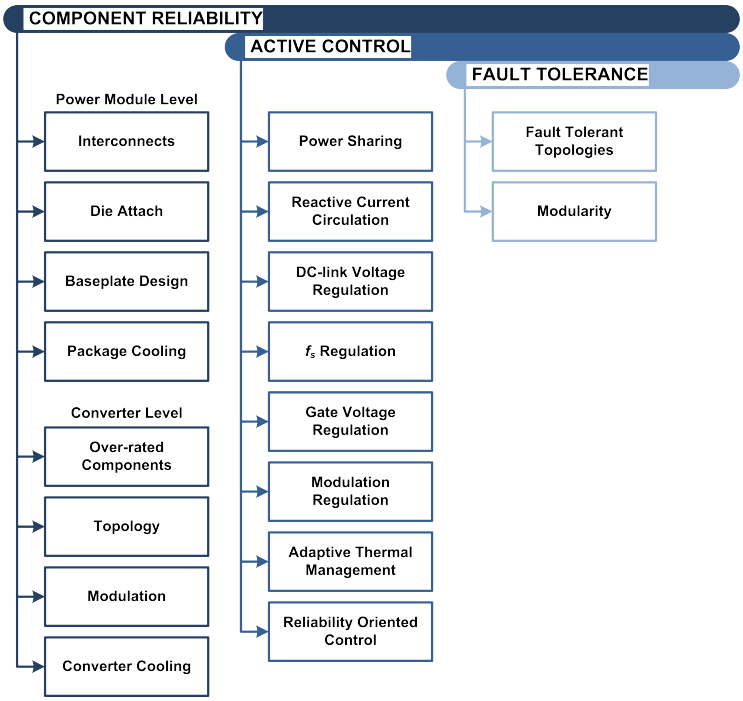

Figure 3.2 Framework for increasing converter availability.

3.2.1 Component Reliability - Power Module Level

The design for reliability can be tackled at two levels, the power module level and the converter level. At the power module level, connection techniques for interconnects and die attach are reviewed along with the baseplate design and package cooling. These aspects are shown in the schematic in Fig. 3.3.

Interconnects

Wire bonds have been shown to be a limitation for the reliability of power semiconductors. When subjected to thermal and power cycling, the flexure stress can lead to a lift-off or a crack in the

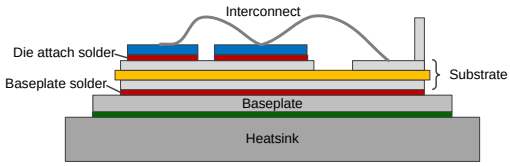

Figure 3.3 Schematic of the power semiconductor module.

heel of the aluminium bond wire; leading to failure. There are a number of methods and design choices that can improve the lifetime performance of these interconnects:

- **Molybdenum Strain Buffers -** bond wire failure occurs due to the stresses caused by the CTE mismatch between the aluminium of the bond wire and the silicon. This stress can be reduced by the addition of a molybdenum strain buffer soldered to the chip [1, 2]. The CTE of molybdenum is close to that of the silicon chip, which reduces the thermal stress and improves the lifetime. *Hamidi et al.* showed that the introduction of these strain buffers could increase lifetimes by a factor of 2-3 [1].

- **Copper Wire Bonding -** in the heel cracking failure mechanism the crack develops in the aluminium bond wire near the semiconductor surface and propagates along the grain boundaries. An increase in the yield strength of the bond wire material will allow the interconnection to sustain the thermal stresses for a longer period of time. Copper is therefore a suitable choice and can increase the lifetimes of bond wires by an order of magnitude under certain test conditions [3, 4]. Fig. 3.4 shows an example of copper wire interconnects. However, the use of copper wires will require a change in the aluminium topside contacts on the chip. Therefore, the use of copper wires clad with aluminium (an example for this is shown in Fig. 3.5 for ribbon bond wires) allows the use of standard chip contacts while increasing the lifetime of the bond wires [5, 6]. Also, research on other materials, usually alloys of aluminium, as a replacement to aluminium have shown promising results [7, 8].

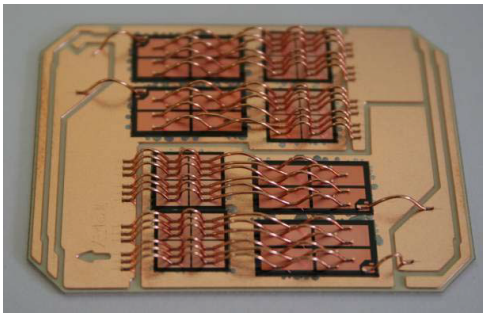

Figure 3.4 Copper wire bonds on Cu metallised IGBTs. Figure from [4]

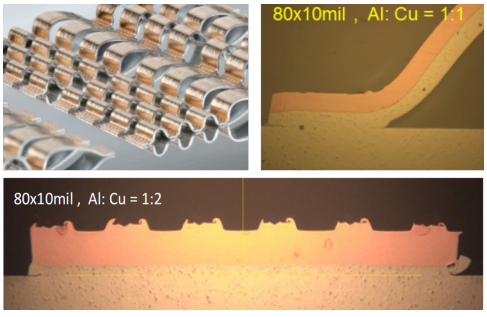

Figure 3.5 Al-Cu ribbon bonds. The figure shows cross-sections of ribbon bonds with different Al:Cu thickness ratios. Figure from [6]

• **Ribbon Bonding -** this technique makes use of rectangular ribbons of bond wire (Fig. 3.5) in place of the round bond wires. This allows better contact with the surface of the die area and lower thicknesses which improves the ultrasonic bonding process [9]. The study in [10] found that lifetime with a ribbon bond wire is 2.3 times that of a round wire bonded technology. This is attributed to the higher contact surface and stiffness which reduces crack propagation.

• **Sintered Interconnects -** this technique eliminates the need for wire bonds by sintering the top side of the power chip to a connector. The connector may be in the form of a flexible circuit board (Fig. 3.6) as in [11, 12] or planar copper interconnects (Fig. 3.7) as in [13, 14]. Such an interconnection gives the opportunity for double-sided cooling that can greatly increase the cooling efficiency.

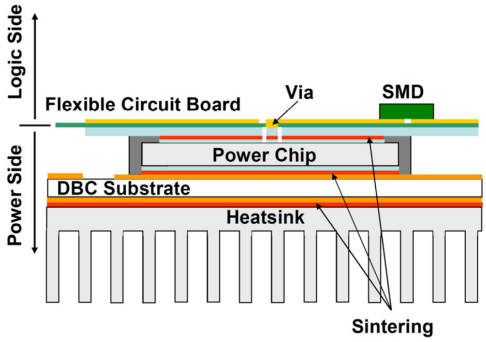

Figure 3.6 Planar interconnects with flexible PCB. Figure from [12]

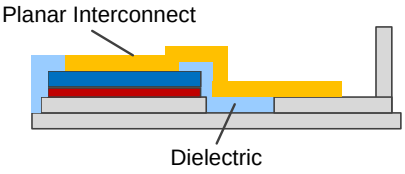

Figure 3.7 Planar copper interconnects. Based on [14]

• **Press-pack -** the press-pack technology uses pressure to obtain electrical and thermal contacts, thus eliminating wirebonds and minimising solder connections. Studies in [15] showed that press-pack IGBTs have improved lifetime performance compared to the flat-pack IGBTs. However, [16] found early failures that could be attributed to damaged gate-oxide and micro-eroding. The press-pack also addresses the solder fatigue failure mechanism.

Die Attach

In a power semiconductor, the silicon die is in most cases attached to the substrate by a solder layer. This introduces a failure mechanism driven by temperature cycles leading to solder fatigue. In [17] it is shown that for power cycling tests with $\Delta T_j < 100K$ the solder fatigue failure mode dominates. Therefore, for wind power applications this failure mode should be the focus for the design for reliability approach.

There are a number of replacements for the conventional lead based solder that have the potential of improving the lifetime with respect to solder fatigue. The use of new solder material such as the lead-free tin-silver based solder in [18] can be one solution, although it brings its own challenges. Another possibility is the use of diffusion bonding which forms bonds based on intermetallics leading to improved performance against thermo-mechanical loading [4, 19].

Another promising technique for the die attach is silver sintering where micro or nano silver particles are applied between the die and the substrate followed by the sintering process resulting in a metallic bond [19]. A number of studies have shown the improvement in lifetime performance of silver sintered joints compared to solder joints [19–22]. However, this is a more expensive technique.

Further, a more focussed and detailed review on the die attach methods and materials can be found in [23].

Baseplate Design

The power semiconductors have a solder layer between the ceramic substrate and the baseplate. This layer undergoes fatigue under cycling of temperature due to the different expansions the ceramics and the baseplate undergo. This fatigue can be reduced by matching the CTEs of the ceramic substrate and the baseplate. This can be achieved by the use of AlSiC baseplates with AlN substrates. This can reduce fatigue on the solder and increase lifetime [24–26]. However, this comes at the cost of higher temperatures due to the lower thermal conductivity of AlSiC compared to copper [26].

Package Cooling

As failures in the power semiconductor are temperature driven, effective cooling can enhance reliability. One way to do this is the use of micro-channel based water cooled baseplates. [27] shows a 60% reduction in thermal resistance compared to a standard module. This can be extended to jet impingement cooling for the baseplate or the substrate itself [28] with both methods thermally outperforming modules with cold plate technology. The integration of metallic phase change material into the design of the chip silicon as in [29] or the integration at the DBC level as in [30] could also be explored. Furthermore, the use of modules designed as a sandwich between two DBC layers for double-sided cooling as in [31,32] could result in large improvements in thermal performance.

3.2.2 Component Reliability - Converter Level

At the converter level, the use of overrating, topology, modulation and converter cooling are discussed.

Over-rating

For power semiconductors, the failure mechanisms are driven by the cycling of the junction temperature and the mean junction temperature. The use of multiple parallel converters, which

would overrate the switches in use, or the use of switches with a higher rating would reduce the junction temperatures and hence boost reliability. This has been explored for PV systems in [33–35] and can be extended to wind turbine systems.

Topology

The choice of topology can also have an effect on the lifetime of the power semiconductor. The three-level Neutral Point Clamped (3L-NPC) converter is a popular choice for large power wind turbines. This topology has an uneven distribution of losses amongst the semiconductors in each leg. Therefore, topologies that can evenly distribute the losses, and hence the stresses on the semiconductors would result in an increased lifetime of the converter. For this, the T-type and the Active Neutral Point Clamped (ANPC) topologies are promising [36].

Furthermore, the number of converter levels can be extended further than 3. This would introduce additional switching states in the operation and improve thermal performance thereby improving reliability as has been shown with a five-level converter in [37].

Modulation

The use of the Discontinuous PWM technique can reduce the effective switching frequency of a converter and increase lifetime. This use of this modulation strategy has been shown to have a modest effect on the lifetime of the converter for DFIGs in [38]. However, the DPWM leads to increased current harmonics at low modulation levels.

The use of optimal modulation schemes can reduce switching frequencies without increasing harmonic distortion. Reducing switching frequency results in lower losses in the semiconductor which is advantageous from the point of view of reliability. The Synchronous optimal PWM (SoPWM) is one such technique that has been explored and has been shown to be successful in reducing the switching frequency without affecting the harmonic distortion [39–41].

Converter Cooling

The thermal management of the converter is important not only from the point of view of the power semiconductors, but also the other sub-components like the capacitors as well. A number of failure mechanisms in these sub-components can be linked to temperature and therefore, methods that can improve thermal management of the converter can be beneficial for the overall reliability of the converter. The power sandwich integration is one such concept [42, 43] that uses new passive components that have equal heights and are sandwiched between two substrates allowing heat transfer in both directions.

3.2.3 Active Control

Once the converter has been designed there are still opportunities where active control methods can be applied to reduce the stress on components.

Power Sharing

Today's large wind turbine converters are built up of multiple modular converters in parallel to handle the large amount of power they need to process. The variation of components in these converters, even within the tolerance limits, may lead to a variation in junction temperature amongst the parallel converters. This would lead to larger stresses on certain converters and drive them to premature failure. However, if the power processed by each converter is partitioned on the basis of the temperature of the components as in [44, 45], the stresses on converters can be reduced and lifetimes extended. Therefore, the control strategy is based on equalising temperatures in converters rather than current. This method is also shown to improve efficiencies compared to current sharing controls in [46].

Reactive Current Management

Today's wind turbines are required to support the grid with reactive power injection. This can have a significant effect on the lifetimes of the converters. For a DFIG based system, this reactive power injection can be achieved from the grid side converter or the rotor side converter via the stator circuit. It has been shown that injection of reactive power from the rotor side converter produces less current stress and is, therefore, better for lifetimes [47]. Furthermore, the reactive power flow between the grid and rotor side converters has been optimised to achieve an overall balanced lifetime in [48].

The reactive current can further be used to minimise temperature variations in the power semiconductors of the converter. The circulation of reactive power between the rotor side and the grid side converter of a DFIG based system resulting in lower temperature variations during normal operation as well as during gusts is studied in [49]. The circulation between parallel connected converters for full converter based wind turbines is investigated in [50]. Here, as the reactive power is only circulated inside parallel converters in order to heat up the power switching devices the efficiency of the system reduces.

DC-link Voltage Regulation

A DC-link regulation strategy adapts the DC-link voltage to the requirement of the operating point. Such a strategy can reduce losses in the converter significantly resulting in reduced junction temperatures and therefore, increased lifetime. The DC-link voltage regulation strategy can be used in conjunction with the other methods described in this section to further increase the effect

on lifetime. This has been implemented for traction drives in [51]. A drawback here is the addition of a DC-DC converter which adds complexity and cost to the system.

Switching Frequency Regulation

The losses in a power semiconductor are dependant on the switching frequency. Therefore, the control of switching frequency can be used to regulate the temperature of the device.

First, the switching frequency can be used to ensure that semiconductor temperatures remain within the safe limits. As the junction temperature rises to a set value, the switching frequency can be reduced. This would reduce losses and hence protect the semiconductor from overheating. Such a system has been proposed in [52] and for traction applications in [53].

Another regulation method uses the frequency to reduce the amplitudes of temperature cycles in converters. A hysteresis controller is used to regulate switching frequency according to the amplitude of the temperature cycling with the frequency being increased as temperature cycle amplitude reduces, leading to a smaller temperature cycle. A number of variations of this control strategy are available in [54–57]. However, the changing of switching frequency gives rise to harmonics which need to be taken into consideration. Such an analysis of the effect on power quality is missing in literature.

Gate Voltage Regulation

Like with the power sharing method, the gate voltage regulation can be used to prevent thermal imbalance in parallel connected converters. This is achieved by adjusting the gate voltage or the gate resistance. Such a system for the thermal balance of parallel connected converters by active gate control is discussed in [58, 59].

Active gate control can also be used to control the amplitude of temperature cycles in the power semiconductor. Luo *et al.* use a system of switchable gate resistors such that the largest gate resistor is selected when the current is at the low magnitude points while the lowest gate resistor is used at high currents [60]. This results in slow switching at low current magnitudes and fast switching at high currents resulting in reduced losses. However, in this design the trade-off between switching losses and turn-off over-voltage and collector current overshoot have to be considered. Apart from controlling the gate resistance, the control of gate voltage can also be used to regulate losses as proposed in [61].

Modulation Regulation

The Discontinuous PWM (DPWM) has been discussed in section 3.2.2 and has been used to reduce losses in a converter. Using a combination of the Space Vector PWM (SVPWM) and DPWM, the switching losses can be varied within a certain band. This can be used to reduce the junction

temperature cycling amplitude. This Hybrid Discontinuous PWM (HDPWM) technique has been discussed and shown to be effective in [62–64].

Adaptive Thermal Management

The active control methods discussed above are based on controlling electrical parameters. Another opportunity for active control lies in the thermal management system.

Such a system has been proposed by de Rijck *et al.* where the efficiency of the cooling system is adjusted based on the temperature of the power semiconductor [65]. Such a adaptively controlled thermal system can reduce junction temperature cycles leading to higher lifetimes. Furthermore, active cooling regulation by control of forced air speed has been studied in [66, 67].

Reliability Oriented Control

Conventional control schemes for wind turbines are based on the extraction of maximum energy from the wind. However, considering the cost of maintenance for far offshore wind turbines, it may be important to look at reliability oriented control strategies or condition based operation that looks to maximise the availability of the wind turbines rather than maximise the power production at each instant. Such a system is conceptualised in [68, 69].

One possibility is to use a de-rated power curve to reduce the stresses on the converter or generator. For offshore wind turbines, once a failure occurs, there can be considerable time lost in the logistics of organising maintenance visits. If a de-rated power curve would result in lower stresses allowing the converter to operate for a longer period, it could result in an overall improvement in power production. This approach could be extended such that the de-rated power curve is designed to allow the operation of the converter for a longer period, wherein the component is replaced only in the next maintenance visit. These two approaches are represented in Fig. 3.8.

This active control technique would require inputs from the prognostics or condition monitoring mechanism.

3.2.4 Fault Tolerance

This section discusses two aspects of achieving fault tolerance in the converter - fault tolerant topologies, and modularity. This section is based on the review of modularity in [70] and fault tolerance in [71].

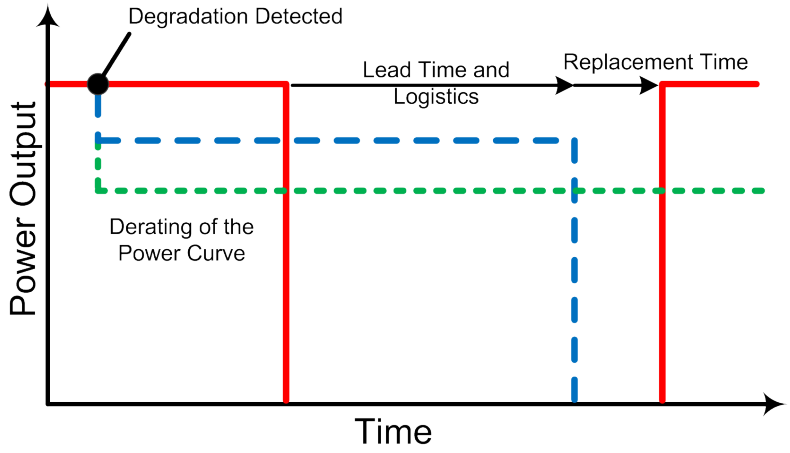

Figure 3.8 Opportunities for increased availability using the de-rating of power curves.

Fault Tolerant Topologies

There are a number of topologies that can be used to make the converter system tolerant to faults. A review of such topologies can be found in [72–74]. Fault tolerant topologies use redundancy in one form or another to introduce fault tolerant capabilities.

The switch redundant topology introduces extra switches to the two-level converter to make it able to accommodate open phase and switch short circuit faults. The double switch redundant topology (Fig. 3.9) adds an extra leg connected to the neutral point of the machine. This has the advantage of making the converter tolerant to switch short and open circuits along with phase leg short and open circuits. However, the power handling capability of the topology, during the faulted condition, is reduced. The phase redundant topology (Fig. 3.10) adds an extra phase leg that can be connected to any leg of the machine by triggering connecting switches. This topology too is tolerant to most types of faults and is capable of handling rated power.

In back to back converters, the phase redundant topology can be used with a common redundant phase leg for both (Fig. 3.11), the generator side and the grid side converters [75]. This reduces the overall cost for redundancy without affecting the fault tolerant capability. Furthermore, a converter topology without redundancy but with the possibility of reconfiguration which allows operation after a switch fault as a five-leg converter is proposed in [76].

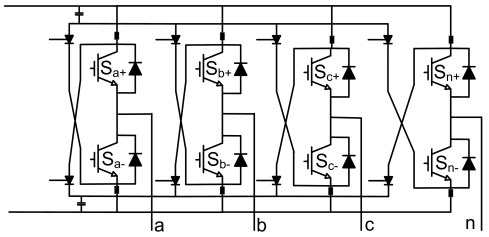

Figure 3.9 Double switch redundant topology.

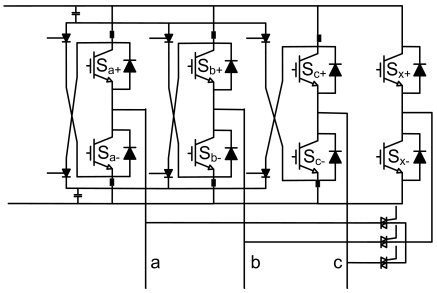

Figure 3.10 Phase redundant topology.

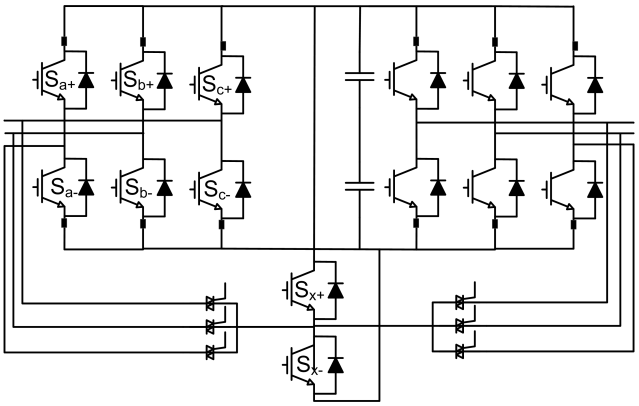

Figure 3.11 Phase redundant topology with a common redundant phase leg.

Modularity

This section is based on the review of modularity in [70]. The use of multiple modules in a converter also introduces a degree of redundancy in the system. In the event of a failure in a module, it can be disconnected from the system and allow the rest of the converter modules to process the generated power. As wind turbines operate at partial load for significant periods of time, such a system can be especially attractive. Modularity can be introduced in two layers - the first is the functional layer, where the modules operate as separate functional blocks. The second is the physical layer, which builds on functional modularity by adding physical separation.

[77, 78] discuss the use of six parallel converter modules for a 4.5MW turbine. The study shows that the system not only increases efficiency and reduces grid harmonics, but it also boosts availability when mean time to repair is considered. [79] shows the improvement in reliability with modular converters using Markov models.

One method of increasing the modularity of the system is the use of tooth wound concentrated

modular windings with a converter unit. This system brings in modularity both in the converter unit and the generator unit. There have been a number of applications where such a system has been employed as a means of incorporating fault tolerance. [80–82] uses this design concept for traction applications and [83] uses this for aerospace applications.

With a high level of physical modularity, such as with modular stator windings with independent H-bridge converters for each coil, there is an opportunity to design compact converters that would reduce replacement costs. Converter modules can be designed so that they can be replaced by a single worker without heavy lifting equipment. This would increase the maintainability of the converters and increase the availability of the converter system [70].

3.3 Addressing Generator Availability

The framework for improving generator availability is shown in Fig. 3.12.

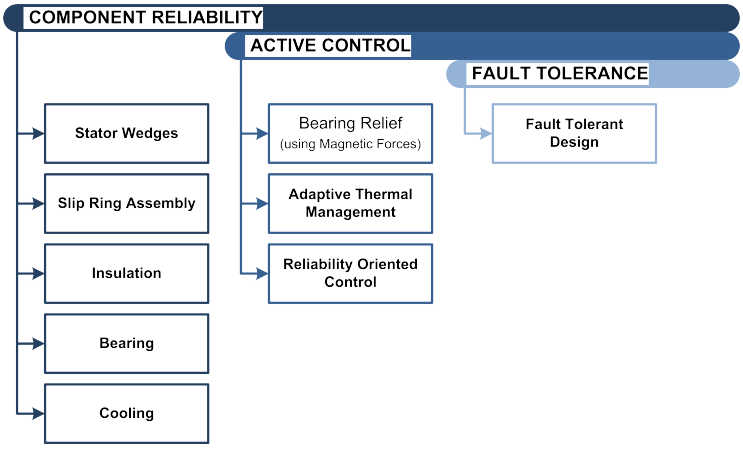

Figure 3.12 Framework for increasing generator availability.

3.3.1 Component Reliability

This section discusses design solutions for the magnetic stator wedges, slip ring assemblies, winding insulation, bearings, and cooling systems because they are the major sources of failure in the generator.

Magnetic Stator Wedges

A study of failures of wind turbine generators and found that approximately 15% of failures in generators rated above 2MW were due to stator wedges [84]. One explanation of this is that when magnetic stator wedges are used, they are subjected to pulsating forces which speed up the failure process.

Magnetic wedges offer a number of improvements to machines resulting in increased efficiency [85–87]. However, looking at their propensity to failure in wind turbines, it may be important to look at their impact once again. Here, generator designs from [88] were modified to include magnetic wedges. Analytical models were used to compare the performance of wind turbines with and without magnetic wedges. The comparison includes the DFIG with a three stage gearbox, and the permanent magnet direct drive. The results of this comparison are shown in Table 3.1. However, this is a simplified comparison that does not consider the reduction in harmonics.

These results do show that the advantage offered by the inclusion of magnetic wedges is small. Therefore, replacing the magnetic wedges with non-magnetic wedges could increase reliability without a large effect on energy production, leading to a net reduction in Cost of Energy (CoE).

	DFIG 3-stage Gearbox	PM Direct Drive
Without Magnetic Stator Wedges		
Annual Energy Yield (GWh)	7.73	8.04
With Magnetic Stator Wedges		
Optimal μ_{wedge}	9.1	10
Annual Energy Yield (GWh)	7.73	8.05
Difference in Annual Energy Yield (MWh)	0.97	8.42
Equivalent hours of Energy Production	1.1	9.16

Table 3.1 Effect of magnetic stator wedges on electrical performance.

Slip Ring Assembly

The brush and slip ring assembly is a major contributor to failures in DFIG based wind turbine systems. According to [89], more than half the failures in DFIGs are brush-slip ring failures. Even though more than half these failures are classified as minor repairs, for far offshore wind turbines minor failures can be very expensive. This failure mode can be addressed by either doing away with the slip ring system or by improving the design such that it fails less often. Apart from the slip ring in the generator, turbines using electrical pitch actuators require slip ring assemblies to transfer power to the rotating hubs.

- **Brushless DFIG -** The B-DFIG is yet to be commercialised for use in wind turbine generators. A 250kW machine has been designed and tested in [90]. The B-DFIG eliminates the need of brushes and slip rings which can be especially beneficial for wind turbines in offshore applications. However, it has lower efficiencies [91] and the trade-off between higher reliability and a lower efficiency (compared to the conventional DFIG) needs to be explored further. Another advantage of the B-DFIG is its improved low voltage ride through capability [92]. The B-DFIG is able to handle low voltage events without the use of an extra crowbar circuit. Therefore, the power electronic converter is protected without the use of extra components, improving reliability. However, the use of brushless excitation in full-converter based technologies makes the B-DFIG less relevant.

- **Brushless Excitation -** The slip ring assembly can also be avoided by the use of brushless excited machines. Apart from the permanent magnet synchronous machine, the use of rotary transformers for contactless power transfer to the rotor is also a solution. Examples of the design of such systems can be found in [93, 94].

- **Lubricated Slip Ring Assemblies -** In sliding contacts, the conduction takes place across an insulating film (which is a moisture film in many applications) by the tunnel effect, which is where a particle passes through a potential barrier that it classically cannot pass [95]. In the absence of such a film, the two clean metallic surfaces will cold weld such that the surfaces will be destroyed during sliding and the wear on the brushes will be very high [95]. One of the ways of improving the wear resistance of the brush/slip-ring assembly is by the use of boundary lubrication. This is done through the formation of thin films on the contact surfaces that do not strongly affect the current but reduce the wear [96]. The use of oil that is a suspension of conducting particles has been shown to have good results [97]. Apart from improving the wear characteristics, a good lubricant could damp vibrations leading to lower noise levels in the transmitted signal (this is more important in the use of slip rings for signals and instrumentation) as well as act as protection against corrosion of the slip ring assembly. As wind turbines, especially those erected offshore, operate in harsh and corrosive conditions (salt spray etc.) protection from corrosion is an important aspect of lubricants in slip-ring assemblies for wind turbines.

Insulation

Thermal degradation is a dominant factor in the ageing of electrical machine winding insulation systems [98, 99]. Lifetimes of insulation can be estimated using the Arrhenius rate law. The thermal class of the insulation has an effect on the lifetime. Therefore, using an insulation with a higher thermal class would increase the life expectancy of the insulation.

The use of PWM based converters can cause electrical stresses in the insulation due to the voltage spikes created by the fast front voltage waves [100]. Further, this large dV/dt due to switching of the converter can give rise to large capacitive currents in the insulation, and voltage gradients within windings. [101] gives an overview of possible solutions for relieving these stresses. These solutions could be design choices like the length of connecting cables, the switching speed, the machine insulation material as well as the use of additional components like filters.

Bearings

Bearings are a major reason for failures in wind turbines. The causes of failure may be due to problems in lubrication, contamination, misalignment etc. The solutions to such problems are beyond the scope of this thesis.

However, another reason for accelerated bearing wear is bearing current. These bearing currents can be produced by high motor frame voltage due to common mode current, high frequency axial shaft voltage due to circumferential magnetic flux around the motor shaft, the coupling of common mode voltage via the bearing capacitances [102]. It is possible to prevent the discharge of current through the bearings by using insulation in the bearings or by creating alternative paths for the current like using a grounding brush [102, 103]. Furthermore, converter design to minimise the common mode voltage can also help reduce bearing currents [104].

Eccentricity in the machine rotor may be caused by a manufacturing defect or from wear in the bearings. This eccentricity causes Unbalanced Magnetic Pull (UMP) which can further effect an increase in bearing wear. This UMP is damped to some extent by the cage in the caged induction machines and by the pole dampers in synchronous machines [105, 106], however, wound rotor machines (like the DFIG) can still benefit from the addition of damper windings. The use of stator damper windings to attenuate UMP in induction machines has been investigated in [107].

Generator Cooling

As the temperature is the main driving factor for insulation ageing, improved cooling systems for generators would prolong lifetimes of windings. Liquid cooling is one such technology that can give good results. Many high power wind turbines today already use liquid cooling for the generator and converter [108]. This cooling performance may be improved by using hydrogen cooling as in [109].

Another possibility is to use liquid flow within the stator winding to remove heat. This uses hollow conductors which allows the cooling liquid to flow within them and remove heat straight from the source. Such a system has been proposed in [110] and [111].

3.3.2 Active Control

This section looks at opportunities for reducing stress on components of the wind turbine generator.

Bearing Relief

One of the ways of addressing the bearing failures is the use of the inherent magnetic forces in the machines to reduce the load on the bearings and hence accomplish bearing relief. For large direct

drive generators, the weight of the rotor is carried by the generator bearings. The use of magnetic forces to take this load off the mechanical bearing would reduce their wear and hence increase their lifetime. Here, the weight of the turbine and the moments generated by it would have to be handled. A number of methods can be used to reduce bearing forces, of which the passive damper windings have been discussed in section 3.3.1:

- **Control Windings -** One possibility is the use of an additional winding in the stator which can be controlled to produced the required radial forces. This may be compared to a magnetic bearing or bearingless machine, however, the idea here is to keep the mechanical bearing and only use the additional winding to reduce the load on the bearing thus reducing the load handled by such windings. One of the disadvantages of such a system is the additional need for control. This would require the addition of power electronic converters, controllers and sensors [112]. A system that uses additional windings to generate radial forces and cancel the rotor weight to effect bearing relief has been investigated in [113].

- **Active Generator Control -** Another option is the use of control schemes in existing machine systems to reduce the rotor radial forces [114]. This would have the advantage of not requiring additional windings, however, it would make the control of the machine more complex. The use of modular machine concepts (with tooth wound generators with independent h-bridge converters for each turn) could be extended to include active generator control to counteract the weight of the rotor and reduce the load on the bearings. The use of sensorless control would also reduce the need for sensors and has been proposed in [115, 116] for small bearingless machines.

Furthermore, the use of active magnetic force control in modular generators also affords the opportunity to counteract dynamic bearing forces that may arise, for example, due to wind gusts. The challenge here is being able to measure the stress in the bearing system to be able to counter them.

Adaptive Thermal Management

It has been discussed in section 2.4.1 that temperature cycling of the winding could lead to accelerated failure, therefore, adaptive thermal management as discussed for the converter in section 3.2.3 could reduce the temperature cycling.

Reliability Oriented Control

Reliability based control or condition based operation has been described in section 3.2.3 and can be used to extend the lifetime of generator components as well. [117] explores a prognostics based life extension methodology for generation systems and focusses on the bearing system.

3.3.3 Fault Tolerance

This section is also based on the review of modularity in [70] and fault tolerance in [71]. For a machine to be tolerant to its failures, it has to satisfy certain requirements [118],

- **Electrical Isolation -** to limit the effect of the faulty winding on the healthy part of the machine, the different 'modules' of the machine should be electrically isolated. For modular systems that use independent converters for each module (be it a single coil or three phase coil module) this requirement is already built into the design.

- **Limiting Fault Current -** if the short circuit fault occurs at the machine winding terminal or in the converter, both scenarios could result in large currents. To limit the fault current, stator phase inductance has to be designed to be close 1 pu inductance so that fault current is limited to the rated value. Furthermore, techniques for reducing the short circuit current by using magnet subdivisions have been investigated in [119, 120].

- **Magnetic Isolation -** fault current will induce a voltage in the neighbouring phases, because of the presence of mutual inductance between phases. This would make control of the machine difficult. To reduce the effect of one phase on another, the mutual inductance between phases or modules must be small.

- **Thermal Isolation -** short circuit current can produce large amounts of heat in the slot, therefore, thermal isolation between the different windings is recommended. Modular stator windings with a single coil in each slot would serve this need well.

The use of a modular design with a distributed control architecture with multiple processors would allow operation under the failure of control modules as well. The addition of physical modularity to the generator design by using segmented cores introduces the ability of a core module of the generator being replaced in case of any winding failure. Stator winding failures account for about 20-30% of all generator failures [84]. These failures are expensive to fix and take considerable time. According to [121], a generator failure averages about 150 hours of downtime. The use of segmentation would reduce the time and cost of faulty winding replacement. Physical modularity in the form of segmentation could, therefore, be especially attractive for offshore wind turbines [70]. Such a system is proposed in [122] where the direct drive PM generator is constructed from physically separate E-core modules as shown in Fig. 3.13.

Fault tolerance can also be included by the use of multiple phases. [123] describes an AC drive with multiple independent phase driving units. For wind turbines, such a multiple phase system with nine phases constructed with classical three phase converters was described in [124].

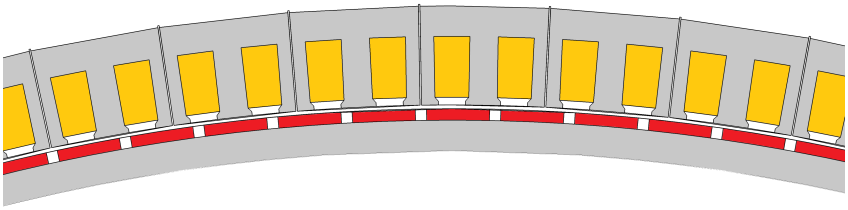

Figure 3.13 Physical modularity in the generator.

3.4 Promising Research Directions

The previous sections have examined some methods that aim to increase the availability of wind turbine generator systems by the design for component reliability, the active control for reliability, and the design for fault tolerance approaches. This section highlights promising directions for investigation that form the basis for the remaining chapters in this thesis.

- **Converter Design for Improved Lifetimes -** the use of design concepts at a converter level to increase reliability can be applied to commercially available power modules. Even with advancement in power module technology, the failure mechanisms are still driven by thermal and power cycling (the examples being press-pack technology, silver sintering methods etc.). Therefore, with the advances in power module technology, these design concepts will only help boost the reliability of the converter (until other failure mechanisms become the limiting factor in reliability).

A number of avenues for further research exist in this field. First, a comparison of the effects of overrated components and overrated topologies on the lifetime of the converter is required. This will allow the identification of an optimal topology from the point of view of reliability. Further, the use of dynamic switching strategies that distribute the losses based on the temperatures of the semiconductors can be investigated.

- **Adaptive Thermal Management -** many active control methods use the control of electrical parameters to reduce the amplitude of temperature cycles in the junction of the power semiconductors (ΔT_j) and increase the lifetime. The essence of this concept is to increase the losses when the junction temperature is low so that ΔT_j is reduced. However, the reduction of ΔT_j can also be achieved by controlling the effectiveness of the thermal circuit. Without the need to increase losses, this method has the potential of improving the lifetime without considerable effect on the efficiency of the converter. The case for the use of adaptive thermal management is further strengthened by the fact that a majority of wind turbine converters already use liquid cooling. Therefore, aspects of this method can be included into the design without major re-engineering.

There are a number of opportunities for research in this field. First, different configurations that are possible need to be identified and evaluated. One possibility is the use of the generator as

thermal capacitance by the integration of the converter and generator cooling circuits. This could be used to counter medium term temperature cycles. Another possibility is the use of differential heat production in separate parts of the component for dynamic thermal management i.e. use heat from one place to reduce thermal efficiency at another.

- **Fault Tolerance with Modularity -** systems, no matter how well designed, can suffer from random failures. This is more so in the case of complex systems like wind turbines. Therefore, the use of fault tolerant design can play an important role in increasing the availability of such systems. Modularity is interesting because it is already used to some extent in large wind turbine generator systems. Furthermore, the use of modularity can benefit other aspects such as maintainability and the installation of generator systems.

This area of research presents a number of opportunities some of which have been listed in [70]. These include: the design of compact physically modular converters that can be replaced by a single worker without heavy lifting equipment, a detailed investigation of physically modular generator topologies for use in wind turbines, and the optimal sizing of generator modules considering electrical, structural, and post fault performance. Further, as the converter has a majority of the failures when compared to the machine winding, it must be investigated if the generator needs to be designed for fault tolerance.

3.5 Conclusions

The increased availability of wind turbine generator systems is based on five pillars - design for component reliability, active control for reliability, design for fault tolerance, prognostics, and design for maintainability. This chapter has reviewed methods focussing on the first three pillars and identified a few promising directions for further research. With a holistic approach based on these five design approaches, methods can be adopted at each level such that they result in the required availability with an acceptable increment in the cost.

Further, the following conclusions are made for the wind turbine power electronic converter:

- A majority of the failure mechanisms are driven by junction temperature and the amplitude of junction temperature variation. Therefore, the methods described under the design for components reliability and the active control for reliability approaches focus on these issues.

- Methods for design for converter reliability are promising because they address reliability at a system level and can be applied with advancing technology as long as temperature is the driving factor in failures.

- Dynamic thermal management reduces the amplitude of junction temperature cycles without significantly increasing the electrical losses. Furthermore, a comparison of electrical parameter control and thermal control based on the improvement in the lifetime as well as the electrical performance is required.

- Wind turbine control is based on extracting maximum power from wind. However, the use of reliability oriented control (or condition based operation) that would focus on increasing

availability could help in lowering cost of energy, especially in far offshore wind farms. Reliability oriented control can be used to reduce the maintenance costs by allowing operation of the converter until the next scheduled maintenance visit. Thus, removing the need for unscheduled maintenance visits.

- Fault tolerance through modularity is also promising because apart from the advantage of fault tolerance, it can improve the maintainability of the converter.

Also, the following conclusions are made for the wind turbine generator:

- Choices in the design of the generator can have a large impact on the reliability of the generator. The examples of this are the use of non-magnetic stator wedges, and the use of brushless excitation. Magnetic stator wedges fail often in wind turbine generators. Therefore, replacing them with non-magnetic wedges will help in improving reliability. The slip rings and brush system are major contributors to failures in DFIG wind turbine generators. Apart from adding to failures, the wear of brushes causes brush dust which can act as an environmental stress for the insulation of generator windings. Therefore, a shift to brushless excitation or the improvement in brush-slip ring technology could lead to improvements in generator reliability.

- Bearing relief from the dynamic forces could be an important step in improving the lifetime of generator bearings. However, the real-time identification of the stresses is a challenge that has to be overcome for this.

- Dynamic thermal management can be used to reduce temperature cycling stresses on the winding insulation. However, further studies are required to confirm the effect of the temperature cycling stresses on the insulation lifetime in wind turbine applications.

- Modularity in the generator system can be used to improve maintainability as well as the ease of installation. However, the trade-off between the maintainability, the electrical performance, and the structural requirements needs analysis.

The remainder of this thesis devotes one chapter to each of the promising research directions discussed in section 3.4. Chapter 4 analyses converter topologies from the viewpoint of reliability, in particular it examines the effect of over-rating. Chapter 5 analyses adaptive cooling as an active control method to reduce temperature cycling of power semiconductors. The effect of modularity on the availability of wind turbine generator systems is examined in chapter 6. Finally, conclusions on this study are detailed in chapter 7.

Bibliography

[1] A. Hamidi, N. Beck, K. Thomas, and E. Herr, "Reliability and Lifetime Evaluation of Different Wire Bonding Technologies for High Power IGBT Modules," *Microelectronics Reliability*, vol. 39, pp. 1153–1158, 1999.

[2] B. Baliga, "Package and Module Design," in *The IGBT Device*. Elsevier Ltd, 2015, p. 732.

[3] R. Bayerer, "Advanced Packaging Yields Higher Performance and Reliability in Power Electronics," *Microelectronics Reliability*, vol. 50, pp. 1715–1719, 2010.

[4] K. Guth, D. Siepe, J. Görlich, H. Torwesten, R. Roth, F. Hille, and F. Umbach, "New Assembly and Interconnects Beyond Sintering Methods," in *International Conference on Power Conversion and Intelligent Motion (PCIM)*, 2010, pp. 219–224.

[5] R. Schmidt, U. Scheuermann, and E. Mike, "Al-clad Cu Wire Bonds Multiply Power Cycling Lifetime of Advanced Power Modules," in *International Conference on Power Conversion and Intelligent Motion (PCIM)*, 2012.

[6] J. Ling, T. Xu, R. Chen, O. Valentin, and C. Luechinger, "Cu and Al-Cu composite-material interconnects for power devices," in *2012 IEEE 62nd Electronic Components and Technology Conference*. IEEE, May 2012, pp. 1905–1911.

[7] Y. Fujii, Y. Ishikawa, S. Takeguchi, and J. Onuki, "Development of High-Reliability Thick Al-Mg2Si Wire Bonds for High-Power Modules," in *International Symposium on Power Semiconductor Devices and ICs*, 2012, pp. 279–282.

[8] U. Geißler, J. Göhre, S. Thomas, M. Schneider-Ramelow, and K.-D. Lang, "A new Aluminium Alloy for Heavy Wire Bonding in Power Electronics - First Tests of Bonding Behaviour and Reliability Specification of the AlX-alloy," in *International Conference on Power Conversion and Intelligent Motion (PCIM)*, 2013, pp. 14–16.

[9] B. Ong, M. Helmy, S. Chuah, C. Luechinger, and G. Wong, "Heavy Al Ribbon Interconnect: An Alternative Solution for Hybrid Power Packaging," in *IMAPS*, 2004, pp. 1–11.

[10] S. Jacques, R. Leroy, and M. Lethiecq, "Impact of Aluminum Wire and Ribbon Bonding Technologies on D2PAK Package Reliability during Thermal Cycling Applications," *Microelectronics Reliability*, vol. 55, no. 9-10, pp. 1821–1825, Aug. 2015.

[11] T. Stockmeier, P. Beckedahl, C. Gobl, and T. Malzer, "SKiN: Double Side Sintering Technology for New Packages," in *2011 IEEE 23rd International Symposium on Power Semiconductor Devices and ICs*. IEEE, May 2011, pp. 324–327.

[12] U. Scheuermann, "Reliability of Planar SKiN Interconnect Technology," in *7th International Conference on Integrated Power Electronics Systems (CIPS)*, 2012, pp. 464–471.

[13] Y. Wang, X. Dai, G. Liu, D. Li, and S. Jones, "An Overview of Advanced Power Semiconductor Packaging for Automotive System Packaging of Power Module," in *9th International Conference on Integrated Power Electronics Systems (CIPS 2016)*, 2016, pp. 1–6.

[14] R. Dudek, R. Doring, M. Hildebrandt, S. Rzepka, S. Stegmeier, S. Kiefl, V. Sommer, G. Mitic, and K. Weidner, "Analyses of Thermo-mechanical Reliability Issues for Power Modules Designed in Planar Technology," in *2016 17th International Conference on Thermal, Mechanical and Multi-Physics Simulation and Experiments in Microelectronics and Microsystems (EuroSimE)*. IEEE, Apr. 2016, pp. 1–8.

[15] N. Benavides, T. McCoy, and M. Chrin, "Reliability Improvements in Integrated Power Systems with Pressure-Contact Semiconductors," in *Proc. ASNE*, 2009.

[16] L. Tinschert, A. R. Årdal, T. Poller, M. Bohlländer, M. Hernes, and J. Lutz, "Possible Failure Modes in Press-Pack IGBTs," *Microelectronics Reliability*, vol. 55, no. 6, pp. 903–911, 2015.

[17] U. Scheuermann, "Packaging and Reliability of Power Modules – Principles , Achievements and Future Challenges General Design Principles of Power Modules," in *International Conference on Power Conversion and Intelligent Motion (PCIM)*, 2015, pp. 35–50.

[18] A. Morozumi, K. Yamada, T. Miyasaka, S. Sumi, and Y. Seki, "Reliability of Power Cycling for IGBT Power Semiconductor Modules," *IEEE Transactions on Industry Applications*, vol. 39, no. 3, pp. 665–671, May 2003.

[19] K. Guth, N. Oeschler, L. Böwer, R. Speckels, G. Strotmann, N. Heuck, S. Krasel, and A. Ciliox, "New Assembly and Interconnect Technologies for Power Modules," in *International Conferecne on Integrated Power Electronics Systems (CIPS)*, 2012, pp. 380–384.

[20] L. Jiang, T. G. Lei, K. D. T. Ngo, G.-Q. Lu, and S. Luo, "Evaluation of Thermal Cycling Reliability of Sintered Nanosilver Versus Soldered Joints by Curvature Measurement," *IEEE Transactions on Components, Packaging and Manufacturing Technology*, vol. 4, no. 5, pp. 751–761, May 2014.

[21] R. Dudek, R. Doring, S. Rzepka, C. Ehrhardt, M. Gunther, and M. Haag, "Electro-thermo-mechanical Analyses on Silver Sintered IGBT-module Reliability in Power Cycling," in *2015 16th International Conference on Thermal, Mechanical and Multi-Physics Simulation and Experiments in Microelectronics and Microsystems*. IEEE, Apr. 2015, pp. 1–8.

[22] F. Le Henaff, S. Azzopardi, E. Woirgard, T. Youssef, S. Bontemps, and J. Joguet, "Lifetime Evaluation of Nanoscale Silver Sintered Power Modules for Automotive Application Based on Experiments and Finite-Element Modeling," *IEEE Transactions on Device and Materials Reliability*, vol. 15, no. 3, pp. 326–334, Sep. 2015.

[23] V. R. Manikam and Kuan Yew Cheong, "Die Attach Materials for High Temperature Applications: A Review," *IEEE Transactions on Components, Packaging and Manufacturing Technology*, vol. 1, no. 4, pp. 457–478, Apr. 2011.

[24] T. Schutze, H. Berg, and M. Hierholzer, "Further Improvements in the Reliability of IGBT Modules," in *Conference Record of 1998 IEEE Industry Applications Conference. Thirty-Third IAS Annual Meeting (Cat. No.98CH36242)*, vol. 2. IEEE, 1998, pp. 1022–1025.

[25] G. Coquery and L. R., "Failure Criteria for Long Term Accelerated Power Cycling Test Linked to Electrical Turn Off SOA on IGBT Module. A 4000 Hours Test on 1200A-3300V Module with AlSiC Base Plate," *Microelectronics Reliability*, vol. 40, pp. 1665–1670, 2000.

[26] U. Scheuermann, "Reliability Challenges of Automotive Power Electronics," *Microelectronics Reliability*, vol. 49, no. 9-11, pp. 1319–1325, Sep. 2009.

[27] J. Schulz-Harder, "Efficient Cooling of Power Electronics," in *3rd International Conference on Power Electronics Systems and Applications (PESA 2009)*, 2009, pp. 1–4.

[28] R. Skuriat and C. M. Johnson, "Direct Substrate Cooling of Power Electronics," in *2008 5th International Conference on Integrated Power Systems (CIPS)*, 2008.

[29] R. W. Bonner, T. Desai, F. Gao, X. Tang, T. Palacios, S. Shin, and M. Kaviany, "Die Level Thermal Storage for Improved Cooling of Pulsed Devices," in *2011 27th Annual IEEE Semiconductor Thermal Measurement and Management Symposium*. IEEE, Mar. 2011, pp. 193–197.

[30] U. Soupremanien, H. Szambolics, S. Quenard, P. Bouchut, M. Roumanie, R. Bottazzini, and N. Dunoyer, "Integration of Metallic Phase Change Material in Power Electronics," in *2016 15th IEEE Intersociety Conference on Thermal and Thermomechanical Phenomena in Electronic Systems (ITherm)*. IEEE, May 2016, pp. 125–133.

[31] C. Gillot, C. Schaeffer, C. Massit, and L. Meysenc, "Double-sided Cooling for High Power IGBT Modules using Flip Chip Technology," *IEEE Transactions on Components and Packaging Technologies*, vol. 24, no. 4, pp. 698–704, 2001.

[32] C. M. Johnson, C. Buttay, S. J. Rashid, F. Udrea, G. A. J. Amaratunga, P. Ireland, and R. K. Malhan, "Compact Double-Side Liquid-Impingement-Cooled Integrated Power Electronic Module," in *Proceedings of the 19th International Symposium on Power Semiconductor Devices and IC's*, vol. 3. IEEE, May 2007, pp. 53–56.

[33] H. Calleja, F. Chan, and I. Uribe, "Reliability-Oriented Assessment of a DC/DC Converter for Photovoltaic Applications," in *2007 IEEE Power Electronics Specialists Conference*. IEEE, 2007, pp. 1522–1527.

[34] G. Petrone, G. Spagnuolo, R. Teodorescu, M. Veerachary, and M. Vitelli, "Reliability Issues in Photovoltaic Power Processing Systems," *IEEE Transactions on Industrial Electronics*, vol. 55, no. 7, pp. 2569–2580, Jul. 2008.

[35] F. Chan and H. Calleja, "Reliability Estimation of Three Single-Phase Topologies in Grid-Connected PV Systems," *IEEE Transactions on Industrial Electronics*, vol. 58, no. 7, pp. 2683–2689, Jul. 2011.

[36] S. Gierschner and H.-G. Eckel, "Lifetime Estimation of the BIGT in ANPC Converter and T-Type Converter for Wind Energy Application," in *8th IET International Conference on Power Electronics, Machines and Drives (PEMD 2016)*. IET, 2016, pp. 1–6.

[37] K. Ma and F. Blaabjerg, "Multilevel Converters for 10 MW Wind Turbines," in *14th European Conference on Power Electronics and Applications (EPE 2011)*, 2011, pp. 1–10.

[38] M. Morisse, A. Bartschat, J. Wenske, and A. Mertens, "Converter Lifetime Assessment for Doubly-Fed Induction Generators Considering Derating Control Strategies at Low Rotor Frequencies," *Journal of Physics: Conference Series*, vol. 753, pp. 1–10, Sep. 2016.

[39] J. Holtz and N. Oikonomou, "Synchronous Optimal Pulsewidth Modulation and Stator Flux Trajectory Control for Medium-Voltage Drives," *IEEE Transactions on Industry Applications*, vol. 43, no. 2, pp. 600–608, 2007.

[40] ——, "Optimal Control of a Dual Three-Level Inverter System for Medium-Voltage Drives," *IEEE Transactions on Industry Applications*, vol. 46, no. 3, pp. 1034–1041, 2010.

[41] C. A. dos Santos and F. L. M. Antunes, "Losses Comparison Among Carrier-Based PWM Modulation Strategies in Three- Level Neutral-Point-Clamped Inverter Key words The Three-level NPC Inverter," in *International Conference on Renewable Energies abd Power Quality*, vol. 1, no. 9, 2011, pp. 1035–1040.

[42] I. Josifovic, J. Popovic-Gerber, and J. Ferreira, "A PCB System Integration Concept for Power Electronics," in *2009 IEEE 6th International Power Electronics and Motion Control Conference*, vol. 3. IEEE, May 2009, pp. 756–762.

[43] ——, "Power Sandwich Industrial Drive with SiC JFETs," in *14th European Conference on Power Electronics and Applications (EPE 2011)*, 2011.

[44] C. Joseph, M. Zolghadri, A. Homaifar, F. Lee, and R. Lorenz, "Novel Thermal Based Current Sharing Control of Parallel Converters," in *2004 10th International Workshop on Computational Electronics*. IEEE, 2004, pp. 647–653.

[45] C. Nesgaard and M. Andersen, "Optimized Load Sharing Control by means of Thermal Reliability Management," in *IEEE Power Electronics Specialists Conference*. IEEE, 2004, pp. 4901–4906.

[46] ——, "Efficiency Improvement in Redundant Power Systems by means of Thermal Load Sharing," in *IEEE Applied Power Electronics Conference and Exposition.*, vol. 1. IEEE, 2004, pp. 433–439.

[47] D. Zhou, F. Blaabjerg, M. Lau, and M. Tonnes, "Reactive Power Impact on Lifetime Prediction of two-level Wind Power Converter," in *International Conference on Power Conversion and Intelligent Motion (PCIM)*, 2013, pp. 564–571.

[48] ——, "Optimized Reactive Power Flow of DFIG Power Converters for Better Reliability Performance Considering Grid Codes," *IEEE Transactions on Industrial Electronics*, vol. 62, no. 3, pp. 1552–1562, Mar. 2015.

[49] Dao Zhou, F. Blaabjerg, M. Lau, and M. Tonnes, "Thermal Behavior Optimization in Multi-MW Wind Power Converter by Reactive Power Circulation," *IEEE Transactions on Industry Applications*, vol. 50, no. 1, pp. 433–440, Jan. 2014.

[50] K. Ma, M. Liserre, and F. Blaabjerg, "Reactive Power Influence on the Thermal Cycling of Multi-MW Wind Power Inverter," *IEEE Transactions on Industry Applications*, vol. 49, no. 2, pp. 922–930, Mar. 2013.

[51] J. Lemmens, J. Driesen, and P. Vanassche, "Dynamic DC-link Voltage Adaptation for Thermal Management of Traction Drives," in *2013 IEEE Energy Conversion Congress and Exposition*. IEEE, Sep. 2013, pp. 180–187.

[52] V. Blasko, R. Lukaszewski, and R. Sladky, "On line Thermal Model and Thermal Management Strategy of a Three Phase Voltage Source Inverter," in *Conference Record of the 1999 IEEE Industry Applications Conference. Thirty-Forth IAS Annual Meeting (Cat. No.99CH36370)*, vol. 2. IEEE, 1999, pp. 1423–1431.

[53] J. Lemmens, J. Driesen, and P. Vanassche, "Thermal Management in Traction Applications as a Constraint Optimal Control Problem," in *2012 IEEE Vehicle Power and Propulsion Conference*. IEEE, Oct. 2012, pp. 36–41.

[54] M. Weckert and J. Roth-Stielow, "Lifetime as a Control Variable in Power Electronic Systems," in *2010 Emobility - Electrical Power Train*, no. 1. IEEE, Nov. 2010, pp. 1–6.

[55] ——, "Chances and Limits of a Thermal Control for a Three-Phase Voltage Source Inverter in Traction Applications using Permanent Magnet Synchronous or Induction Machines," in *2011 13th European Conference on Power Electronics and Applications (EPE'11 ECCE Europe)*, 2011, pp. 1–10.

[56] Lixiang Wei, J. McGuire, and R. a. Lukaszewski, "Analysis of PWM Frequency Control to Improve the Lifetime of PWM Inverter," *IEEE Transactions on Industry Applications*, vol. 47, no. 2, pp. 922–929, Mar. 2011.

[57] J. Falck, M. Andresen, and M. Liserre, "Active Thermal Control of IGBT Power Electronic Converters," in *IECON 2015 - 41st Annual Conference of the IEEE Industrial Electronics Society*. IEEE, Nov. 2015, pp. 000 001–000 006.

[58] P. Hofer, N. Karrer, and C. Gerster, "Paralleling Intelligent IGBT Power Modules with Active Gate-controlled Current Balancing," in *PESC Record. 27th Annual IEEE Power Electronics Specialists Conference*, vol. 2. IEEE, 1996, pp. 1312–1316.

[59] X. Wang, Z. Zhao, and L. Yuan, "Current Sharing of IGBT Modules in Parallel with Thermal Imbalance," in *2010 IEEE Energy Conversion Congress and Exposition*. IEEE, Sep. 2010, pp. 2101–2108.

[60] H. Luo, F. Iannuzzo, K. Ma, F. Blaabjerg, W. Li, and X. He, "Active Gate Driving Method for Reliability Improvement of IGBTs via Junction Temperature Swing Reduction," in *2016 IEEE 7th International Symposium on Power Electronics for Distributed Generation Systems (PEDG)*. IEEE, Jun. 2016, pp. 1–7.

[61] L. Wu and A. Castellazzi, "Temperature Adaptive Driving of Power Semiconductor Devices," in *2010 IEEE International Symposium on Industrial Electronics*. IEEE, Jul. 2010, pp. 1110–1114.

[62] J. F. Wolfle and J. Roth-Stielow, "A Hybrid Discontinuous Modulation Technique to Influence the Switching Losses of Three Phase Inverters," in *2015 17th European Conference on Power Electronics and Applications (EPE'15 ECCE-Europe)*. IEEE, Sep. 2015, pp. 1–10.

[63] D. Kaczorowski, M. Mittelstedt, and A. Mertens, "Investigation of Discontinuous PWM as Additional Optimization Parameter in an Active Thermal Control," in *2016 18th European Conference on Power Electronics and Applications (EPE'16 ECCE Europe)*. IEEE, Sep. 2016, pp. 1–10.

[64] J. Wolfle, M. Nitzsche, J. Weimer, M. Stempfle, and J. Roth-Stielow, "Temperature Control System using a Hybrid Discontinuous Modulation Technique to Improve the Lifetime of IGBT Power Modules," in *2016 18th European Conference on Power Electronics and Applications (EPE'16 ECCE Europe)*. IEEE, Sep. 2016, pp. 1–10.

[65] A. C. de Rijck and H. Huisman, "Power Semiconductor Device Adaptive Cooling Assembly," Patent WO 2010-041 175, 2010.

[66] M. Foster, D. Stone, and J. Davidson, "Real-time Temperature Monitoring and Control for Power Electronic Systems under Variable Active Cooling by Characterisation of Device Thermal Transfer Impedance," in *7th IET International Conference on Power Electronics, Machines and Drives (PEMD 2014)*. Institution of Engineering and Technology, 2014, pp. 1–6.

[67] J. N. Davidson, D. A. Stone, M. P. Foster, and D. T. Gladwin, "Real-Time Temperature Estimation in a Multiple Device Power Electronics System Subject to Dynamic Cooling," *IEEE Transactions on Power Electronics*, vol. 31, no. 4, pp. 2709–2719, Apr. 2016.

[68] L. Hao, "Degradation-Based Control of Multi-Component Systems Degradation-Based Control of Multi-Component Systems," PhD diss., Georgia Institute of Technology, 2015.

[69] L. Hao, K. Liu, N. Gebraeel, and J. Shi, "Controlling the Residual Life Distribution of Parallel Unit Systems Through Workload Adjustment," *IEEE Transactions on Automation Science and Engineering*, pp. 1–11, 2015.

[70] U. Shipurkar, H. Polinder, and J. A. Ferreira, "Modularity in Wind Turbine Generator Systems — Opportunities and Challenges," in *European Conference on Power Electronics and Applications (EPE'16 ECCE Europe)*. IEEE, Sep. 2016, pp. 1–10.

[71] H. Polinder, H. Lendenmann, R. Chin, and W. Arshad, "Fault Tolerant Generator Systems for Wind Turbines," in *2009 IEEE International Electric Machines and Drives Conference*. IEEE, May 2009, pp. 675–681.

[72] B. Welchko, T. Lipo, T. Jahns, and S. Schulz, "Fault Tolerant Three-phase AC Motor Drive Topologies: a Comparison of Features, Cost, and Limitations," in *IEEE International Electric Machines and Drives Conference, 2003. IEMDC'03.*, vol. 1, no. 4. IEEE, 2003, pp. 539–546.

[73] C.-C. Yeh and N. A. O. Demerdash, "Induction Motor-Drive Systems with Fault Tolerant Inverter-Motor Capabilities," in *2007 IEEE International Electric Machines & Drives Conference*, vol. 2. IEEE, May 2007, pp. 1451–1453.

[74] Zhou Junwei, Qiu Yingning, Feng Yanhui, and Feng Kai, "Fault Tolerance for Wind Turbine Power Converter," in *2nd IET Renewable Power Generation Conference (RPG 2013)*. IET, 2013, pp. 3.24–3.24.

[75] A. Gaillard, S. Karimi, P. Poure, S. Saadate, and E. Gholipour, "A Fault Tolerant Converter Topology for Wind Energy Conversion System with Doubly Fed Induction Generator," in *2007 European Conference on Power Electronics and Applications*. IEEE, 2007, pp. 1–6.

[76] A. Gaillard, P. Poure, and S. Saadate, "FPGA-based Reconfigurable Control for Switch Fault Tolerant Operation of WECS with DFIG without Redundancy," *Renewable Energy*, vol. 55, pp. 35–48, Jul. 2013.

[77] J. Birk and B. Andresen, "Parallel-connected Converters for Optimizing Efficiency, Reliability and Grid Harmonics in a Wind Turbine," in *2007 European Conference on Power Electronics and Applications*. IEEE, 2007, pp. 1–7.

[78] B. Andresen and J. Birk, "A High Power Density Converter System for the Gamesa G10x 4,5 MW Wind Turbine," in *2007 European Conference on Power Electronics and Applications*. IEEE, 2007, pp. 1–8.

[79] T. Zhang and A. Zain, "Modular Converter System Reliability & Performance Analysis in Design," in *The 2nd International Symposium on Power Electronics for Distributed Generation Systems*. IEEE, Jun. 2010, pp. 252–258.

[80] N. R. Brown, T. M. Jahns, and R. D. Lorenz, "Power Converter Design for an Integrated Modular Motor Drive," in *2007 IEEE Industry Applications Annual Meeting*. IEEE, Sep. 2007, pp. 1322–1328.

[81] M. D. Hennen, M. Niessen, C. Heyers, H. J. Brauer, and R. W. De Doncker, "Development and Control of an Integrated and Distributed Inverter for a Fault Tolerant Five-Phase Switched Reluctance Traction Drive," *IEEE Transactions on Power Electronics*, vol. 27, no. 2, pp. 547–554, Feb. 2012.

[82] A. Shea and T. M. Jahns, "Hardware Integration for an Integrated Modular Motor Drive Including Distributed Control," in *2014 IEEE Energy Conversion Congress and Exposition (ECCE)*. IEEE, Sep. 2014, pp. 4881–4887.

[83] J. Wolmarans, M. Gerber, H. Polinder, S. de Haan, J. Ferreira, and D. Clarenbach, "A 50kW Integrated Fault Tolerant Permanent Magnet Machine and Motor Drive," in *2008 IEEE Power Electronics Specialists Conference*. IEEE, Jun. 2008, pp. 345–351.

[84] K. Alewine and W. Chen, "A Review of Electrical Winding Failures in Wind Turbine Generators," *IEEE Electrical Insulation Magazine*, vol. 28, no. 4, pp. 8–13, Jun. 2012.

[85] M. Davis, "Problems and Solutions with Magnetic Stator Wedges," in *IRIS Rotating Machine Conference*, 2007.

[86] R. Curiac and H. Li, "Improvements in Energy Efficiency of Induction Motors by the use of Magnetic Wedges," in *2011 Record of Conference Papers Industry Applications Society 58th Annual IEEE Petroleum and Chemical Industry Conference (PCIC)*. IEEE, Sep. 2011, pp. 1–6.

[87] K. Alewine and C. Wilson, "Magnetic Wedge Failures in Wind Turbine Generators," in *2013 IEEE Electrical Insulation Conference (EIC)*, no. June. IEEE, Jun. 2013, pp. 244–247.

[88] H. Polinder, F. Van Der Pijl, G.-J. De Vilder, and P. Tavner, "Comparison of Direct-Drive and Geared Generator Concepts for Wind Turbines," *IEEE Transactions on Energy Conversion*, vol. 21, no. 3, pp. 725–733, Sep. 2006.

[89] J. Carroll, A. McDonald, and D. McMillan, "Reliability Comparison of Wind Turbines With DFIG and PMG Drive Trains," *IEEE Transactions on Energy Conversion*, vol. 30, no. 2, pp. 663–670, Jun. 2015.

[90] R. McMahon, E. Abdi, P. Malliband, S. Shao, M. Mathekga, and P. Tavner, "Design and Testing of a 250 kW Medium-speed Brushless DFIG," in *6th IET International Conference on Power Electronics, Machines and Drives (PEMD 2012)*. IET, 2012, pp. D12–D12.

[91] T. D. Strous, U. Shipurkar, H. Polinder, and J. A. Ferreira, "Comparing the Brushless DFIM to other Generator Systems for Wind Turbine Drive-Trains," *Journal of Physics: Conference Series*, vol. 753, p. 112014, Sep. 2016.

[92] U. Shipurkar, T. D. Strous, H. Polinder, and J. A. Ferreira, "LVRT Performance of Brushless Doubly Fed Induction Machines — A Comparison," in *2015 IEEE International Electric Machines & Drives Conference (IEMDC)*, no. 6. IEEE, May 2015, pp. 362–368.

[93] H. Krupp and A. Mertens, "Rotary Transformer Design for Brushless Electrically Excited Synchronous Machines," in *2015 IEEE Vehicle Power and Propulsion Conference (VPPC)*. IEEE, Oct. 2015, pp. 1–6.

[94] S.-A. Vip, J.-N. Weber, A. Rehfeldt, and B. Ponick, "Rotary Transformer with Ferrite Core for Brushless Excitation of Synchronous Machines," in *2016 XXII International Conference on Electrical Machines (ICEM)*. IEEE, Sep. 2016, pp. 890–896.

[95] K. Sawa and E. I. Shobert, "Sliding Electrical Contacts (Graphitic Type Lubrication)," in *Electrical Contacts: principles and applications*, P. G. Slade, Ed. CRC Press, 2013, pp. 1042–1079.

[96] M. Braunovic, "Sliding Contacts," in *Electrical Contacts: Fundamentals, Applications and Technology*, M. Braunovic, N. K. Myshkin, and V. V. Konchits, Eds. CRC Press, 2006, pp. 369–494.

[97] M. van der Laan and H. Hoelman, "Method and device for reducing the resistance between two conductors," Patent WO 2015-183 081, 2015.

[98] M. Botha, "Electrical Machine Failures, Causes and Cures," in *Eighth International Conference on Electrical Machines and Drives*, vol. 1997, no. 444. IEE, 1997, pp. 114–117.

[99] G. Stone, I. Culbert, E. Boulter, and H. Dhirani, *Electrical Insulation for Rotating Machines: Design, Evaluation, Aging, Testing, and Repair*, 2nd ed. Wiley-IEEE Press, 2014.

[100] Weijun Yin, "Failure Mechanism of Winding Insulations in Inverter-fed Motors," *IEEE Electrical Insulation Magazine*, vol. 13, no. 6, pp. 18–23, Nov. 1997.

[101] M. Melfi, "Low-Voltage PWM Inverter-fed Motor Insulation Issues," *IEEE Transactions on Industry Applications*, vol. 42, no. 1, pp. 128–133, Jan. 2006.

[102] H. W. Oh and A. Willwerth, "Shaft Grounding — A Solution to Motor Bearing Currents," *ASHRAE Transactions*, vol. 114, 2008.

[103] R. Schiferl and M. Melfi, "Bearing Current Remediation Options," *IEEE Industry Applications Magazine*, vol. 10, no. 4, pp. 40–50, Jul. 2004.

[104] Fei Wang, "Motor Shaft Voltages and Bearing Currents and their Reduction in Multilevel Medium-voltage PWM Voltage-source-inverter Drive Applications," *IEEE Transactions on Industry Applications*, vol. 36, no. 5, pp. 1336–1341, 2000.

[105] M. BeBortoli, S. Salon, D. Burow, and C. Slavik, "Effects of Rotor Eccentricity and Parallel Windings on Induction Machine Behavior: a Study Using Finite Element Analysis," *IEEE Transactions on Magnetics*, vol. 29, no. 2, pp. 1676–1682, Mar. 1993.

[106] A. Di Gerlando, G. M. Foglia, and R. Perini, "Analytical Modelling of Unbalanced Magnetic Pull in Isotropic Electrical Machines," in *Proceedings of the 2008 International Conference on Electrical Machines, ICEM'08*, 2008.

[107] D. G. Dorrell, J. K. H. Shek, M. A. Mueller, and M. F. Hsieh, "Damper Windings in Induction Machines for Reduction of Unbalanced Magnetic Pull and Bearing Wear," *IEEE Transactions on Industry Applications*, vol. 49, no. 5, pp. 2206–2216, 2013.

[108] Y. Jiang, "Wind Turbine Cooling Technologies," in *Critical Infrastructure Security: Assessment, Prevention, Detection, Response*, Jun. 2010, vol. 54, pp. 613–640.

[109] R. Gray, L. Montgomery, R. Nelson, J. Pipkin, S. Joki-Korpel, and F. Caguiat, "Designing the Cooling Systems for the World's Most Powerful Turbogenerator - Olkiluoto Unit 3," in *IEEE Power Engineering Society General Meeting*. IEEE, 2006, p. 5 pp.

[110] R. Scott Semken, M. Polikarpova, P. Roytta, J. Alexandrova, J. Pyrhonen, J. Nerg, A. Mikkola, and J. Backman, "Direct-drive Permanent Magnet Generators for High-power Wind Turbines: Benefits and Limiting Factors," *IET Renewable Power Generation*, vol. 6, no. 1, p. 1, 2012.

[111] J. Pyrhönen, J. Nerg, H. Jussila, Y. Alexandrova, M. Polikarpova, R. S. Semken, and P. Röyttä, "Stator of an Electrical Machine and an Electrical Machine," Patent WO 2012-052 618, 2013.

[112] J. Shek, D. Dorrell, M. Hsieh, D. Macpherson, and M. Mueller, "Reducing Bearing Wear in Induction Generators for Wave and Tidal Current Energy Devices," in *IET Conference on Renewable Power Generation (RPG 2011)*, vol. 2011, no. 579 CP. IET, 2011, pp. P23–P23.

[113] U. Ungku Amirulddin, G. Asher, P. Sewell, and K. Bradley, "Dynamic Field Modelling of Torque and Radial Forces in Vector-controlled Induction Machines with Bearing Relief," *IEE Proceedings - Electric Power Applications*, vol. 152, no. 4, p. 894, 2005.

[114] M. Osama and T. A. Lipo, "A Magnetic Relief Scheme for Four Pole Induction Motors," in *International Conference on Electrical Machines, Converters and Systems*, 1999, pp. 115–121.

[115] T. Tera, Y. Yamauchi, A. Chiba, T. Fukao, and M. Rahman, "Performances of Bearingless and Sensorless Induction Motor Drive Based on Mutual Inductances and Rotor Displacements Estimation," *IEEE Transactions on Industrial Electronics*, vol. 53, no. 1, pp. 187–194, Feb. 2006.

[116] K. Raggl, B. Warberger, T. Nussbaumer, S. Burger, and J. Kolar, "Robust Angle-Sensorless Control of a PMSM Bearingless Pump," *IEEE Transactions on Industrial Electronics*, vol. 56, no. 6, pp. 2076–2085, Jun. 2009.

[117] S. A. Niknam, "Prognostic-based Life Extension Methodology with Application to Power Generation Systems," PhD diss., University of Tennessee, 2014.

[118] B. Mecrow, A. Jack, J. Haylock, and J. Coles, "Fault-tolerant Permanent Magnet Machine Drives," *IEE Proceedings - Electric Power Applications*, vol. 143, no. 6, p. 437, 1996.

[119] C. Noel, N. Takorabet, and F. Meibody-Tabar, "Short-circuit Current Reduction Technique for Surface Mounted PM Machines High Torque-low Speed Applications," in *Conference Record of the 2004 IEEE Industry Applications Conference, 2004. 39th IAS Annual Meeting.*, vol. 3. IEEE, 2004, pp. 1427–1433.

[120] B. Vaseghi, N. Takorabet, and F. Meibody-Tabar, "Short-circuit Current Reduction of PM Motors by Magnet Segmentation Technique," in *14th Biennial IEEE Conference on Electromagnetic Field Computation*. IEEE, 2010, pp. 1–1.

[121] F. Spinato, P. Tavner, G. van Bussel, and E. Koutoulakos, "Reliability of Wind Turbine Subassemblies," *IET Renewable Power Generation*, vol. 3, no. 4, pp. 387–401, 2009.

[122] E. Spooner, A. C. Williamson, and G. Catto, "Modular Design of Permanent-magnet Generators for Wind Turbines," *IEE Electrical Power Applications*, vol. 143, no. 5, pp. 388–395, 1996.

[123] T. M. Jahns, "Improved Reliability in Solid-State AC Drives by Means of Multiple Independent Phase Drive Units," *IEEE Transactions on Industry Applications*, vol. IA-16, no. 3, pp. 321–331, May 1980.

[124] D. Vizireanu, X. Kestelyn, S. Brisset, P. Brochet, Y. Milet, and D. Laloy, "Polyphased Modular Direct-drive Wind Turbine Generator," in *2005 European Conference on Power Electronics and Applications*. IEEE, 2005, p. 9.

CHAPTER 4

Converter Topologies for Improved Semiconductor Lifetimes

The power electronic converter, especially the power semiconductor, is a major contributor to the failure rates of the wind turbine drivetrain. As the temperature is a major driving factor behind the failure mechanisms of these power semiconductors the choice of topology and switching strategy can have a significant effect on the reliability of the converter. This chapter presents a detailed comparison of several three level converter topologies and switching strategies on the basis of loss distribution, thermal, and lifetime performance. This investigation is done through simulations on a 10MW direct drive permanent magnet drivetrain. The study shows that over-rating in the form of using overrated topologies, or the use of overrated components can result in large gains in lifetime expectancy and quantifies these gains. It concludes that the improvements offered by overrated topologies and overrated components are comparable and that use of the overrated topologies do not offer a significant advantage over the use of topologies with overrated components.

Based on:
U. Shipurkar, E. Lyrakis, K. Ma, H. Polinder and J. A. Ferreira, "Lifetime Comparison of Power Semiconductors in Three-Level Converters for 10MW Wind Turbine Systems," in *IEEE Journal of Emerging and Selected Topics in Power Electronics*, vol. 6, no. 3, pp. 1366–1377, Sept. 2018.
This chapter updates the results.

4.1 Introduction

It has been discussed in previous chapters that the major driving force behind the failure mechanisms of power semiconductors is temperature - i.e. mean junction temperature and the amplitude of junction temperature cycles. For this reason, the focus now is to develop power converter topologies with an extended reliability which would result in increased energy yields and reduced costs. The current practice is to do this by using over-rated components, however, another solution could be the use of over-rating in terms of topology - i.e., the designing of more complex topologies or control strategies that offer a more evenly distributed loading of the power converter or even topologies that can sustain faults and preserve their functioning ability.

The two level back to back voltage source converter has been the most popular converter topology in wind turbines [1,2]. However, with the increasing power rating of turbines leading to higher voltage ratings, the increased switching losses in a two level converter make this prohibitive. For this reason multi-level converter topologies, especially the Neutral Point Clamped topology, are becoming popular. Their operation is based on the composition of sinusoidal output using multiple levels of DC voltage [3]. By going up a level in a multilevel converter, the maximum voltage that each switch has to sustain is decreased. Additionally, the output power quality is improved as the levels of voltage increase and the need for filtering the output decreases. Consequently the total harmonic distortion (THD) tends to decrease [4]. However the cost of the converter is increased because of the additional power electronic components. Moreover, the PWM methods used by converters with higher levels become complicated.

This thesis investigates multilevel converter topologies to compare their reliability. Although the range of multilevel converters can in theory be extended to any $(2n+1)$-level topology, this chapter limits itself to a comparison of topologies from the three level family. The three level topologies are chosen as they are the next step-up from the two level converters and address their issues while not complicating design and control to a large extent. Further, a number of different topologies for multilevel converters can be found in literature [5–8], however, this analysis is limited to the Neutral Point Clamped (NPC), Active Neutral Point Clamped (ANPC), H- Bridge and T-type topologies as these are the most prominent ones. The approach followed in this work uses stress and strength modelling to map the loads that drive the failure mechanisms in the considered components [9]. The assessment is based on the power losses of each converter, the distribution of these losses through their components and the impact that they have on the thermal behaviour of the power electronic components. The study of the power loss and the thermal behaviour of the components offers useful conclusions about their lifetimes and their improvement.

Prior comparisons of converters focussed on aspects of efficiency and harmonic distortion as in [5], as well as a host of other parameters as in [10]. However, with the growth of interest in reliability, this has become an important comparison criteria for modern converter topologies and some studies have focussed on this aspect. Ma *et al.* compared 3L and 5L H-bridge topologies with the 3L-NPC topology in [11] and extended this study to a comparison of reliability for these

topologies in [12]. Also, Gierschner *et al.* have compared the lifetime estimation of Bi-Mode Insulated Gate Transistor (BIGT) based A-NPC and T-type converters in [13]. This thesis extends the available comparisons to include the most prominent three-level topologies and modulation techniques, thus leading to a comprehensive comparison with the aim to draw conclusions on the suitability of these topologies from the viewpoint of reliability. Further, these configurations are built into complete drivetrain models and evaluated on wind distribution over an annual cycle which gives a realistic comparison.

This chapter describes multilevel converter topologies in section 4.2 and details the converter topologies and switching strategies compared in this work. Further, in section 4.3 it details the system analysed and its modelling. Section 4.4 compares the performance of topologies and switching strategies. Finally, section 4.5 gives the conclusions drawn from this study.

4.2 Multilevel Power Electronic Converters

For this thesis the power-electronic converters that are investigated include topologies and switching regimes of 3-level converters as well as those of the classical 2-level converter. The basic 2-level VSC topology is used as a reference model; primarily because it represents the most simple and basic building block of power electronic converters. The topologies analysed in this study are listed below:

- Two Level Voltage Source Converter (2L-VSC)
- Three-level Neutral Point Clamped (3L-NPC)
- Three-level Active Neutral Point Clamped (3L-ANPC)
  - ▷ Double Frequency (3L-ANPC-DF)
  - ▷ Adjustable Loss Distribution (3L-ANPC-ALD)
- Three-level H-Bridge (3L-HB)
- Three-level T-Type (3L-T2C)

The 3-level NPC (3L-NPC) requires double the number of IGBTs as a 2-level converter and also has two additional diodes that clamp the neutral point as can be seen in Fig. 4.1. These two diodes provide the neutral or zero state. Even though the overall number of the power electronic components is higher, their voltage rating is half compared to that of the 2-level converter topology with the same DC-link voltage. The main drawback of this topology is the uneven loss distribution among its power components as can be seen in the figure.

The 3-level active neutral-point-clamped (3L-ANPC) topology is derived from the 3L-NPC with the aim of reducing or better distributing losses amongst the components. The fundamental difference between them is that the 3L-ANPC topology has two additional IGBT switches that clamp the neutral point. The two active switches that replace the diodes give the topology the capability of more than one way of neutral point clamping. With the use of the right switching strategies, the switching losses can be controlled by using the variety of different commutations

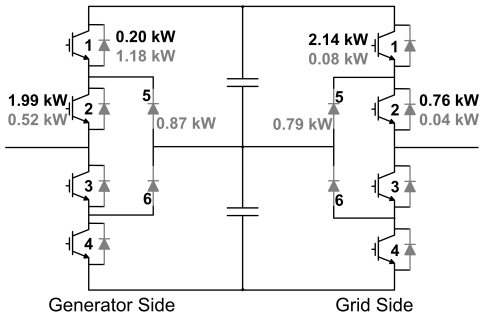

Figure 4.1 Neutral Point Clamped (3L-NPC) with losses at rated operation. The values in black represents the losses in the IGBT and the values in grey represent the losses in the Diode. These are calculated based on the equations in Section 4.3.

that are now available. This study analyses the system with two different switching strategies for the ANPC - Double Frequency (DF), and Adjustable Loss Distribution (ALD).

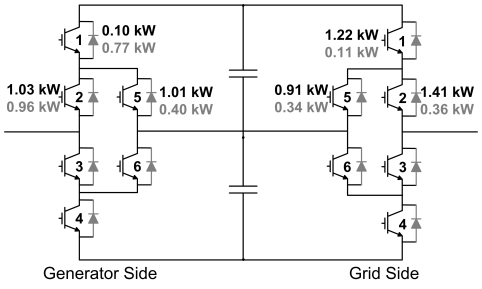

Figure 4.2 Active Neutral Point Clamped - Double Frequency (3L-ANPC-DF) with losses

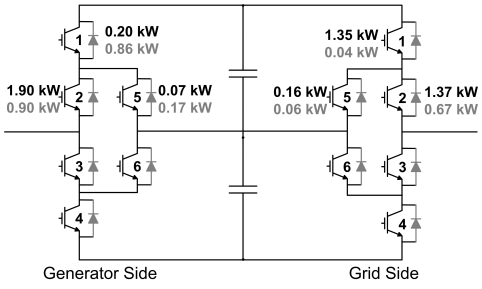

Figure 4.3 Active Neutral Point Clamped - Adjustable Loss Distribution (3L-ANPC-ALD) with losses

In the PWM-DF (Fig. 4.2) switching strategy for the 3L-ANPC converter [14, 15] the output phase voltage has an apparent switching frequency that is double the switching frequency, even though all switches do not switch more than once per switching period; this feature enables this switching strategy to produce the same output as any other ANPC PWM strategy with only half of the switching frequency, resulting in lower switching losses. The PWM-ALD (Fig. 4.3) strategy introduces a new way of distributing the switching losses and is explained in detail in [16]. During certain commutations where IGBT modules have to switch-on and off simultaneously, one switch can switch-on earlier and switch-off later than the other. As a result the switching losses load only one of the switches as the other turns-on and off with zero current. Each voltage period is featured by a stress-in/stress-out percentage which defines the proportionality of loading the inner or the outer IGBT modules with the switching losses during the extent of a voltage period. This way, the ALD-PWM strategy can achieve a more even distribution of overall losses among the power

electronic components as can be seen from Fig. 4.3.

Another topology is the 3-level H-bridge (3L-HB) that consists of two single-leg converters or it can be said that it is the combination of two half-bridge converters as seen in Fig. 4.4. It only needs half of the DC-link voltage to produce the same voltage output as any other 3-level converter. If each one of the two legs of the H-bridge are seen individually, the voltage output of each is the output of a 2L-VSC. Due to this, the DC-link voltage that is needed for the 3L-HB is half of that needed for the rest of topologies that have been mentioned. Instead of a reference or neutral point, the 3L-HB ends in an open winding.

The 3-level T-type (3L-T2C) converter is a topology that combines the structural and operational characteristics of the 2L-VSC and the 3L-NPC converters. Structurally, the 3L-T2C converter can be considered a development of the 2L-VSC with an extension of one bidirectional switch to clamp the neutral point of the DC-link as can be seen in Fig. 4.5. A unique feature of the T-type converter is that it uses switches of two different voltage ratings. Its outer switches block the full dc-link voltage. On the other hand, the middle switches are designed to have half the voltage rating of the two outer switches. Even though the outer switches block the DC-link voltage they only switch at half the DC-link voltage and therefore experience reduced switching losses. Table 4.1 summarises the prominent features of the topologies under consideration.

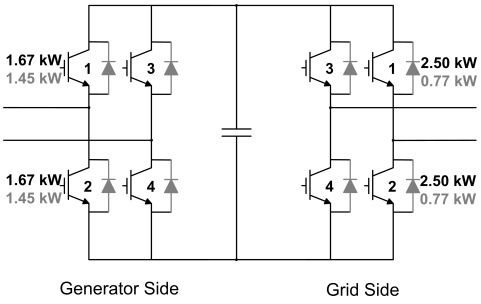

Figure 4.4 H-Bridge (3L-HB) with losses

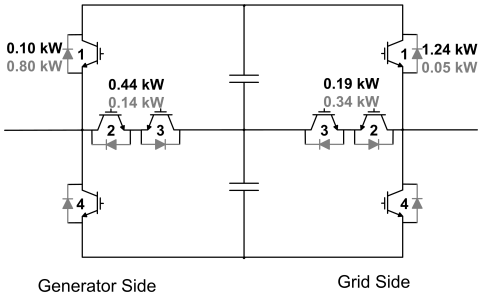

Figure 4.5 T-Type (3L-T2C) with losses

	2L-VSC	3L-NPC	3L-ANPC	3L-HB	3L-T2C
No. of Converters	8	4	4	4	8
Types of Switches	1	1	1	1	2
No. of IGBTs	12	24	36	24	24
No. of Diodes	12	36	36	24	24
DC-Link Voltage	$2kV$	$4kV$	$4kV$	$2kV$	$2kV$
Converter IGBT Rating*	$96 \cdot V_s I_s$	$96 \cdot V_s I_s$	$144 \cdot V_s I_s$	$96 \cdot V_s I_s$	$144 \cdot V_s I_s$
Converter Diode Rating*	$96 \cdot V_s I_s$	$144 \cdot V_s I_s$	$144 \cdot V_s I_s$	$96 \cdot V_s I_s$	$144 \cdot V_s I_s$

* V_s and I_s are the rated voltage and current of each switch which is common to all topologies.

Table 4.1 Summary of topologies

4.3 System Modelling

A detailed model of the wind turbine drivetrain is constructed to compare the lifetimes of power semiconductors in wind turbine converters. The schematic is shown in Fig. 4.6. The input is wind speed, this is fed to the mechanical model which generates the load torque signal. Based on the generator, control block, and converter models the required electrical signals are generated. These are used by the loss models to calculate the losses in the switches and diodes. This is converted to a temperature signal by the thermal model of the power semiconductors. Furthermore, a rainflow counter and lifetime models are used to calculate the consumed lifetimes.

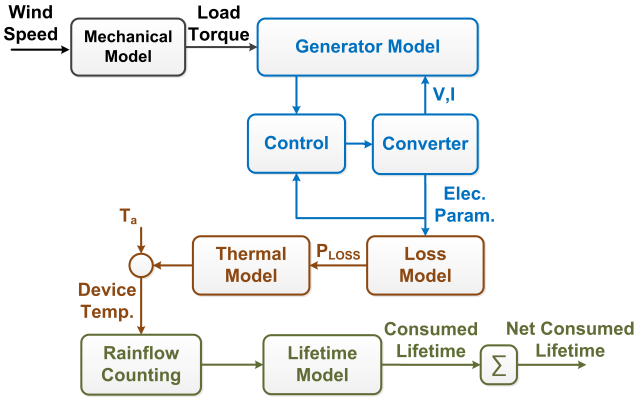

Figure 4.6 Schematic of system model.

The drivetrain under consideration is a 10MW direct drive permanent magnet generator with fully rated converters. The turbine is based on the design proposed by Polinder *et al.* [17]. For a fair comparison between topologies, the switch rating in each topology is identical. This results in the 2L-VSC and 3L-T2C topologies employing half the DC-link voltage and twice the number of converters compared to the rest. This also has consequences for the design of the generator and therefore, two different generator designs have been used in this study. Section 4.3.1 describes the used wind scenario and Section 4.3.2 describes the mechanical and generator model of the turbine. Similarly, Section 4.3.3 develops the converter design and modelling. Section 4.3.4 and Section 4.3.5 describe the loss and thermal models used in this study respectively. Finally, Section 4.3.6 describes the lifetime model.

4.3.1 Wind Model

Wind turbines are designed based on wind classes according to IEC61400-1. For the purpose of this comparison the wind class Ia has been selected as it poses the highest wind speeds and turbulence intensities. Further, the wind model is based on measured data of a KNMI (The

Royal Netherlands Meteorological Institute) offshore weather station (L9-FF-1) . The wind speed distribution used is shown in Fig. 4.7 and the main characteristics of the wind profile are described in Table 4.2.

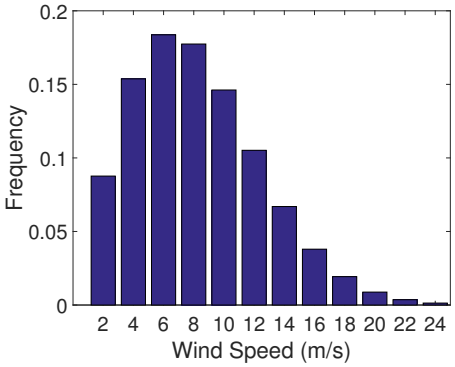

Figure 4.7 Distribution of mean wind speed

Wind Characteristics	
Mean Wind Speed (m/s)	8.2
Turbulence Intensity(%)	16
Weibull Parameters	
Shape Parameter	2.01
Scale Parameter (m/s)	9.30

Table 4.2 Turbine characteristics

4.3.2 Turbine and Generator Model

The mechanical model describes the wind turbine rotor and is modelled to convert a wind speed input to the appropriate shaft power and torque. The shaft power, neglecting mechanical losses, is described by

$$P_{shaft} = \frac{1}{2} \cdot \rho_{air} \cdot C_p(\lambda, \theta) \cdot A \cdot v_{wind}^3, \tag{4.1}$$

where ρ_{air} is the density of air, C_p is the power coefficient that is a function of tip speed ratio (λ) and pitch angle (θ), and A is the area of the turbine rotor. The characteristics of the wind turbine rotor are detailed in Table 4.3. The variation of the power coefficient, C_p with the tip speed ratio is plotted in Figure 4.8.

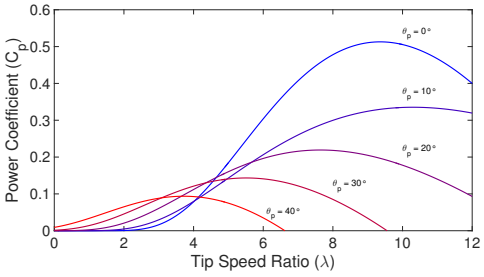

Figure 4.8 Power coefficient curve

10 MW Turbine Characteristics	
Rotor Diameter (m)	170
Hub Height (m)	100
Rated Wind Speed (m/s)	12
Rated Rotor Speed (rpm)	10
Optimum Tip Speed Ratio	9.5
Maximum Power Coefficient	0.515

Table 4.3 Turbine characteristics

The design of the generator is based on the design by *Polinder et al.* in [17]. As there are two levels of topologies that are compared, the design of the generator is adapted for use with both two and three level converters. The details of the generator are given in Table 4.4 and Table 4.5. Design I is the generator used with 3-level converters, while design II is used with the 2-level converter. The dynamic model of a permanent magnet synchronous generator has been covered extensively in literature [18, 19] and is not presented here.

10 MW Generator Geometry Characteristics	
Stator Diameter (m)	10
Stack Length (m/s)	1.6
Pole Pairs	160
Air-gap (mm)	10
Stator Slot Width (mm)	16.4
Stator Tooth Width (mm)	16.4
Stator Slot Height (mm)	80
Stator and Rotor Yoke Height (mm)	40
Magnet Height (mm)	20

Table 4.4 Generator characteristics - Geometry

10 MW Generator Electrical Characteristics		
	I	II
Generator Rating (MVA)	12	12
Rated Line Voltage (kV)	2.5	1.5
Rated Current (kA)	2.75	4.50
Stator Resistance (pu)	0.02	0.03
Stator Leakage Inductance (pu)	0.35	0.51
Stator Main Inductance (pu)	0.21	0.30
Rated Electrical Frequency (Hz)	26.67	

Table 4.5 Generator characteristics - Electrical

4.3.3 Converter Model

The main design parameters for this converter are summarised in Table 4.6, these are for a 10MW application. Design I is for the 3-level converters, while design II is for the 2-level converter.

DC-Link

The DC-link voltage is related to the ac voltage in the lines through

$$V_{DC} = x \cdot \frac{2\sqrt{2}}{\sqrt{3}} \cdot \frac{1}{m} \cdot V_{l-l}, \tag{4.2}$$

where m is the modulation ratio, and V_{l-l} is the rms line voltage of the ac side. For space vector modulation strategy the value of m is limited to 1.15. Further, to account for grid fluctuations the DC-link voltage is scaled with an overvoltage factor, x, which is 1.15 for medium voltage systems [20, 21]. This results in a 4kV DC-link voltage for a 2.5kV AC system (3L converter) and a 2kV DC-link voltage for a 1.5kV system (2L converter).

DC-Link Capacitance

The sizing of the DC-link capacitor is done based on the allowed voltage ripple [21] through

$$C = \frac{S}{4\pi f V_{DC} \Delta V_{DC}}, \tag{4.3}$$

where S is the apparent power of each converter, f is the nominal generator side frequency, V_{DC} is DC-link voltage, and ΔV_{DC} is the allowed voltage ripple which is taken as 2% of the DC-link voltage [21].

Grid Side Line Reactor

The line reactor is used for protection and filtering. As proposed in [21], the line reactor resistance and inductance are taken as 0.003pu and 0.15pu respectively. Converters also usually include filters as they can improve quality of the energy exchanged. This has not been considered in this study, however, details about sizing a filter can be found in [22].

Switch Ratings

The selection of switches are based on their blocking voltage and their rated currents. The switches are required to block the DC-link voltage. Further, a safety margin of 50% or 60% on this DC-link voltage is used for the selection of the voltage rating of the switches [20]. For the purpose of this study, Infineon switch - FZ1000R33HE3 is selected fro all topologies.

The rated current that needs to be processed by the three level converter is 2.75kA. To handle this current a set of parallel converters are used. Each topology uses four parallel converters. Similarly, the 2L-VSC and 3L-T2C topologies use eight parallel converters.

Heat Sink

As the switches used are high power modules, liquid cooled heat sinks are considered in this study. The heat sink used in the model is an exposed tube 6-pass cold plate (Wakefield-Vette #120460) with water as the coolant [23]. The details are given in Table 4.7. In the converters one heat sink module is used for four switches in the grid side and one switch per heat sink for the generator side.

Converter Characteristics		
	I	II
Parallel Converters	4	8
Switching Frequency (kHz)	2	
DC Link		
DC Link Voltage (kV)	4	2
DC Link Capacitance (mF)	97	160
Grid Side		
Line Voltage (kV)	2.5	1.5
Grid Frequency (Hz)	50	
Line Reactance (pu)	0.15	
Line Resistance (pu)	0.003	
Power Factor	0.9	
Generator Side		
Line Voltage (kV)	2.5	1.5
Rated Frequency (Hz)	26.67	

Table 4.6 Converter characteristics

Switch and Heat Sink Characteristics	
Switch Selection	
Converter Switch Rating (kV)	3.3
Converter Switch Rating (kA)	1
Switch Characteristics	
Switch Thermal Impedence (K/kW)	11.10
Switch Thermal Time Constants (s)	1.47
Diode Thermal Impedence (K/kW)	19.80
Diode Thermal Time Constants (s)	1.29
Heat Sink Details	
Fluid Flow Rate (l/min)	5
Fluid Inlet Temperature (°C)	40
Thermal Impedence (K/kW)	4.24
Thermal Time Constants (s)	21.2

Table 4.7 Switch and Heat Sink Characteristics

Control

The generator-side converter controller regulates the current through the stator of the generator controlling the rotational speed of the rotor speed so as to extract maximum power from the wind. The grid-side converter controls the power flow to the grid. Current in the d-axis maintains the dc-link voltage level controlling the amount of real power that is being fed to the grid and reactive power is regulated by the q-axis current. In this study the power factor of the grid side controller is maintained at 0.9.

The converters use the sinusoidally modulated PWM for controlling the modules. Although, a number of other modulation strategies are available, studies in [24, 25] show that the effect of these is not significant compared to the results in this study. Therefore, these different modulation strategies have not been considered.

4.3.4 Loss Model

The models that are described for the calculation of the losses are based on work by *Ma et al.* in [26, 27]. The conduction loss, averaged over a switching period, can be calculated by

$$P_{cond,IGBT} = u_{CE}(i) \cdot i \cdot d_{IGBT}, \tag{4.4}$$

$$P_{cond,Diode} = u_F(i) \cdot i \cdot d_{Diode}, \tag{4.5}$$

where u is the on-state voltage that is a function of the current and is estimated on the basis of datasheet curves, i is the current through the component, and d is the duty cycle. The conduction

loss, therefore, requires the knowledge of the duty cycle of the component and the current through it. This loss is further dependant on the junction temperature and a linear interpolation of losses is used to calculate the loss for the component. The switching loss can be calculated by

$$P_{sw,IGBT} = (E_{on,IGBT} + E_{off,IGBT}) \cdot f_{sw}, \tag{4.6}$$

$$P_{sw,Diode} = (E_{on,Diode} + E_{off,Diode}) \cdot f_{sw}, \tag{4.7}$$

where E_{on} and E_{off} are the switching energy for the components that are a function of the current through the component and the switched voltage and are estimated using datasheet curves, and f_s is the switching frequency of the component. The switching loss, therefore, requires the knowledge of the current, switched voltage, and the switching frequency of the component. Again, the loss is further dependant on the junction temperature and a linear interpolation is used to calculate the loss for the component.

The on-state voltage and switching energy are obtained from the datasheet. These are plotted in Fig. 4.9 and Fig. 4.10 for a junction temperature of $125°C$. These plots from the datasheet are used to extract the required data for the modelling. The resulting loss profile is shown in Fig. 4.11.

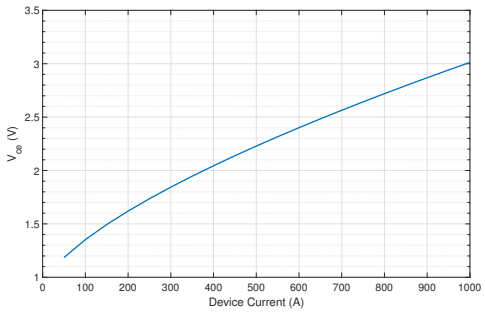

Figure 4.9 IGBT characteristics - V_{ce}

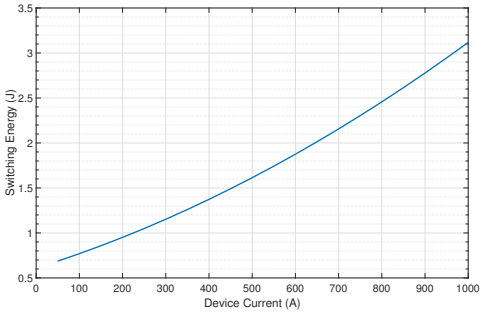

Figure 4.10 IGBT characteristics - E_{sw}

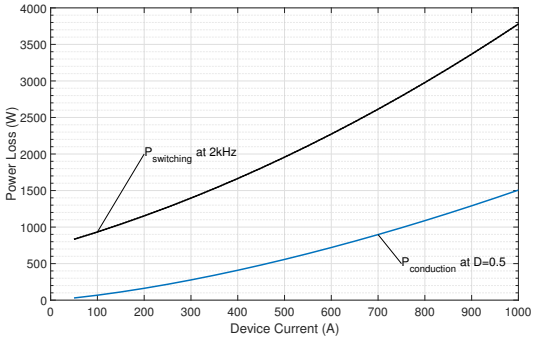

Figure 4.11 IGBT conduction and switching losses.

These results show that the switching losses are a major share of the losses in the case considered

here. Therefore, this is a good candidate for using topologies that level stresses on different switches though modulation.

4.3.5 Thermal Model

The thermal model used in this study is based on [26, 28]. This model combines Cauer and Foster thermal networks to address shortcomings of both models and is shown in Fig. 4.12. The single layer Cauer model of the switch is generated from the curve fitting of the four layer Foster model from the datasheet. The equivalent parameters are given in Table 4.7.

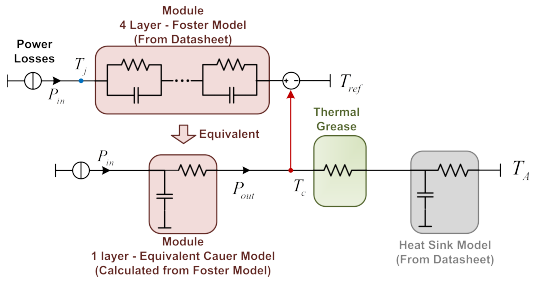

Figure 4.12 Thermal model of the power semiconductor. From [28].

4.3.6 Calculation of Lifetime

Lifetime Model

The lifetime model used in this study is based on the work by Bayerer *et al.* [29]. The number of cycles to failure is given by

$$N_f = A \cdot \Delta T_j^{\beta_1} \cdot e^{\frac{\beta_2}{T_j+273}} \cdot t_{on}^{\beta_3} \cdot I^{\beta_4} \cdot V^{\beta_5} \cdot D^{\beta_6}, \tag{4.8}$$

where A is a technology factor, ΔT_j is the amplitude of the thermal cycling, T_j is the mean junction temperature, t_{on} is the pulse duration, I is the current per wire, V is the blocking voltage of the chip, and D is the diameter of the bonding wire. The impact of these factors are represented by power laws with exponents $\beta_1 - \beta_6$. Here, the exponential factors used are, $\beta_1 = -4.416$, $\beta_2 = 1.285 \times 10^3$, $\beta_3 = -0.463$, $\beta_4 = -0.716$, $\beta_5 = -0.761$, and $\beta_6 = -0.5$. The value of A depends on the type of switch, $A = 2.03 \times 10^{14}$ for standard packages and $A = 9.34 \times 10^{14}$ for IGBT4 modules [30].

The experiments on which this lifetime model is based, use a minimum junction temperature cycling of approximately 40K. The extension of this model to cycling amplitudes much below

this value could introduce large error in the results. Therefore, this model has been extended based on work by Kovacevic-Badstuebner *et al.* [31]. The updated model has two asymptotic linear dependancies in a log-log plot. One is for large-amplitude cycling derived from the Bayerer model discussed above with $m = \beta_1 \approx 4$, and the other for low-amplitude cycling by extending the model with an asymptotic slope $m = 13$. This is shown in Fig. 4.13. The use of this updated lifetime model increases the accuracy of the lifetime prediction and, therefore, results in a more realistic comparison.

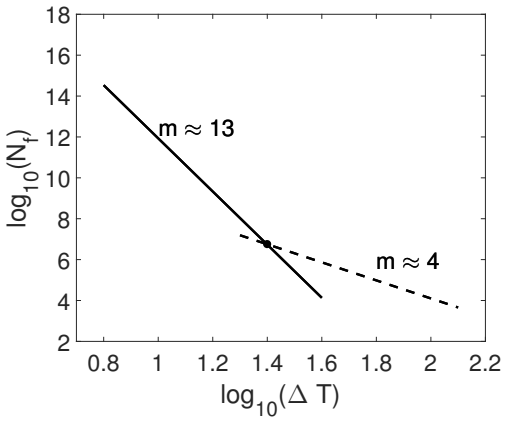

Figure 4.13 Lifetime Model. From [29, 31].

Calculation Procedure

The lifetime calculation in this study involves analysing the system for wind profiles with two different time scales (shown schematically in Fig. 4.14):

- **Long duration profile -** this uses the annual wind profile with wind speed averaged over 10 minute periods. As the 10 minute period is large enough for the wind turbine drivetrain to have reached an equilibrium, the steady state model is used to generate a temperature profile. This profile is used to calculate the damage (or lifetime) due to the long duration profile.
- **Short duration profile -** this uses stochastic 10 minute profiles. The profiles are generated such that each has a particular mean wind speed (the number of profiles depend on the number of bins in the selected weibull distribution). These profiles represent the wind speed variation within the 10 minutes over which the measured wind speed is averaged and recorded.

  The short duration profiles are used in conjunction with the dynamic model of the drivetrain to generate the temperature profile of the semiconductors. This temperature profile is

used to calculate the damage due to each 10 minute profile. This damage along with the frequency of occurrence of the respective 10 minute profile is used to calculate the net consumed lifetime for the short duration profiles. This contribution of the frequency of occurrence from the Weibull Distribution is represented by the connection to the Lifetime Model block in Fig. 4.14.

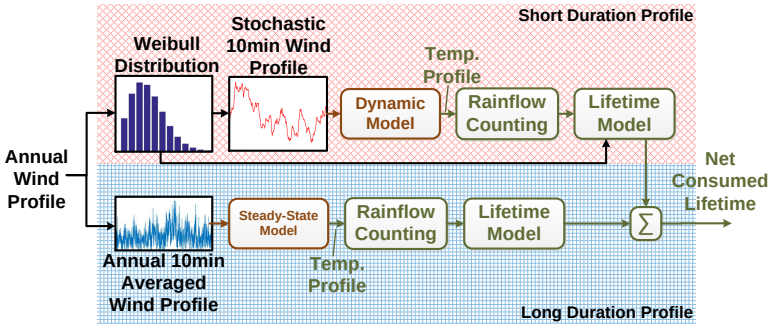

Figure 4.14 Lifetime Calculation Procedure

4.3.7 Limitations of the Study

There are a number of assumptions taken in this work that may give rise to inaccuracy in the results. However, the results presented in this chapter remain a good indication of the lifetime performance of the topologies considered, especially with regard to a comparative study.

- Thermal effect of IGBT on diode and vice versa - In the modules considered, the IGBT and the anti-parallel diode are part of the same package and share the baseplate. This would mean that the losses of the IGBT would influence the temperature of the diode junction and vice versa. However, the thermal model used has not considered this effect. This would lead to the introduction of error but as the model considers the effect of these two components on each other through the heat sink, this inaccuracy is minimised.

- Disturbances - The model used in this study neglects grid disturbances as well as the effect of wind gusts. Therefore, the results obtained do not consider these aspects as well.

- Reactive Power - In this study a constant power factor of 0.9 for the grid side converter is considered. Apart from increasing losses with the increase in reactive power required by the grid, varying reactive power is another source of power cycling and can therefore affect lifetimes. However, these effects have not been considered in this study.

4.4 Comparison of Topologies

The comparison of topologies presented in this chapter is based on three aspects – the distribution of losses, the thermal performance, and the lifetimes of the power semiconductors. As this chapter focusses on the power semiconductors, it does not consider the effects (or lifetimes) of the other components of the converter. Furthermore, as reliability can be linked to the reliability of the most stressed or weakest component, the focus of this study is the reliability of its most stressed power semiconductor component.

4.4.1 Loss Distribution

A topology that distributes the stresses more evenly amongst its power semiconductors would result in a higher lifetime of the weakest (or most stressed) power semiconductor, therefore, the loss distribution amongst the components is an important consideration. Fig. 4.15 and Fig. 4.16 show the distribution of losses amongst the power semiconductor components, in both the generator and grid side converters, for an operating point with an average wind speed equal to 12m/s. In these figures, the 3L-T2C losses are for a set of two parallel converters to keep the rating of the compared topologies equal. However, the 2L-VSC losses are for a single converter (therefore, half the rating of the rest) so that its results do not skew the scale of the figures.

Grid Side Converter

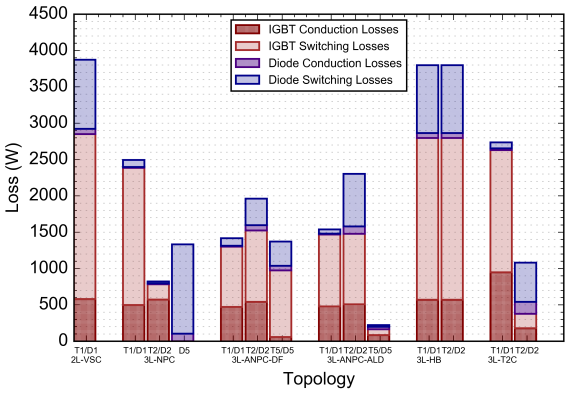

Figure 4.15 Loss distribution for the grid side converter with $v_{wind} = 12m/s$.

3L-NPC - For the 3L-NPC converter the outer switches (T1 and T4) experience the most losses. The inner IGBTs suffer the most conduction losses as they conduct during both positive and

neutral states. However the switching losses of the outer switches are significantly higher than those of the inner modules. This highlights the problem of inequality of loss distribution.

3L-ANPC-DF - In the DF strategy of the ANPC converter, the halving of switching frequency creates a better distribution of losses among the components. As a result of this switching technique the switching losses of the active switches increase but their losses remain lower than those of the other two types of switches. The resulting losses are more evenly distributed.

3L-ANPC-ALD - In the ALD strategy a 25-75 percentage of Stress-in-Stress-out has been chosen for the Grid-side converter. The choice of this factor depends on a number of factors, such as power factor, current, and voltage. This selection has been made so that the total losses of the most heavily loaded components (in this case the inner and outer IGBTs) are as balanced as possible. As a result the switches are observed to have the best distribution of losses among the tested topologies. The neutral-point-clamping modules switch with voltage frequency and thus are lightly stressed compared to the other types of switches.

3L-HB - For this converter, even though the losses are optimally distributed among the switches, the magnitude of losses are higher compared to other topologies. This is due to the larger conduction times as well as the continuous switching during both voltage cycles.

3L-T2C - Here, the components with the heaviest loading are the outer switches which also have a higher voltage rating. However, because these switches switch at only half the DC-link voltage, the losses are reduced when compared to the 2L-VSC.

Generator Side Converter

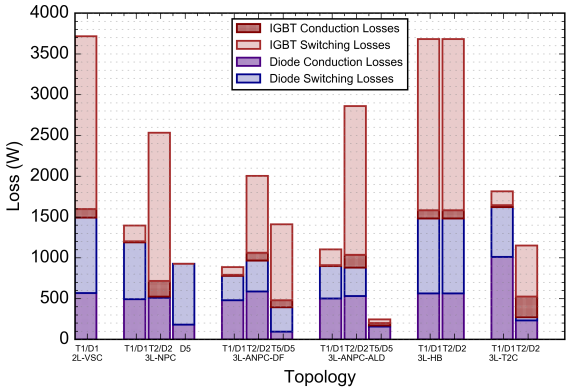

Figure 4.16 Loss distribution for the generator side converter with $v_{wind} = 12m/s$.

3L-NPC - For the 3L-NPC converter the largest part of losses are at the inner modules (T2/D2 module). However the conduction losses are now better distributed between the inner diodes and IGBTs.

3L-ANPC-DF - In the DF strategy of the ANPC generator-side converter, the smaller switching frequency has the same impact as in grid-side converter. Switching losses are also shared between the inner and outer modules. However, when it comes to the inner power module, the diode is taking most of the conduction losses. This makes the inner diode the most heavily loaded component of the converter.

3L-ANPC-ALD - In the ALD strategy of the generator-side converter a 33-67 percent Stress-in-Stress-out strategy has been chosen. This selection has again been made in an attempt to balance the losses between the most heavily loaded components. Therefore the total amount of the distributable switching losses loads the outer switches in order to relieve the inner module which displays the largest part of dissipated losses. Even though the inner module still experiences the largest losses, the distribution among the individual parts of each module is improved.

3L-H Bridge - Again, for the 3L-HB converter even though the losses are almost optimally distributed among the switches, the amount of losses is higher than in the other converters.

3L-T Type - In the 3L-T2C converter, although the inner switch has large losses, the poorer thermal properties of the outer diode couples with the large losses make this also heavily loaded.

4.4.2 Thermal Performance

The thermal response of the power semiconductors to the losses that they are subjected to is closely linked to their reliability. In particular, the junction temperature and the amplitude of temperature cycling affect the lifetime of the power semiconductor as seen in (4.8). For the comparison here, two quantities are being compared - the mean temperature for each converter over a 10 minute period and the range of temperature cycling amplitudes. Further, this comparison is presented for the most stressed power semiconductor of each topology. These quantities for the grid side converter are shown in Fig. 4.17 and Fig. 4.19, while those for the generator side converter are presented in Fig. 4.18 and Fig. 4.20.

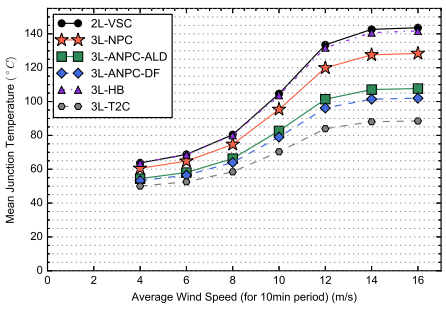

Figure 4.17 Mean temperatures - Grid Side Converter

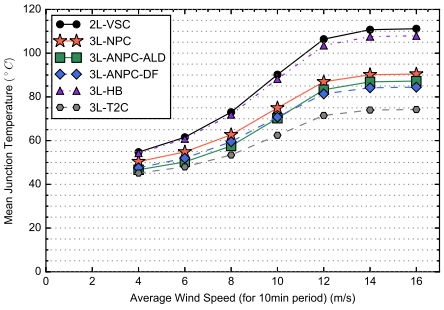

Figure 4.18 Mean temperatures - Generator Side Converter

The 2L-VSC develops high mean temperatures as well as high temperature cycle amplitudes both in the grid and the generator-side. In the 3L-ANPC topologies the improvement in the distribution of losses is reflected in the temperature profiles, resulting in a lower mean temperature as well as lower temperature cycling amplitudes. Even though the 3L-HB displays an excellent distribution of losses amongst its components, compared to other topologies the amount of losses increase the mean temperature and cycling amplitude. Finally, the 3L-T2C, also shows low mean temperatures and lower temperature cycling amplitudes.

In all cases the loading of the generator side converter is higher which is attributed to the lower frequency of the generator side which account for higher temperature cycling amplitude being attained as well as the poorer thermal characteristics of the diode which takes a bulk of the load in the generator side converters.

4.4.3 Lifetime

Following the analysis of the thermal performance of the examined converters, the temperature profiles generated for the different wind profiles are used as input to the lifetime model. The individual consumed lifetimes for each mean wind speed profile are multiplied by the frequency of occurrence (based on the weibull distribution of Figure 4.7) and added to give the total life consumption for a period of one year. In the lifetime model, the damage is assumed to be linear and the sequence at which the power and temperature cycles occur do not have any effect according to Palmgren-Miner's rule

$$LC = \sum_{i=1}^{k} \frac{n_i}{N_i}, \tag{4.9}$$

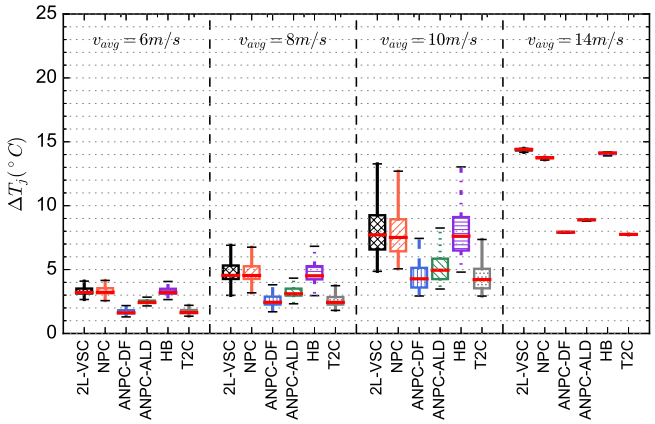

Figure 4.19 Distribution of temperature cycling amplitudes for the grid side converter.

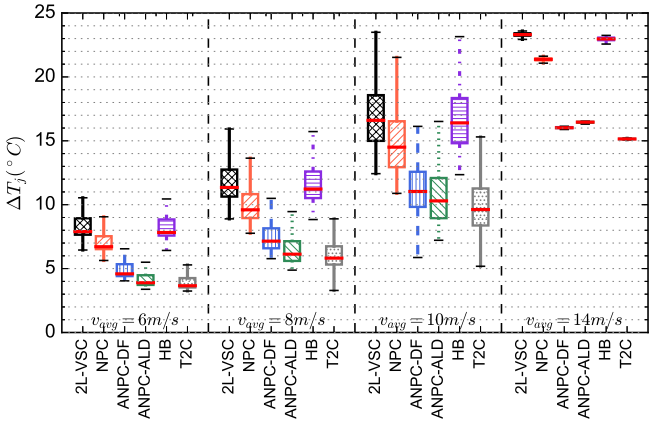

Figure 4.20 Distribution of temperature cycling amplitudes for the generator side converter.

where N_i is the lifetime for the i-th load, n_i is the number of cycles the component has been exposed to the i-th load profile, and k is the total number of load profiles. To this, the consumed lifetime based on the long duration profile (using the annual 10 minute averaged wind speed profile) is added. Failure occurs when the lifetime consumption LC equals one. Table 4.8 gives the lifetimes of the most stressed power semiconductors of each topology, both in terms of years as well as a factor in relation to the 3L-NPC topology. It also shows the annual semiconductor power loss.

It is important to state that although all the modelling-related choices and assumptions have been made so that the drivetrain model is a suitable design for a 10MW wind turbine, there are a number of limitations when calculating the absolute lifetime of the topologies in terms of years (see Section 4.3.7). As a result, the consumed lifetime values of each converter topology should not be considered in absolute terms, however, the fact that all the simulations and calculations are executed based on the same references offers a solid basis upon which a fruitful reliability comparison can be conducted.

It is noted that there is a consistency between the thermal response of the power semiconductors and their reliability. The switches or diodes that display high temperatures and large temperature cycles have been proved to have a smaller expected lifetime. The results show that the 3L-ANPC topology with the DF and ALD switching strategies, and the T2C topology show a large improvement over the 2L-VSC, 3L-HB, and the 3L-NPC. In both these cases the improvement in the grid side is larger than that of the generator side converter.

Topology Lifetimes (in years)					
	Grid Side Converter		Generator Side Converter		Annual Losses (GWh)
2L-VSC	**5.94**	$(\frac{X}{1.82})$	**0.83**	$(\frac{Y}{3.69})$	1.67
3L-NPC	**10.81**	(X)	**3.07**	(Y)	0.98
3L-ANPC-DF	**84.63**	$(7.83X)$	**57.01**	$(18.58Y)$	0.98
3L-ANPC-ALD	**54.21**	$(5.01X)$	**37.20**	$(12.13Y)$	0.98
3L-HB	**6.47**	$(\frac{X}{1.67})$	**0.90**	$(\frac{Y}{3.39})$	1.60
3L-T2C	**227.88**	$(21.08X)$	**129.75**	$(42.29Y)$	1.15

Table 4.8 Comparison of lifetimes of the most stressed power semiconductors. X and Y represent the lifetimes for the 3L-NPC converter.

4.4.4 Effect of Over-rating

The lifetime performance with the use of overrated topologies (3L-ANPC and the 3L-T2C) has been explored in the previous sections. This comparison was based on designs with the same total power rating. Another possibility is the use of overrated components, which is explored in this section. As the 3L-NPC is a popular converter topology for high power wind turbine generator systems, it is important to consider the effect of overrating this converter.

This comparison is done for a 1.25 and a 1.5 times overrated NPC topology (resulting in a 5 and 6 parallel converter system) with the 3L-ANPC-DF and 3L-T2C converter topologies (with 4 parallel converters). The 1.5 times rated NPC topology results in a net IGBT rating (VA) equal to that of the 3L-ANPC and 3L-T2C topologies but a 50% overrating of the diodes. The IGBT VA ratings is another benchmark for comparison and the 1.5x3L-NPC topology is equal to the 3L-ANPC and 3L-T2C topology in this aspect. Also, as the VA rating is an indicator of cost, this benchmark can be used as an indicator for power semiconductor cost. The resultant lifetimes for this comparison are given in Table 4.9.

Topology Lifetimes (in years)					
	Grid Side Converter		Generator Side Converter		Annual Losses (GWh)
3L-ANPC-DF	**84.63**	$(7.83X)$	**57.01**	$(18.58Y)$	0.98
3L-T2C	**227.88**	$(21.09X)$	**129.75**	$(42.29Y)$	1.15
1.25 x 3L-NPC	**57.36**	$(5.30X)$	**51.52**	$(16.79Y)$	1.05
1.50 x 3L-NPC	**197.96**	$(18.32X)$	**355.97**	$(116.03Y)$	1.10

Table 4.9 Comparison of lifetimes of the most stressed power semiconductors. X and Y represent the lifetimes for the rated 3L-NPC converter.

These results also show that over-rating the components of the 3L-NPC leads to a large improvement in lifetime performance. The use of the 1.25x3L-NPC results in a grid and generator side lifetime that is about 5 and 16 times that of the rated 3L-NPC, and this increases to 18 and 116 times when a 1.5x3L-NPC is considered. The calculated lifetimes for the 1.5 times overrated 3L-NPC topology has the highest lifetimes, except for the grid side of the T2C topology. However, the loss performance of the 3L-ANPC remains better than that of the overrated NPC topologies. The reduced losses in the power semiconductors would result in an approx. 0.2% increase in the annual energy production.

4.5 Conclusions

This chapter has compared the lifetime performance of the power seimconductors in a number of three-level topologies for use in the wind turbine drivetrain. This comparison has been done on the basis of loss distribution, thermal performance, and a final lifetime number.

It has been found that in a comparison of different three-level topologies, the 3L-ANPC and the 3L-T2C show the highest lifetimes. When a component over-rating is considered, the 3L-NPC topology shows a large improvement and the lifetime performance is comparable to that of the overrated topologies. However, the loss performance of the 3L-ANPC remains marginally better than the other cases considered in this study.

In conclusion, the use of over-rating - be it in the form of overrated topologies (like the ANPC and the T2C), or the use of overrated components - is successful in improving the lifetime performance of power semiconductors in converters. However, the improvement offered by overrated topologies over the use of overrated components is not significant and it is unlikely to replace the current practice of using overrated components.

Bibliography

[1] M. Liserre, R. Cardenas, M. Molinas, and J. Rodriguez, "Overview of multi-MW wind turbines and wind parks," *IEEE Transactions on Industrial Electronics*, vol. 58, no. 4, pp. 1081–1095, 2011.

[2] F. Blaabjerg, M. Liserre, and K. Ma, "Power electronics converters for wind turbine systems," in *IEEE Transactions on Industry Applications*, vol. 48, no. 2, 2012, pp. 708–719.

[3] J. S. Lai and F. Z. Peng, "Multilevel converters - A new breed of power converters," *IEEE Transactions on Industry Applications*, vol. 32, no. 3, pp. 509–517, 1996.

[4] R. Melicio, V. M. F. Mendes, and J. P. S. Catalao, "Power converter topologies for wind energy conversion systems: Integrated modeling, control strategy and performance simulation," *Renewable Energy*, vol. 35, no. 10, pp. 2165–2174, 2010.

[5] O. S. Senturk, L. Helle, S. Munk-Nielsen, P. Rodriguez, and R. Teodorescu, "Medium voltage three-level converters for the grid connection of a multi-MW wind turbine," in *Power Electronics and Applications, 2009. EPE'09. 13th European Conference on*. IEEE, 2009, pp. 1–8.

[6] S. Kouro, M. Malinowski, K. Gopakumar, J. Pou, L. Franquelo, B. Wu, J. Rodriguez, M. A. Perez, and J. I. Leon, "Recent advances and industrial applications of multilevel converters," *IEEE Transactions on Industrial Electronics*, vol. 57, no. 8, pp. 2553–2580, 2010.

[7] T. M. Iversen, S. S. Gjerde, and T. Undeland, "Multilevel converters for a 10 MW, 100 kV transformer-less offshore wind generator system," in *Power Electronics and Applications (EPE), 2013 15th European Conference on*. IEEE, 2013, pp. 1–10.

[8] K. Ma, "Promising topologies and power devices for wind power converter," in *Power Electronics for the Next Generation Wind Turbine System*. Springer, 2015, pp. 19–29.

[9] K. Ma, D. Zhou, and F. Blaabjerg, "Evaluation and design tools for the reliability of wind power converter system," *Journal of Power Electronics*, vol. 15, no. 5, pp. 1149–1157, 2015.

[10] M. Schweizer, T. Friedli, and J. W. Kolar, "Comparative evaluation of advanced three-phase three-level inverter/converter topologies against two-level systems," *IEEE Transactions on Industrial Electronics*, vol. 60, no. 12, pp. 5515–5527, 2013.

[11] K. Ma, F. Blaabjerg, and D. Xu, "Power devices loading in multilevel converters for 10 mw wind turbines," in *Industrial Electronics (ISIE), 2011 IEEE International Symposium on*. IEEE, 2011, pp. 340–346.

[12] K. Ma and F. Blaabjerg, "Multilevel converters for 10 MW wind turbines," in *Power Electronics and Applications (EPE 2011), Proceedings of the 2011-14th European Conference on*, 2011, pp. 1–10.

[13] S. Gierschner and H. Eckel, "Lifetime Estimation of the BIGT in ANPC Converter and T-Type Converter for Wind Energy Application," in *IET International Conference on Power Electronics, Machines and Drives (PEMD)*, 2016, pp. 1–6.

[14] D. Floricau, E. Floricau, and M. Dumitrescu, "Natural doubling of the apparent switching frequency using three-level anpc converter," in *Nonsinusoidal Currents and Compensation, 2008. ISNCC 2008. International School on*. IEEE, 2008, pp. 1–6.

[15] X. Jing, J. He, and N. A. Demerdash, "Application and losses analysis of anpc converters in doubly-fed induction generator wind energy conversion system," in *Electric Machines & Drives Conference (IEMDC), 2013 IEEE International*. IEEE, 2013, pp. 131–138.

[16] L. Ma, T. Kerekes, P. Rodriguez, X. Jin, R. Teodorescu, and M. Liserre, "A new PWM strategy for grid-connected half-bridge active NPC converters with losses distribution balancing mechanism," *IEEE Transactions on Power Electronics*, vol. 30, no. 9, pp. 5331–5340, 2015.

[17] H. Polinder, D. Bang, R. P. J. O. M. van Rooij, A. S. McDonald, and M. A. Mueller, "10 MW wind turbine direct-drive generator design with pitch or active speed stall control," in *Electric Machines & Drives Conference, 2007. IEMDC'07. IEEE International*, vol. 2, 2007, pp. 1390–1395.

[18] O. Anaya-Lara, N. Jenkins, J. Ekanayake, P. Cartwright, and M. Hughes, *Wind Energy Generation: Modelling and Control*. Wiley, 2009.

[19] P. C. Krause, O. Wasynczuk, S. D. Sudhoff, and S. Pekarek, *Analysis of Electric Machinery and Drive Systems*. Wiley-IEEE Press, 2013.

[20] B. Backlund, M. Rahimo, S. Klaka, and J. Siefken, "Topologies, voltage ratings and state of the art high power semiconductor devices for medium voltage wind energy conversion," in *Power Electronics and Machines in Wind Applications. PEMWA 2009. IEEE*. IEEE, 2009, pp. 1–6.

[21] L. Quéval and H. Ohsaki, "Back-to-back converter design and control for synchronous generator-based wind turbines," in *Renewable Energy Research and Applications (ICRERA), 2012 International Conference on*. IEEE, 2012, pp. 1–6.

[22] E. J. Bueno, S. Cóbreces, F. J. Rodríguez, A. Hernádez, and F. Espinosa, "Design of a back-to-back NPC converter interface for wind turbines with squirrel-cage induction generator," *IEEE Transactions on Energy Conversion*, vol. 23, no. 3, pp. 932–945, 2008.

[23] Wakefield-Vette. Exposed tube liquid cold plates. [Online]. Available: http://www.wakefield-vette.com/products/liquid-cooling/liquid-cold-plates/standard-liquid-cold-plates.aspx

[24] C. A. Santos and F. L. M. Antunes, "Losses Comparison Among Carrier-Based PWM Modulation Strategies in Three- Level Neutral-Point-Clamped Inverter Key words The Three-level NPC Inverter," in *International Conference on Renewable Energies and Power Quality*, vol. 1, no. 9, 2011, pp. 1035–1040.

[25] M. Morisse, A. Bartschat, J. Wenske, and A. Mertens, "Converter lifetime assessment for doubly-fed induction generators considering derating control strategies at low rotor frequencies," *Journal of Physice: Conference Series*, vol. 753, p. 10, 2016.

[26] K. Ma, Y. Yang, and F. Blaabjerg, "Transient modelling of loss and thermal dynamics in power semiconductor devices," in *Energy Conversion Congress and Exposition (ECCE), 2014 IEEE*. IEEE, 2014, pp. 5495–5501.

[27] K. Ma, M. Liserre, F. Blaabjerg, and T. Kerekes, "Thermal loading and lifetime estimation for power device considering mission profiles in wind power converter," *IEEE Transactions on Power Electronics*, vol. 30, no. 2, pp. 590–602, 2014.

[28] K. Ma, "Electro-thermal model of power semiconductors dedicated for both case and junction temperature estimation," in *Power Electronics for the Next Generation Wind Turbine System*. Springer, 2015, pp. 139–143.

[29] R. Bayerer, T. Herrmann, T. Licht, J. Lutz, and M. Feller, "Model for power cycling lifetime of IGBT modules-various factors influencing lifetime," in *Integrated Power Systems (CIPS), 2008 5th International Conference on*. VDE, 2008, pp. 1–6.

[30] A. Wintrich, U. Nicolai, W. Tursky, and T. Reimann, "Application Manual Power Semiconductors," Semikron International GmbH, Tech. Rep., 2015.

[31] I. Kovacevic-Badstuebner, J. Kolar, and U. Schilling, "Modelling for the Lifetime prediction of power semiconductor modules," in *Reliability of Power Electronic Converter Systems*, 2015, pp. 103–140.

CHAPTER 5

Adaptive Cooling in Wind Turbine Converters

Active control techniques can be used to reduce stresses on the power semiconductors in a wind turbine converter. Considering that the major failure mechanisms are related to temperature and temperature cycling, active control can be used to enhance lifetime in these power semiconductors. This chapter investigates adaptive cooling as one such active control technique. It proposes a simple control structure based on the junction temperature of the power semiconductor to adapt the cooling system that results in reduced temperature cycling. The chapter analyses and compares control strategies, and quantifies the performance of the system in a case study turbine. Finally, it demonstrates the adaptive cooling technique using an experimental setup.

Based on:
U. Shipurkar, F. Wani, Z. Qin, J. Dong, H. Polinder and J. A. Ferreira, "Adaptive Cooling for Improved Power Semiconductor Lifetime in Wind Turbine Converters," submitted to *IEEE Journal of Emerging and Selected Topics in Power Electronics*, 2018.

5.1 Introduction

A number of studies have been carried out on failure rates of wind turbine components, however, there is little data in the public sphere about failures at a sub-component level. Lyding *et al.* have studied failure rates of power electronic converters at a sub-component level with data from the WMEP Database [1], and found that about half of all the faults in the power electronic converters are due to faults in semiconductors. An industry based survey by Yang *et al.* [2] gave similar results, with maximum respondents selecting semiconductor power devices as the most fragile component in converters.

Junction Temperature (T_j) and Junction Temperature Cycling (ΔT_j) are two dominant driving factors of failure mechanisms in power semiconductors [3–5]. The LESIT study conducted extensive tests to verify the correlation between the possible number of power cycles (N_f), the temperature cycling amplitude (ΔT_j) and the mean junction temperature ($T_{j,m}$) [6, 7]. This is represented by Fig. 5.1.

Previous studies have shown that active control concepts [8] such as power sharing [9], manipulation of switching frequency [10–15], reactive current circulation [16], DC-link regulation [17], advanced modulation schemes [18], and active gate control [19] can successfully increase the lifetimes of power semiconductors in converters. Another possibility is the use of controlled adaptive cooling to reduce the amplitude of temperature cycles. De Rijck *et al.* propose an invention that uses an actively cooled heat sink and controller to adjust the cooling efficiency of the heat sink depending on the temperature of the semiconductor [20] and Anderl *et al.* proposed a real time adaptive fluid flow cooling system for electronic systems [21]. Davidson *et al.* studied aspects of active cooling regulation by the control of air speed in forced air cooling [22, 23], and Wang *et al.* proposed a full-order observer based temperature control cooling strategy for power electronics cooling [24]. Similarly, Lewis *et al.* proposed an invention that enhances reliability with the use of

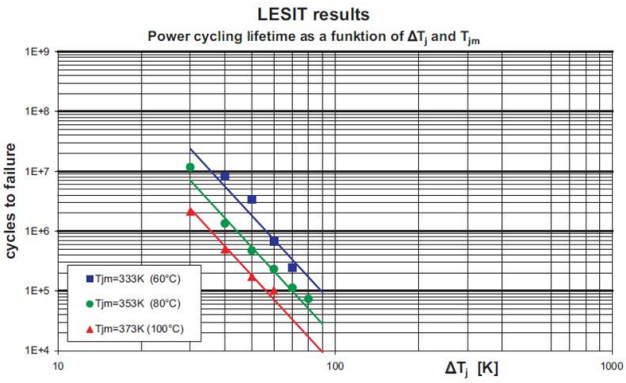

Figure 5.1 Number of cycles to failure (N_f) as function of ΔT_j with T_{jm} as parameter. From [7].

a thermal electric cooling (TEC) device attached between the chip and the heat sink [25].

However, a detailed analysis of controlled adaptive cooling for wind turbine converters is missing in literature. Therefore, the objective of this chapter is to analyse controlled adaptive cooling for wind turbine converters with the aim of improving lifetime of power semiconductors. Also, existing studies analyse systems where the control is based on a pre-determined reference temperature, which is not valid for the case of wind turbines where the variations in load lead to large variations in temperature.

The first contribution of this chapter is the investigation of the adaptive cooling method for liquid cooled wind turbine power converters with experimental validation. The second contribution is the quantification of the lifetime improvement of power semiconductors using the proposed method in a 10 MW case study turbine. The chapter is divided into four main parts. Section 5.2 details the adaptive cooling system, discusses the control structures analysed in the study, and comments on the measurement of temperature (which is the feedback signal for the control in the system). Section 5.3 starts with the description of the models used in the study followed by simulation results. Section 5.4 demonstrates the validity of the concept using a scaled-down laboratory setup. Section 5.5 uses a case study 10MW turbine to quantify the effect of adaptive cooling on the lifetime of the power semiconductors. Finally, conclusions of the study are given in section 5.6.

5.2 Adaptive Cooling System

The cycles to failure of the power semiconductor is described by the equation

$$N_f = A\Delta T_j^{-\alpha} e^{\frac{E_a}{k_b T_{j,m}}}, \tag{5.1}$$

and shows that lifetime depends on both the mean junction temperature and the amplitude of temperature cycles [6, 7]. Here, A and α are curve fitting constants, E_a is the activation energy, and k_b is the Boltzmann constant. While the lifetime of power semiconductors depends on a number of parameters such as humidity, vibration etc., this chapter focusses only on temperature driven failure mechanisms. Also, more detailed lifetime models have been developed since the LESIT study (for example the model used in this chapter to calculate the lifetime of the power semiconductors in the case study is based on [26]), however, this section uses the simplicity of Eq. 5.1 to explain the adaptive cooling concept.

Eq. 5.1 shows that lifetime depends on two parameters – $T_{j,m}$ and ΔT_j. The effect of these parameters on the lifetime (or the number of cycles to failure) can be compared through the sensitivity of N_f to ΔT_j and $T_{j,m}$, given by $\frac{\partial N_f}{\partial \Delta T_j}$ and $\frac{\partial N_f}{\partial T_{j,m}}$ in equations:

$$\frac{\partial N_f}{\partial \Delta T_j} = A(-\alpha \Delta T_j^{-\alpha-1}) e^{\frac{E_a}{k_b T_{j,m}}} = -\frac{\alpha}{\Delta T_j} N_f, \text{and}$$
$$\frac{\partial N_f}{\partial T_{j,m}} = A \Delta T_j^{\alpha} e^{\frac{E_a}{k_b T_{j,m}}} \frac{E_a}{k_b T_{j,m}^2} = -\frac{E_a}{k_b T_{j,m}^2} N_f. \tag{5.2}$$

The impact of these two parameters ($T_{j,m}$ and ΔT_j) can be compared using the ratios of sensitivities

$$\frac{\partial N_f / \partial \Delta T_j}{\partial N_f / \partial T_{j,m}} = \frac{\alpha k_b}{E_a} \frac{T_{j,m}^2}{\Delta T_j}. \tag{5.3}$$

This is greater than 1 when $T_{j,m}^2 > 1.4 \times 10^3 \cdot \Delta T_j$, which is valid over the operating range except when large cycling occurs at low mean temperatures. Therefore, temperature cycling has a greater effect on the lifetime of the power semiconductor although this difference reduces as both parameters increase to the outer limits. Control of the amplitude of temperature cycling is therefore a more efficient way of improving reliability in power semiconductors.

The adaptive cooling system aims to increase lifetime of power semiconductors by reducing the cycling amplitude. It comprises of an actively cooled heat sink with control that dynamically adapts the coolant flow rate of the heat sink. When the temperature of the semiconductor decreases, the controller reduces coolant flow leading to a lower heat transfer. This results in a lower amplitude of thermal cycling when compared to the case with constant flow rate. Such a system can take many forms, but this chapter limits the study to systems that use liquid cooling.

An adaptive cooling system schematic is shown in Fig. 5.2. This is similar to the system proposed in [20]. The junction temperature is measured and fed as input to the controller, based on this the control signal to the pump is regulated resulting in a reduced temperature cycling.

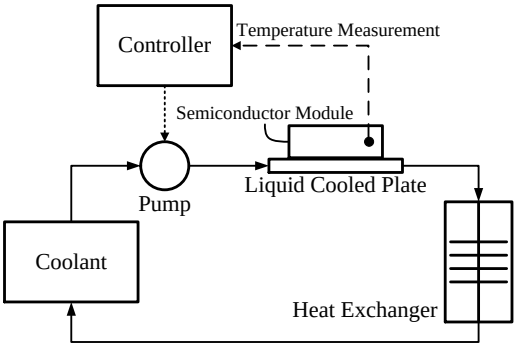

Figure 5.2 Schematic of the adaptive cooling system to reduce the thermal cycling amplitudes in power semiconductors.

5.2.1 Adaptive Cooling Concept

The proposed adaptive cooling system reduces thermal cycling by adapting the cooling efficiency via the coolant flow rate in the liquid cooled plate.

The heat transfer coefficient (h) for fluid flow in tubes is given by

$$h = \frac{Nu \cdot k}{D_t}, \tag{5.4}$$

where Nu is the Nusselt number, k is the thermal conductivity of the coolant, and D_t is the inner diameter of the tube. Further, the Nusselt number can be estimated using the Gnielinski formulation for turbulent flow in smooth surface tubes[27, 28], given by

$$Nu = \frac{\frac{\xi}{8} \cdot (Re - 1000) \cdot Pr}{1 + 12.7\sqrt{\frac{\xi}{8}}(Pr^{\frac{2}{3}} - 1)}, \tag{5.5}$$

where ξ is the friction factor for smooth tubes, Re is the Reynolds number and Pr is the Prandtl number. This is valid for $3000 \leq Re \leq 10^6$, and $0.5 \leq Pr \leq 200$.

From these equations, it is clear that the heat transfer coefficient of a fluid in a tube is directly related to the Reynolds number, and hence the velocity or flow rate of the coolant through

$$h \propto Re^x \propto Q^x, \tag{5.6}$$

where Q is the flow rate of the coolant, and $x > 0$.

Fig. 5.3 shows an illustrative example of adaptive cooling. It considers the case of a square power profile with semiconductor losses being maximum for the period T_{on} and minimum for the period T_{off}. At point 1, when the junction temperature is maximum, the period T_{off} starts and results in a reduction in temperature. As the temperature drops below $T^{control}$ at point 2, the flow rate (Q) is reduced. This reduces the heat transfer rate of the thermal system and results in a temperature trajectory as shown by the dashed line. At point 3, the power loss increases to its maximum value and temperature rises. When $T_j > T^{control}$ at point 4, the flow rate increases to the maximum value again.

Therefore, adaptive cooling uses the reduction of flow rate as a way to reduce heat transfer during periods of low junction temperature. This results in higher junction temperatures during these periods leading to a lower value of the cycling amplitude (ΔT_j). As the lifetime of power semiconductors is strongly dependant on this cycling amplitude, this results in an increased lifetime.

5.2.2 Control Structure

The aim of the system is to minimise cycling amplitude therefore, the controller reduces flow rate when junction temperature reduces and increases flow rate when junction temperature increases. This can be achieved using a controller shown in Fig. 5.4.

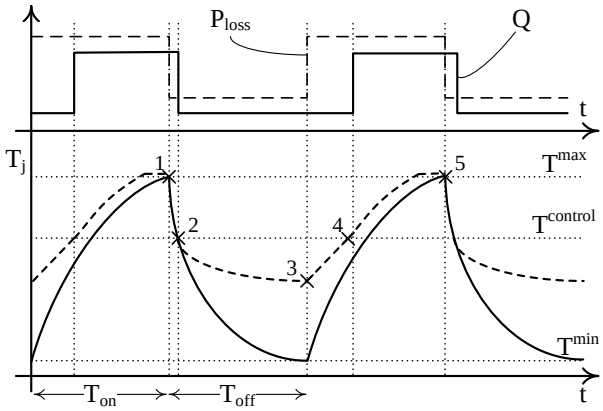

Figure 5.3 Illustrative example of adaptive cooling. In the bottom figure, the bold line depicts the variation of junction temperature with constant coolant flow rate, while the dotted line represents the expected junction temperature when the flow rate is varied, leading to a reduced junction temperature cycle.

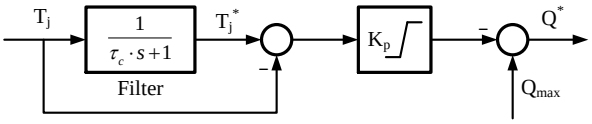

Figure 5.4 Schematic of the adaptive cooling controller.

Compared to the previous adaptive cooling controllers [22, 24] the control is not based on a pre-determined reference temperature, but measured signals. The filtered junction temperature is the reference signal and its difference with the actual value is the temperature difference that the adaptive cooling aims to reduce. A simple gain block is used to calculate the deviation from the set maximum flow rate and used to calculate the reference flow rate. A limiter is used to ensure the flow rate remains between zero and the maximum allowed flow. Finally, the reference and the measured flow rates are used by the pump controller to generate the required voltage (or duty cycle) for pump control. There are two parameters that affect the performance of the system – the gain (K_p) and the filter cut-off frequency ($\omega_c = \frac{1}{\tau_c}$). The tuning of these parameters for this study is explained in Section 6.6.

While there are two sources of temperature cycles in the power semiconductor:

- The variation of wind speed resulting in varying power being processed by the converter,
- and the power cycling due to AC current,

the adaptive cooling system is unable to respond to the higher frequencies of power cycling due

to the dynamic response of the mechanical components (e.g., pump). Therefore, this is filtered out of the temperature measurement for use in the adaptive cooling system.

5.2.3 Temperature Measurement

The estimation or measurement of the junction temperature is an important consideration as the control is based on this temperature. This may be done in the following ways:

- measurement using optical methods,
- measurement using physical contact methods,
- estimation using thermo-sensitive electrical parameters of the semiconductor device,
- and estimation using device models.

Optical methods use the temperature dependant optical properties of the devices. A number of indicators can be used including, luminescence, the Raman effect, refraction index, reflectance, and variation of infra-red radiation. However, these methods require a modification in the power module and the package and dielectric gel need to be removed. A review of these optical measurement methods can be found in [29, 30].

Junction temperature measurement is also possible using contact methods. This includes the use of thermal probes, liquid crystals and thermographic phosphors, and microprobes [29, 30]. One solution is the use of fiber-optic temperature sensors in direct contact with the chip [31].

All these methods require visible or mechanical access to the chip which is difficult in a commercial converter, therefore, to overcome this limitation, thermo-sensitive electrical parameters (TSEP) are used. There are a number of different parameters that can be used: collector-emitter voltage (V_{ce}), switching times, and threshold voltage [30, 32, 33]. This study uses the online V_{ce} measurement method proposed in [34], to estimate junction temperature for the controller in the experimental setup. This study also utilises a fiber-optic temperature sensor to calibrate the TSEP as well as validate the results of the proposed solution.

Finally, temperature can also be estimated using loss and thermal models. There are a number of examples where such systems have been used [23, 35, 36].

5.3 Simulation Results

5.3.1 Simulation System Description

The simulations are performed on a wind turbine drivetrain model for a 10 MW direct permanent magnet generator with a fully rated converter. The converter uses the 3-level Neutral Point Clamped (3L-NPC) topology. Further, design and modelling details are summarised below and can be found in [37] and Chapter 4.

10 MW Turbine Characteristics	
Rotor Diameter (m)	170
Hub Height (m)	100
Rated Wind Speed (m/s)	12
Rated Rotor Speed (rpm)	10
Optimum Tip Speed Ratio	9.5
Maximum Power Coefficient	0.515

Table 5.1 Turbine characteristics

10 MW Generator Electrical Characteristics	
Generator Rating (MVA)	12
Rated Line Voltage (kV)	2.5
Rated Current (kA)	2.75
Stator Resistance (pu)	0.02
Stator Leakage Inductance (pu)	0.35
Stator Main Inductance (pu)	0.21
Rated Electrical Frequency (Hz)	26.67

Table 5.2 Generator characteristics - Electrical

Converter Characteristics	
Parallel Converters	4
Switching Frequency (kHz)	2
DC Link	
DC Link Voltage (kV)	4
DC Link Capacitance (mF)	97
Grid Side	
Line Voltage (kV)	2.5
Grid Frequency (Hz)	50
Line Reactance (pu)	0.15
Line Resistance (pu)	0.003
Power Factor	0.9
Generator Side	
Line Voltage (kV)	2.5
Rated Frequency (Hz)	26.67

Table 5.3 Converter characteristics

Switch and Heat Sink Characteristics	
Switch Selection	
Converter Switch Rating (kV)	3.3
Converter Switch Rating (kA)	1
Switch Characteristics	
Switch Thermal Impedence (K/kW)	11.10
Switch Thermal Time Constants (s)	1.47
Diode Thermal Impedence (K/kW)	19.80
Diode Thermal Time Constants (s)	1.29
Heat Sink Details	
Rated Fluid Flow Rate (l/min)	5
Fluid Inlet Temperature (°C)	40
Rated Thermal Impedence (K/kW)	4.24
Rated Thermal Time Constants (s)	21.2

Table 5.4 Switch and Heat Sink Characteristics

The heat sink used in the model is an exposed tube 6-pass cold plate (Wakefield-Vette #120460) with water as the coolant [38]. The liquid cooled plate (LCP) is modelled as per Eq. 5.4 and 5.5. The variation of thermal resistance of the LCP with the coolant flow rate is shown in Fig. 5.5 along with values from the datasheet. The values represent the thermal resistance from the LCP plate to the inlet water. For the simulations, a maximum flow rate of 5 lpm is used.

Under rated flow conditions, heat transfer to the environment is usually insignificant enough to be ignored, however, in this case we consider flow rates that can be zero as well. Therefore, two additional components of heat transfer are added to the model – heat transfer due to natural convection and radiation. For this, the LCP is modelled as a vertical plate with only one side exposed (as the top side is covered by the semiconductor modules). The component due to

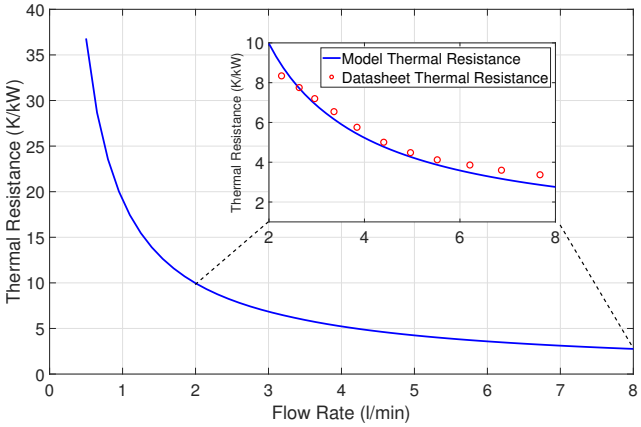

Figure 5.5 Thermal resistance of liquid cooled heatsink from plate to inlet coolant. The solid line represents the results of the heat sink model while the red scatter points are the datasheet values.

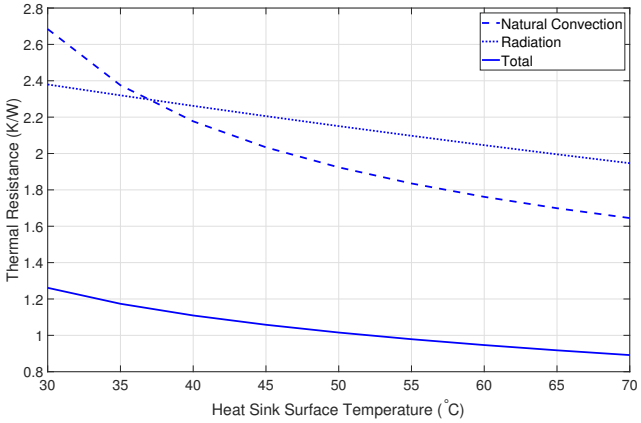

Figure 5.6 Thermal resistance of liquid cooled heatsink due to natural convection and radiation. The values are calculated considering an ambient temperature of $20°C$.

natural convection is calculated [39] using

$$Ra_L = \frac{g\beta(T_s - T_\infty)L_c^3}{\nu^2} \cdot Pr,$$
$$Nu = \left(0.825 + \frac{0.387Ra_L^{1/6}}{[1+(0.492/Pr)^{9/16}]^{8/27}}\right)^2, \tag{5.7}$$

where g is gravitational acceleration, β is the coefficient of volume expansion, T_s and T_∞ are the temperatures at the surface and ambient, L_c is the characteristic length of the geometry, ν

is the kinematic viscosity of air, and Pr is the Prandtl number. The heat lost due to radiation is calculated using

$$\dot{Q}_{rad} = \epsilon A_s \sigma (T_s^4 - T_\infty^4), \tag{5.8}$$

where ϵ is the emissivity of the LCP material, A_s is the surface area, and σ is the Stefan-Boltzmann constant. The resulting thermal resistance due to natural convection and radiation for different heat sink temperatures is shown in Fig. 5.6. A model based on the combination of all these heat transfers is implemented in the simulation.

5.3.2 Controller Tuning

There are two parameters that have to be selected – controller gain (K_p) and filter cut-off frequency (ω_c). First, the tuning of the filter is considered. The equivalent controller transfer function is

$$C = \frac{\tau_c \cdot K_p \cdot s}{\tau_c \cdot s + 1}. \tag{5.9}$$

The controller is simulated for different cut-off frequency ω_c on a sweep of power cycling frequency from 1–100 mHz. The equivalent gain of the controller ($\tau_c \cdot K_p$) is held constant in this analysis. The results are plotted in Fig. 5.7. The plot shows that ω_c >2 rad/s shows maximum reduction of temperature cycling amplitude, and this value is selected for the system.

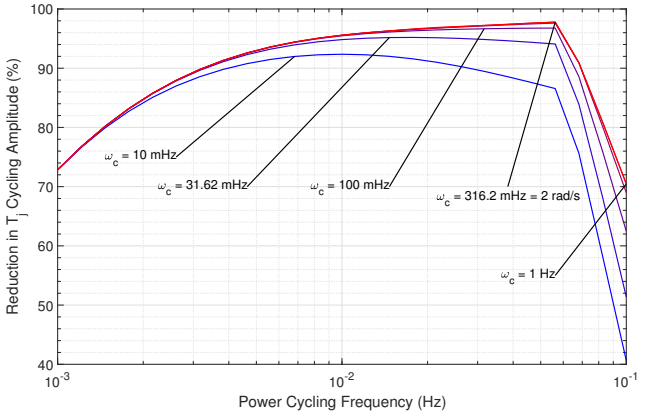

Figure 5.7 Comparison of damage distribution in the generator side converter with an extra converter in parallel.

The gain is tuned according to the Ziegler-Nichols method [40] and the value of $K_p = 10000$ is selected.

5.3.3 Simulation Results

The control structure described in Fig. 5.4 is implemented in the drivetrain model described in Sec. 5.3.1. First, the response of the system to different frequencies of wind speed cycling is analysed. Cycling wind speed signals with amplitude (Δv) from 2–8 m/s in steps of 2 m/s and frequencies between 1–100 mHz is simulated and analysed. A gain of K_p = 10000, and filter cut-off frequency of ω_c =2 rad/s is used for the simulation. The choice of these parameters is explained in Section 6.6. Fig. 5.8 plots the results of junction temperature cycling amplitude. Here, the power cycling is filtered out of the junction temperature and the temperature cycling amplitude is calculated.

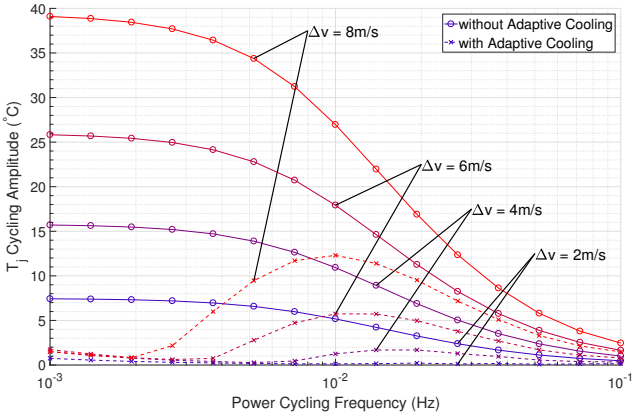

Figure 5.8 The simulated temperature cycling amplitude ΔT_j for different power cycling frequencies with and without mean temperature control based adaptive cooling. The results are for simulations performed for wind speed cycling with v_{mean} = 8 m/s, and amplitude ranging from Δv = 2 m/s for the blue curves, to Δv = 8 m/s for the red curve.

The solid lines show the junction temperature cycling amplitude with constant flow rate in the heatsink while the dashed lines the cycling amplitude with the adaptive cooling system implemented. In all cases, the maximum flow rate with the adaptive cooling equals the constant flow rate without the system. The constant flow rate system is used in the comparison as it is a common method of cooling used in industrial applications. The amplitude of the wind speed cycle increases from the blue line (Δv=2 m/s) to the red line (Δv=8 m/s).

It is observed that the junction temperature cycling amplitude reduces with increasing frequency of the applied wind speed cycling. This is because different steps of power conversion act as low pass filters – the large rotor mass filters cycling in the wind speed, the thermal structure of the IGBT filters cycling in power loss, and the thermal capacitance of the heat sink also filters oscillations in heat dissipation. This results in the reduction of temperature cycling amplitude with increasing wind speed cycling frequency both with and without adaptive cooling.

Furthermore, the results show that the reduction in ΔT_j further reduces with frequency. This can

be expected because the thermal mass of the heat sink causes a further delay in the rise of heat sink temperature which is required to raise the minimum temperature in cycle. Also, it is observed that even at low frequencies (around 1 mHz in Fig. 5.8) there is a limit to the reduction in cycling amplitude which is due to the time taken for the temperature to drop below the calculated mean. This delay is represented by the time between Point-1 and Point-2 in Fig. 5.3, which becomes more significant in sinusoidal shaped wind speed cycling.

While the ability of mean temperature based adaptive cooling to reduce junction temperature cycling has been demonstrated for wind speed cycling, typical wind speed profiles are not as regular. Therefore, it is important to consider the performance of the system for realistic wind speed profiles. As a test case, a 20 minute wind speed profile with 18 % turbulent intensity based on the Kaiman spectra is used [41]. This profiles is shown in Fig. 5.9.

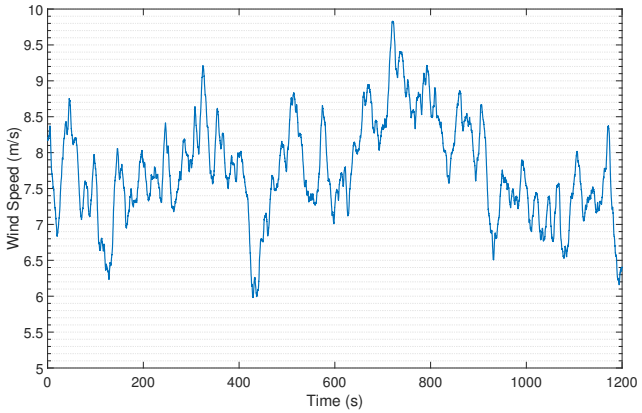

Figure 5.9 Wind speed profile used in the simulation.

This is used to generate the junction temperature profiles both with, and without the adaptive cooling system. The lifetime model from [37] is then used to calculate the cumulative damage from the temperature cycles in the converter switch. Fig. 5.10 plots the junction temperature profiles. The use of adaptive cooling results in a reduction of damage by 96.5 %.

The simulation results show that adaptive cooling is very effective in reducing the damage caused by temperature cycling. The next section uses a scaled-down experimental setup to demonstrate adaptive cooling and validate the system by comparing the experimental and simulation results of the setup.

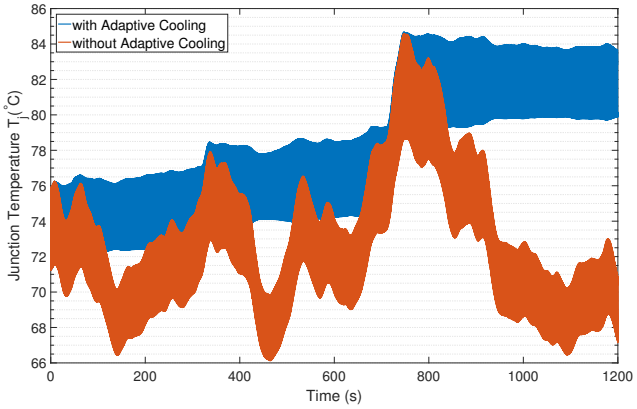

Figure 5.10 The simulated temperature with and without adaptive cooling for the case when ω_c = 7.5 mHz. The power cycling has been filtered out. The adaptive cooling results in a ≈96% reduction in damage compared to the case without any adaptive cooling.

5.4 Experimental Demonstration

5.4.1 System Description

To demonstrate the proposed adaptive cooling concept, a scaled-down setup is used. Fig. 5.11 shows a schematic of the setup and Table 5.5 details the components used.

Table 5.5 Components of the experimental setup.

Components		
IGBT Module	FS10R06VE3-B2	
Pump	M500M-V-EQi	Centrifugal pump with max. flow of 8.7 L/min
Liquid Cold Plate	Wakefield-Vette 120455	Exposed Tube 2- Pass Coldplate
Flow Sensor	FT-110M	1 L/min – 10 L/min
Heat Exchanger	ATS-HE20-C2-R0	
Temperature Sensor	Neoptix Reflex	Signal Conditioner and T1 probe
V_{ce} Measurement		Based on [34]
Microcontroller	LAUNCHXL F28027F	C2000 Piccolo Launchpad

This scaled-down setup uses a six switch 10 A, 600 V IGBT module. However, only one switch is utilised in this case as only one T_j measurement is used. Furthermore, no switching is used and

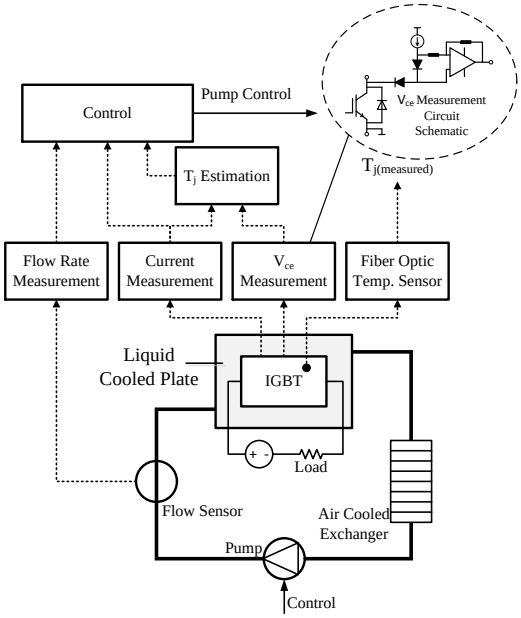

Figure 5.11 Schematic of experimental setup.

thermal cycling is achieved by varying current.

5.4.2 T_j Measurement

The junction temperature is measured using an fiber optic temperature sensor with signal conditioner as detailed in Table 5.5. To test the temperature measurement in the setup, simulation results for junction temperature based on datasheet parameters are compared to the measured junction temperature at steady state for five operating points.

For the measurements, the IGBT module is fixed onto a liquid cooled heat sink connected to refrigerated circulator (Julabo FP50 with Thermal H10S). This circulator is used to maintain a controlled heat sink temperature of 20 °C. A controlled DC source is used to maintain a set current in the module. For the simulation, loss and thermal parameters from the datasheet are used to calculate junction temperature based on the schematic in Fig. 5.12.

The comparison of simulated and measured temperature is presented in Table 5.6. The comparison shows that there is an error of upto ≈17 %. This may be due to,

- the use of only one chip, whereas the datasheet parameters give an average for all the chips,
- the inclusion of a safety factor in the datasheet values,

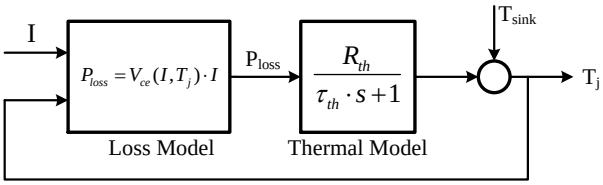

Figure 5.12 Schematic of simulation for calculation of junction temperature. From [42, 43]. The loss and thermal parameters are taken from the datasheet of the used IGBT module.

Table 5.6 Comparison of simulated and measured junction temperatures.

I (A)	Simulated T_j ($^\circ C$)	Measured T_j ($^\circ C$)	Error in $T_j - T_{sink}$ (%)
2	27.88	26.59	16.37
4	37.57	34.55	17.19
6	49.35	44.92	15.10
8	63.64	56.98	15.26
10	81.00	71.32	15.79

- or the placement of the sensor closer to the edge or corner of the chip.

However, the deviation is small enough to allow the fiber optic temperature sensor reading to be considered the junction temperature.

5.4.3 T_j Estimation Calibration

The control uses the junction temperature of the IGBT module which is estimated using the collector-emitter voltage (V_{ce}) as the thermo-sensitive electrical parameter. A circuit as described in [34] is used to measure the V_{ce} during operation. The circuit uses two serial diodes and a current source forward-biases them during the transistor on time (see Fig. 5.11). When the device is conducting the voltage on the second diode is measured to compensate for the voltage drop on the protection diode thus eliminating voltage offset due to diode forward voltage temperature dependency. When the transistor is off, one diode is blocks the V_{ce} voltage, protecting the measurement circuitry from damage.

The IGBT module fixed on the liquid cooled heat sink connected to refrigerated circulator (Julabo FP50 with Thermal H10S) is operated at different currents and different heat sink temperatures. The junction temperature, current, and V_{ce} are stored. This allows the creation of a 2-D look-up table that predicts the temperature based on the measured current and V_{ce}. Figure 5.13 shows a 2-D representation of the estimation of junction temperature based on current and V_{ce}.

The sensitivity of this TSEP depends largely on the collector current level. It is negative for lower

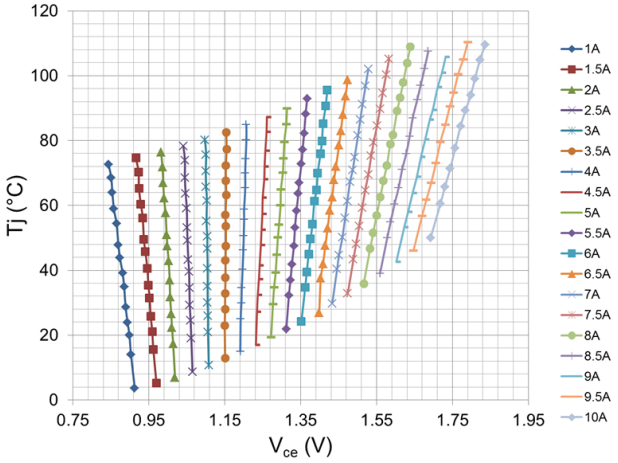

Figure 5.13 Estimation of T_j based on measured I and V_{ce}.

current values and positive for higher values with an inflection point occurring at approximately 3.5 A. This makes it difficult to estimate temperature at currents in this range. This problem could be solved by using a junction temperature measurement that is a hybrid of the TSEP and model based methods [44].

Also, the accuracy of current measurement can be an issue. From Fig. 5.13 it can be seen that a small error in current measurement can lead to large variations in the estimated temperature, especially at low currents. For these reasons the T_j based control in the experimental setup is limited to current cycling between 6.25 A and 9.75 A.

5.4.4 Results

For the demonstrator setup a controller is developed as per the schematic in Fig. 5.4, with the T_j value being generated based on measured V_{ce} and I, and the calibration in Section 5.4.3. Current is cycled between 6.25 A and 9.75 A at different frequency and the measured temperature (using the Fiber Optic Temperature Sensor) is logged. Fig. 5.14 plots the measured junction temperature for a power cycling frequency of 15 mHz. It shows the changing coolant flow rate when the adaptive cooling control is engaged at t=245 s.

This is repeated for a number of different power cycling frequencies. The results of these tests are consolidated in Fig. 5.15. The results show that considerable reduction in ΔT_j can be achieved, however this reduces with an increase in power cycling frequency. This can be explained by the following reasons:

- The time constant of the thermal circuit.

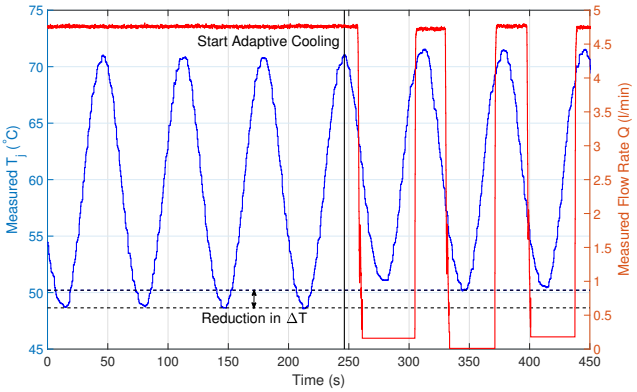

Figure 5.14 Measured junction temperature with and without adaptive cooling for a power cycling of 15 mHz. The figure shows the varying flow rate and the resulting reduction in the temperature cycling amplitude.

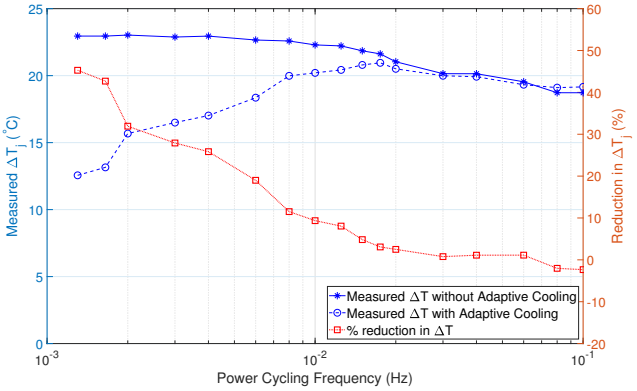

Figure 5.15 The measured temperature cycling amplitude ΔT_j and its reduction for different power cycling frequencies. This ΔT_j reduction ranges from ≈45 % for low power cycling frequencies to 0 % for higher frequencies.

- The dynamics of the cooling system (e.g., the pump dynamics) also play a role. They causes a delayed response in the adaptive cooling and makes cycling performance worse.

These reasons, are also responsible for the higher ΔT measured in the last two readings (0.08 Hz and 0.1 Hz) in Fig. 5.15. Further, Fig. 5.16 compares the results of the measured and simulated values for the same system. Table 5.6 shows that the magnitude of error between the measured and simulated temperature. At the higher range of frequencies (closer to 0.1 Hz), the measured results for cases with and without adaptive cooling have approximately equal temperature waveforms resulting in a negation of the error values. However, this is not the case when the two temperature

waveforms differ (as is the case fore frequencies closer to 1 mHz), resulting in Fig. 5.16. Still, the possible improvements in temperature cycling with adaptive cooling are evident.

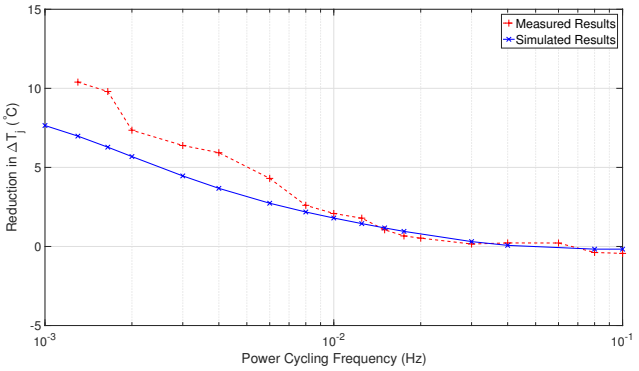

Figure 5.16 A comparison of the reduced junction temperature cycling between simulation and experiments.

5.5 Results for a Case Study Turbine

Finally, to quantify the effect that adaptive cooling could have on the lifetime of the semiconductor, the lifetime with adaptive cooling is investigated for a case study 10MW wind turbine. This analysis is based on the system used in [37] with an updated heat sink as described in Section 5.3.1. The system has been detailed in Table 5.1 – Table 5.4. The wind speed profile used is based on the measured data of a KNMI (The Royal Netherlands Meteorological Institute) offshore weather station. The procedure considers two time scales – the long duration profile, and the short duration profile. The long duration profile uses the annual wind profile with wind speed averaged over 10 minutes and the steady state profile to generate the temperature profile. The short duration profile uses stochastic 10 minute profiles that represent the wind speed variation within the 10 minutes over which the measured wind speed is averaged and recorded. The procedure is shown in Fig. 5.17.

The distribution of damage over the range of temperature cycling frequencies for the outer devices of the 3L-NPC converter is shown in Fig. 5.18 and Fig. 5.19. The outer devices have been shown to be the most stressed switches with the lowest lifetime in [37]. From the distribution it is clear that the majority of the damage in the generator side (in the case considered in this study) is at frequencies above 100 mHz. In fact, a major share of the damage lies in the range of 10–100 Hz. These frequencies are not acted upon by the adaptive cooling system. Therefore, the adaptive cooling would be effective only on the grid side converter.

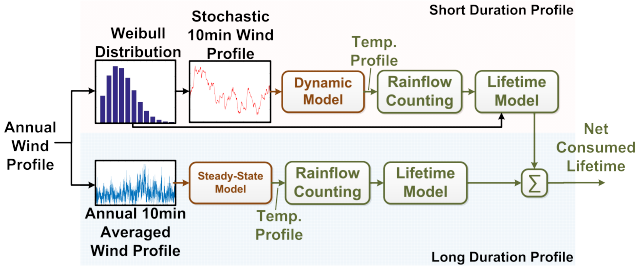

Figure 5.17 Lifetime calculation procedure. From [37].

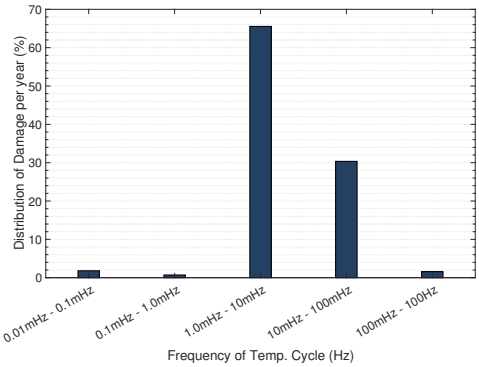

Figure 5.18 Distribution of damage for the grid side converter

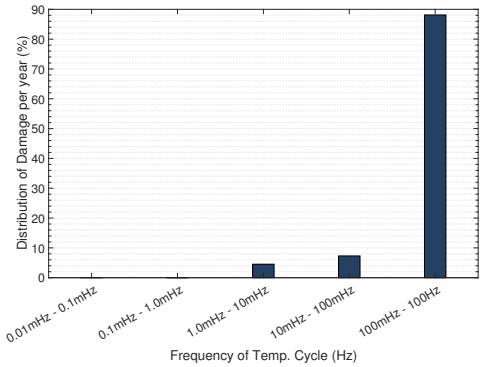

Figure 5.19 Distribution of damage for the generator side converter

The adaptive cooling using a gain $K_p = 10000$, and a filter cut-off frequency $\omega_c = 2$ rad/s is used. The resulting lifetimes for the outer devices are calculated and tabulated in Table 5.7. Here, the effect of adaptive cooling in the long duration profile has been ignored. The results show that significant improvement in lifetime can be achieved with adaptive cooling. Further, the comparison of the distribution of damage is shown in Fig. 5.20. It is clear that there is significant reduction of damage in the frequency range of 1–100 mHz. However, due to the increase in the mean temperature that accompanies adaptive cooling, the damage in the long duration cycling increases and becomes the limiting factor in the improvement achievable with adaptive cooling.

Table 5.7 Comparison of semiconductor lifetime with and without Adaptive Cooling for the grid side converter.

	Lifetime (years)	Normalised
without Adaptive Cooling	10.81	1
with Adaptive Cooling	101.92	9.43

As adaptive cooling involves a change in the temperature profile, it also results in an increase in

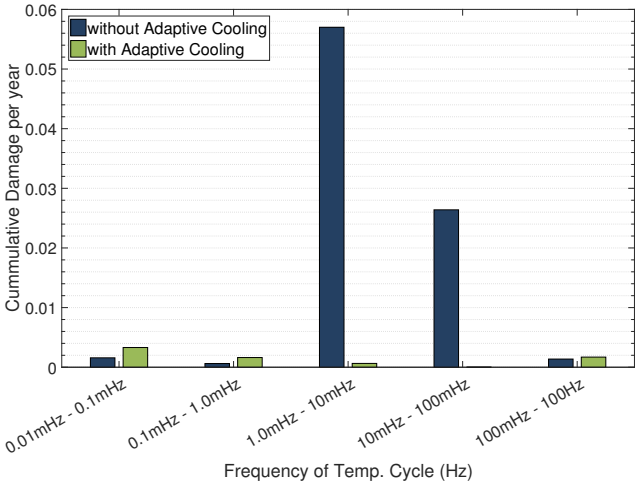

Figure 5.20 Comparison of damage distribution in the grid side converter.

the losses of the semiconductor. However, this increase is small and in the case study considered the increase in losses of the outer switches is calculated to be 2.53%.

For the generator side converter, the fact that the majority of damage occurs at a temperature cycling frequency that is higher than 100 mHz, makes the improvement in lifetime small. In this example an increase of ≈2.5% is achieved. However, when the generator converter is over-rated (an extra converter is used in parallel), there is better distribution of the damage and the results with adaptive cooling using a gain $K_p = 10000$, and a filter cut-off frequency $\omega_c = 2$ rad/s are shown in Fig. 5.21. The result is a 42% improvement in lifetime as detailed in Table 5.8.

Table 5.8 Comparison of semiconductor lifetime with and without Adaptive Cooling for the generator side converter.

	Lifetime (years)	Normalised
without Adaptive Cooling	51.52	1
with Adaptive Cooling	73.30	1.42

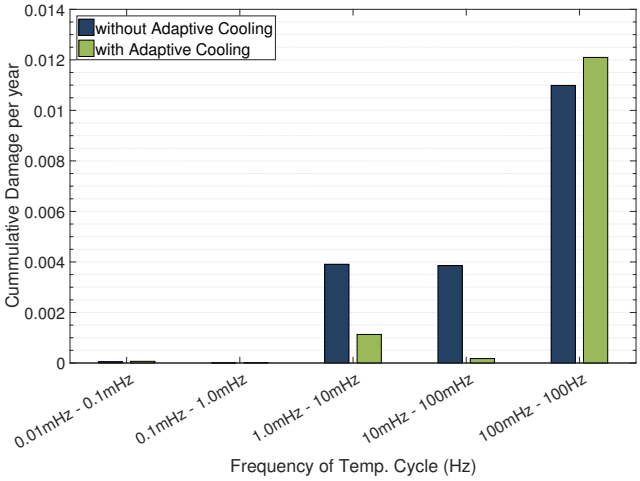

Figure 5.21 Comparison of damage distribution in the generator side converter with an extra converter in parallel.

5.6 Conclusions

This chapter has investigated the use of adaptive cooling to improve lifetimes of power semiconductors in converters by reducing the junction temperature cycling. Simulations have shown that this method displays significant improvement in temperature cycling. In the simulation involving a yearly wind profile, adaptive cooling was shown to increase the power semiconductor lifetime by a factor of ≈ 9.5 for the grid side converter. It has also been seen that the frequency of the cycling is an important consideration. Adaptive cooling (in the presented case study) has a significant reduction of damage upto 100 mHz. Therefore, converters that have a larger share of damage within this range will most benefit from adaptive cooling. This is demonstrated by the difference in lifetime gain for the grid-side and generator-side converters.

Further, the chapter validates the effectiveness of adaptive cooling system using a scaled-down experimental setup. The possible improvements in temperature cycling with adaptive cooling are evident in the results obtained in the experiment. In conclusion, adaptive cooling is a promising method to reduce stresses and increase lifetimes in power semiconductors, especially as most wind turbine converters today use liquid cooling for the converter. The advantage of such a system would be that it uses infrastructure that is already a part of most wind turbine converters and minimal changes would be required for its implementation.

Bibliography

[1] P. Lyding, S. Faulstich, B. Hahn, and P. Tavner, "Reliability of the electrical parts of wind energy systems-a statistical evaluation of practical experiences," in *3rd EPE Wind Energy Chapter Symposium*, 2010, pp. 1–8.

[2] S. Yang, A. Bryant, P. Mawby, D. Xiang, L. Ran, and P. Tavner, "An industry-based survey of reliability in power electronic converters," *IEEE Transactions on Industry Applications*, vol. 47, no. 3, pp. 1441–1451, May 2011.

[3] M. Ciappa, "Selected failure mechanisms of modern power modules," *Microelectronics Reliability*, vol. 42, no. 4, pp. 653 – 667, 2002.

[4] C. Busca, R. Teodorescu, F. Blaabjerg, S. Munk-Nielsen, L. Helle, T. Abeyasekera, and P. Rodriguez, "An overview of the reliability prediction related aspects of high power igbts in wind power applications," *Microelectronics Reliability*, vol. 51, no. 9, pp. 1903 – 1907, 2011.

[5] U. Shipurkar, K. Ma, H. Polinder, F. Blaabjerg, and J. A. Ferreira, "A review of failure mechanisms in wind turbine generator systems," in *2015 17th European Conference on Power Electronics and Applications (EPE'15 ECCE-Europe)*, Sept 2015, pp. 1–10.

[6] M. Held, P. Jacob, G. Nicoletti, P. Scacco, and M. H. Poech, "Fast power cycling test of igbt modules in traction application," in *Proceedings of Second International Conference on Power Electronics and Drive Systems*, vol. 1, May 1997, pp. 425–430 vol.1.

[7] A. Wintrich, U. Nicolai, T. Reimann, and W. Tursky, "Application manual power semiconductors." ISLE, 2011.

[8] M. Andresen, M. Liserre, and G. Buticchi, "Review of active thermal and lifetime control techniques for power electronic modules," in *2014 16th European Conference on Power Electronics and Applications*, Aug 2014, pp. 1–10.

[9] C. J. J. Joseph, M. R. Zolghadri, A. Homaifar, F. Lee, and R. D. Lorenz, "Novel thermal based current sharing control of parallel converters," in *INTELEC 2004. 26th Annual International Telecommunications Energy Conference*, Sept 2004, pp. 647–653.

[10] D. A. Murdock, J. E. R. Torres, J. J. Connors, and R. D. Lorenz, "Active thermal control of power electronic modules," *IEEE Transactions on Industry Applications*, vol. 42, no. 2, pp. 552–558, March 2006.

[11] M. Andresen and M. Liserre, "Impact of active thermal management on power electronics design," *Microelectronics Reliability*, vol. 54, no. 9, pp. 1935 – 1939, 2014.

[12] G. L. Calzo, A. Lidozzi, L. Solero, F. Crescimbini, and V. Cardi, "Thermal regulation as control reference in electric drives," in *2012 15th International Power Electronics and Motion Control Conference (EPE/PEMC)*, Sept 2012, pp. DS2c.18–1–DS2c.18–7.

[13] J. Lemmens, P. Vanassche, and J. Driesen, "Optimal control of traction motor drives under electrothermal constraints," *IEEE Journal of Emerging and Selected Topics in Power Electronics*, vol. 2, no. 2, pp. 249–263, June 2014.

[14] J. Lemmens, J. Driesen, and P. Vanassche, "Thermal management in traction applications as a constraint optimal control problem," in *2012 IEEE Vehicle Power and Propulsion Conference*, Oct 2012, pp. 36–41.

[15] L. Wei, J. McGuire, and R. A. Lukaszewski, "Analysis of pwm frequency control to improve the lifetime of pwm inverter," *IEEE Transactions on Industry Applications*, vol. 47, no. 2, pp. 922–929, March 2011.

[16] K. Ma, M. Liserre, and F. Blaabjerg, "Reactive power influence on the thermal cycling of multi-mw wind power inverter," *IEEE Transactions on Industry Applications*, vol. 49, no. 2, pp. 922–930, March 2013.

[17] M. Weckert and J. Roth-Stielow, "Chances and limits of a thermal control for a three-phase voltage source inverter in traction applications using permanent magnet synchronous or induction machines," in *Proceedings of the 2011 14th European Conference on Power Electronics and Applications*, Aug 2011, pp. 1–10.

[18] K. Ma and F. Blaabjerg, "Thermal optimised modulation methods of three-level neutral-point-clamped inverter for 10 mw wind turbines under low-voltage ride through," *IET Power Electronics*, vol. 5, no. 6, pp. 920–927, July 2012.

[19] L. Wu and A. Castellazzi, "Temperature adaptive driving of power semiconductor devices," pp. 1110–1114, July 2010.

[20] A. C. De Rijck and H. Huisman, "Power semiconductor device adaptive cooling assembly," Patent US 8 547 687, Oct 01, 2013.

[21] W. J. Anderl and C. M. Huettner, "Real time adaptive fluid flow cooling," Patent US 7 733 649, Jun 08, 2010.

[22] J. N. Davidson, D. A. Stone, and M. P. Foster, "Real-time temperature monitoring and control for power electronic systems under variable active cooling by characterisation of device thermal transfer impedance," in *7th IET International Conference on Power Electronics, Machines and Drives (PEMD 2014)*, April 2014, pp. 1–6.

[23] J. N. Davidson, D. A. Stone, M. P. Foster, and D. T. Gladwin, "Real-time temperature estimation in a multiple device power electronics system subject to dynamic cooling," *IEEE Transactions on Power Electronics*, vol. 31, no. 4, pp. 2709–2719, April 2016.

[24] X. Wang, A. Castellazzi, and P. Zanchetta, "Observer based temperature control for reduced thermal cycling in power electronic cooling," *Applied Thermal Engineering*, vol. 64, no. 1, pp. 10 – 18, 2014.

[25] D. A. Lewis and C. Narayan, "Device to monitor and control the temperature of electronic chips to enhance reliability," Patent US 5 569 950, Oct 29, 1996.

[26] R. Bayerer, T. Herrmann, T. Licht, J. Lutz, and M. Feller, "Model for power cycling lifetime of igbt modules-various factors influencing lifetime," in *Proc. CIPS*, vol. 11, 2008, p. 13.

[27] D. Taler, "A new heat transfer correlation for transition and turbulent fluid flow in tubes," *International Journal of Thermal Sciences*, vol. 108, pp. 108 – 122, 2016.

[28] F. Dittus and L. Boelter, "Heat transfer in automobile radiators of the tubular type," *International Communications in Heat and Mass Transfer*, vol. 12, no. 1, pp. 3 – 22, 1985.

[29] D. L. Blackburn, "Temperature measurements of semiconductor devices - a review," in *Twentieth Annual IEEE Semiconductor Thermal Measurement and Management Symposium (IEEE Cat. No.04CH37545)*, Mar 2004, pp. 70–80.

[30] Y. Avenas, L. Dupont, and Z. Khatir, "Temperature measurement of power semiconductor devices by thermo-sensitive electrical parameters - a review," *IEEE Transactions on Power Electronics*, vol. 27, no. 6, pp. 3081–3092, June 2012.

[31] S. Carubelli and Z. Khatir, "Experimental validation of a thermal modelling method dedicated to multichip power modules in operating conditions," *Microelectronics Journal*, vol. 34, no. 12, pp. 1143 – 1151, 2003.

[32] M. Hoeer, M. Meissner, F. Filsecker, and S. Bernet, "Online temperature estimation of a high-power 4.5 kv igbt module based on the gate-emitter threshold voltage," in *2015 17th European Conference on Power Electronics and Applications (EPE'15 ECCE-Europe)*, Sept 2015, pp. 1–8.

[33] N. Baker, M. Liserre, L. Dupont, and Y. Avenas, "Improved reliability of power modules: A review of online junction temperature measurement methods," *IEEE Industrial Electronics Magazine*, vol. 8, no. 3, pp. 17–27, Sept 2014.

[34] S. Beczkowski, P. Ghimre, A. R. de Vega, S. Munk-Nielsen, B. Rannestad, and P. Thogersen, "Online vce measurement method for wear-out monitoring of high power igbt modules," in *2013 15th European Conference on Power Electronics and Applications (EPE)*, Sept 2013, pp. 1–7.

[35] T. K. Gachovska, B. Tian, J. L. Hudgins, W. Qiao, and J. F. Donlon, "A real-time thermal model for monitoring of power semiconductor devices," *IEEE Transactions on Industry Applications*, vol. 51, no. 4, pp. 3361–3367, July 2015.

[36] B. Du, J. L. Hudgins, E. Santi, A. T. Bryant, P. R. Palmer, and H. A. Mantooth, "Transient thermal analysis of power devices based on fourier-series thermal model," in *2008 IEEE Power Electronics Specialists Conference*, June 2008, pp. 3129–3135.

[37] U. Shipurkar, E. Lyrakis, K. Ma, H. Polinder, and J. A. Ferreira, "Lifetime comparison of power semiconductors in three-level converters for 10-mw wind turbine systems," *IEEE Journal of Emerging and Selected Topics in Power Electronics*, vol. 6, no. 3, pp. 1366–1377, Sept 2018.

[38] Wakefield-Vette. Exposed tube liquid cold plates. [Online]. Available: http://www.wakefield-vette.com/products/liquid-cooling/liquid-cold-plates/standard-liquid-cold-plates.aspx

[39] Y. Cengel, *Heat Transfer - A Practical Approach*, 4th ed. London: McGraw-Hill Education - Europe, 2011.

[40] J. G. Ziegler and N. B. Nichols, "Optimum settings for automatic controllers," *trans. ASME*, vol. 64, no. 11, 1942.

[41] F. Iov, A. Hansen, P. Soerensen, and F. Blaabjerg, *Wind Turbine Blockset in Matlab/Simulink. General Overview and Description of the Model.* Institut for Energiteknik, Aalborg Universitet, 2004.

[42] K. Ma, Y. Yang, and F. Blaabjerg, "Transient modelling of loss and thermal dynamics in power semiconductor devices," in *2014 IEEE Energy Conversion Congress and Exposition (ECCE)*, Sept 2014, pp. 5495–5501.

[43] K. Ma, M. Liserre, F. Blaabjerg, and T. Kerekes, "Thermal loading and lifetime estimation for power device considering mission profiles in wind power converter," *IEEE Transactions on Power Electronics*, vol. 30, no. 2, pp. 590–602, Feb 2015.

[44] M. A. Eleffendi and C. M. Johnson, "Application of kalman filter to estimate junction temperature in igbt power modules," *IEEE Transactions on Power Electronics*, vol. 31, no. 2, pp. 1576–1587, Feb 2016.

CHAPTER 6

Modularity in Generator Systems

Modularity is promising from a view to increasing turbine availability through fault tolerant operation as well as reduced downtimes, especially for offshore wind turbines. This chapter examines modular concepts for wind turbine generator systems from the viewpoint of increasing the availability of wind turbines. It explores the modularities possible in wind turbine generator systems at different layers, i.e., the functional and the physical layer. It also attempts to highlight some opportunities and challenges in including modularity in these layers. Next the chapter focuses on a quantitative analysis of large scale (or extreme) modularity in power electronic converters of wind turbine generator systems. It uses mathematical models to investigate the effect of the choice of module number on the availability of a converter.

Based on:
U. Shipurkar, H. Polinder and J. A. Ferreira, "Modularity in wind turbine generator systems – Opportunities and challenges," *2016 18th European Conference on Power Electronics and Applications (EPE'16 ECCE Europe)*, Karlsruhe, 2016, pp. 1–10.
and
U. Shipurkar, J. Dong, H. Polinder and J. A. Ferreira, "Availability of Wind Turbine Converters with Extreme Modularity," in *IEEE Transactions on Sustainable Energy*, doi: 10.1109/TSTE.2018.2813402, 2018.
This chapter merges the two papers and makes editorial changes. Further, one section on extremely modular generators has been added.

6.1 Introduction

The generator systems has been shown to be a major contributor to the failure rates of wind turbine drivetrains [1–7]. This makes addressing its failures and improving its availability an important route towards reducing cost of energy. One method of doing this is though the addition of modularity in the converter system [8]. Modularisation is a design approach that decomposes a system into a number of 'modules'or components. The motivations behind the use of this concept have been diverse: from increasing manufacturability in machines, and standardisation of parts for the supply chain, to improving part load efficiency and system reliability. For wind turbines, this concept is attractive from the perspective of improving the availability of the turbine system predominantly in two ways. First, the introduction of fault tolerance, where the faulted module is bypassed and the remaining system continues operation with the same or a lower rating. Second, the increased maintainability of such a system, by making failed modules easier and cheaper to replace.

This chapter discusses modularity in two layers - the first is functional layer and the second is physical layer. Functional modularity is where the modules operate as separate functional blocks. Physical modularity builds on this layer by adding a physical separation, leading to a possibility to remove/replace such modules. Modularity has been explored in literature, multiple modules that form pairs of interchangeable converter modules is one example [9], and the system with six parallel connected converters for a 4.5 MW commercial wind turbine is another [10]. Further, the integrated modular motor drive concept for traction [11] and aerospace applications [12] utilise modularity to allow for fault tolerant operation. Such a system for wind turbine generators has been investigated by Spooner *et al.* where the direct drive permanent magnet generator is composed of multiple E-core stator segments with tooth wound windings [13–15]. Through a review of existing literature in this field, the chapter first examines the use of these different layers of modularity in wind turbine generator systems from the perspective of improving availability.

Next, the chapter takes a first step towards extremely modular generators by analysing the effect of functional and physical modularity on the availability of the converter in a wind turbine. Furthermore, it focusses on extreme modularity - i.e., designs where the number of modules is much larger than what is used at present (in the industry). It investigates the effect of modularity on the converter availability using Markov state space models [16] to quantify these effects. The use of Markov modelling is one approach towards system level reliability modelling with the advantage that it is an effective tool for fault tolerant systems [17]. Markov models have been used to investigate maintenance planning in [18], optimum maintenance policies in [19], operational comparison of technologies in [20], and reliability of potential wind farms in [21]. In power electronics, this modelling tool has been used by Zhang *et al.* to investigate the reliability of modular converters for wind turbines [22] based on a patented design [9]. Furthermore, Najmi *et al.* use Markov models to model the reliability of capacitor banks for modular multilevel converters [23], and McDonald *et al.* investigate parallel wind turbine powertrains in [24]. Other work has used variations of these methods to investigate redundancy in converters; such as that of HVDC MMC modules in [25], and parallel-inverter systems in [26].

6.2 Functional Modularity

Modularity in the functional layer aims to achieve a system where the modules operate independent of one another leading to a system that can tolerate faults and operate without one or more of these modules.

The use of modular converters is an established method of bringing in redundancy in systems and improving reliability. One way of achieving this is to use multiple converter modules in parallel (or series, or a combination of both) to divide the power generated, as shown in fig. 6.1a. Here, in the event of a failure in any module of the converter, the corresponding module could be switched 'off'and operation could continue with a reduced output. This is especially attractive for wind turbine systems as they do not always operate at rated power and hence power output may not be adversely affected.

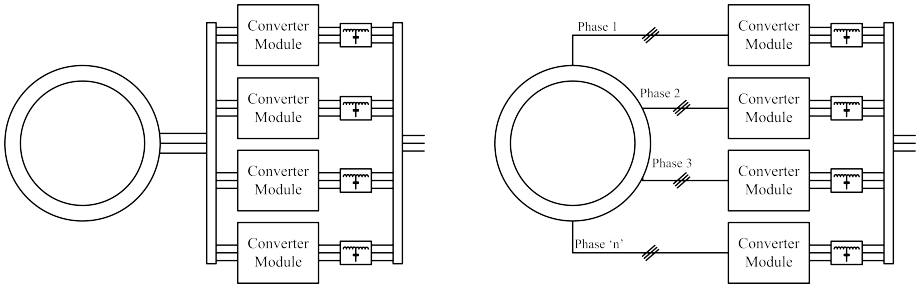

(a) Topology 1 **(b)** Topology 2

Figure 6.1 Modularity in Converters

This concept has been the basis of a number of patents. In [9], Hjort *et al.* describe a converter system comprising multiple modules that form pairs of interchangeable converter modules. This provides a flexible, fully redundant and reliable system. Further, in [27], Mayor *et al.* describe an electric converter system with parallel units and fault tolerance.

In literature, Birk *et al.* describe such a system with six parallel connected converters for a 4.5MW commercial wind turbine [10, 28]. In such a system the converters can be run near rated power, thus optimising efficiency with the added advantage of reduced grid harmonics achieved by shifting the PWM pulses of the modules. These improvements were validated on a 11kW and 2MW test bench. Zhang *et al.* investigated the reliability of such a parallel modular systems using Markov models [29] and show that, as expected, the system reliability improves as more converter modules are added into the system.

The other possible topology, as shown in fig. 6.1b, uses multiple modular converter units each driving an independent phase of the machine. This system allows for operation under failures in the machine phase as well. In [30], a wind power installation with redundancy derived by

multiple, independent power generating systems is described. In [31] an AC drive using multiple independent phase drive units is studied. Such a topology for wind turbine systems consisting of nine phases built using classical three phase converter modules was investigated in [32]. A variation of such a system would be the use of modular converters with parallel machine circuits rather than using machines with a higher number of phases, with most large wind turbines consisting of windings with multiple parallel circuits this would be an attractive option. However, for such a system the design must maintain the tenets of fault tolerant design.

Another promising concept is the use of tooth wound concentrated modular windings with a dedicated converter unit. Fig 6.2 shows an example of such a system. Such a system with permanent magnet synchronous machines has been proposed by Jahns *et al.* as an Integrated Modular Motor Drive (IMMD) for traction applications [11,33] and by Wolmarans *et al.* for aerospace applications [12]. A similar system was developed for a five-phase switched reluctance traction drive with each phase coil having its own modular inverter, thus increasing the redundancy of the drive system [34]. Spooner *et al.* develop such a system built up of stator modular coils wound around modular E-cores for large direct drive wind turbines [13–15], however, the designs proposed by them includes segmented stators and rotors. Some advantages of such a system include, the use of simple structural parts, ease of assembly and the use of common modules for all specifications [13].

This system could be capable of operating with either a fault in a converter module or stator winding module by switching 'off' the particular faulty coil and converter group. As this type of system has a greater degree of modularity that the one with only a modularity in converter (due to the availability of separate converter modules for each stator coil), the system is able to process greater power in the event of a fault, however, this may not be an important factor because wind turbines do not always operate at the rated power. Also, this comes at the expense of increasing the number of components which could have an important bearing on the costs of the system. Another disadvantage of such a system is that the concentrated modular windings give rise to lower winding factors and larger space harmonics which may reduce the efficiency of the system.

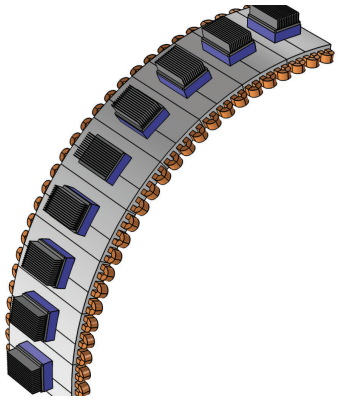

Figure 6.2 Modularity in windings and converter. The blue blocks represent converter modules connected to each tooth wound winding.

The power electronics remain a major contributor to failures in wind turbine generators [3]. Therefore, modular converters are a very attractive solution for improving the availability of wind turbine systems. The following sections discuss some important aspects of modularity in the functional layer. First, the possible connections of the converter modules is discussed in

section 6.2.1. Second, the aspects of fault tolerance are described in section 6.2.2. This is the most important property for the functional modularity layer as the modules must be capable of functioning in the event of a fault in one of the modules. Further, the multiplicity of modules gives rise to different possibilities in their control, this is discussed in section 6.2.3. Finally, the aspects of thermal design for a modular system are described in section 6.2.4.

6.2.1 Connection of Modular Converters

The modular converters can be connected in three possible ways - in series, in parallel and in a combination of both. Most wind turbine generators are designed with operating voltages below 3kV, therefore, as the power rating increases the current generated also increases. Using parallel converter modules is one way to handle this increased current rating. Fig. 6.1a and fig. 6.1b describes such connections. Birk *et al.* investigate the benefits of higher reliability, higher efficiency and reduced grid harmonics for such a configuration of six parallel converters [10,28]. Parallel connected modular converters are also investigated in [35,36].

Another connection possibility for the modular converters is to connect them in series. Such a configuration has a number of advantages - it could be used to form transformer-less grid side connections [37–39], easy integration into HVDC/MVDC connected wind farms, improved fault tolerance (by bypassing failed converter modules) [40,41], and possibility of minimising harmonic distortion [42].

However, operating generator windings at high voltage levels would mean thicker insulation would be required, thereby increasing the area of the slot occupied by the insulation and reducing the area occupied by copper leading to larger machines. Also, this increased voltage offers no added advantage to the machine design, as the voltage across the coil remains a fraction of the total (high) voltage. Therefore, if thicker insulation is to be used, it may be a better option to impress this voltage across the generator coil reducing the current required and hence improving efficiency.

6.2.2 Fault Tolerance

Fault tolerance is the property that enables a system to continue operation with a failure. This is an important tool in improving the availability of wind turbine generator systems. Fault tolerance involves detecting failure, handling the fault, and post fault control. However, the system must first be designed for fault tolerance. This section discusses this aspect for modular designs. It also discusses the problems that may arise in post fault conditions with such a fault tolerant system.

Design for Fault Tolerance - With the aim of designing a generators system that can continue operation with faults, a number of requirements need to be considered in the design [12,43,44].

Complete Electrical Isolation - For modular systems, as the proposal is to use independent converters for each module (be it a single coil or three phase coil module) this requirement is already

built into the design.

Limiting of Fault Currents - It is important to safely handle short circuit currents in wind turbine generators to prevent damage. One possibility is to design the machine with d-axis inductance close to 1pu, thus limiting any fault current to the rated current. Moreover, techniques for reducing the short circuit current without impairing electromechanical performance by using magnet subdivisions have been investigated in literature [45, 46] and could provide interesting alternatives.

Magnetic Isolation - Magnetic isolation is another important factor to consider. Without this, fault currents in one winding would induce large voltages in the other, disrupting the control. Therefore, the design should aim at minimising mutual inductance between windings. A modular winding design has advantages over distributed windings in this regard as some slot/pole combinations have inherent zero mutual inductances. The addition of physical modularity in the stator core, as will be discussed further in this chapter, would only serve to further reduce the mutual inductances between coils and hence may be beneficial for fault tolerant design [47], however, certain configurations would prove to be better than others - this must be investigated.

Thermal Isolation - In machines the windings are at the highest temperature. The heat is produced by copper losses in the slot and is radially transmitted to the stator surface. Windings with short circuit current can produce large amounts of heat in the slot, therefore, in order to protect the healthy windings, thermal isolation between the different windings is recommended. Modular stator windings with a single coil in each slot would serve this need well. Further, physical modularity with the addition of air-gaps in the stator would result in better thermal isolation between the healthy and faulty windings.

Harmonics, Unbalanced Magnetic Pull and Torque Ripple - The operation of the machine with a faulty winding 'switched off 'would give rise to harmonics, unbalanced magnetic pull and torque ripple. While using larger segments may have benefits in the reduced number of components used, they would possible cause larger disturbances when the faulty segment is isolated. The selection of a topology should take these factors into consideration as well. A high level of modularity also presents the opportunity of selecting certain 'healthy' segments to be turned off to minimise the effects of harmonics and unbalanced magnetic pull which may be detrimental to the machine if it is operated for long periods with faults (as may be the case for far offshore turbines). This too is an area requiring further investigation.

6.2.3 Distribution of Intelligence

The control is an important part of the wind turbine generator system. With a modular machine and converter system, there is a need to deliver control signals to each of the module independently.

A possible control structure is to have a single centralised controller that distributes the gate signal to each of the modules. Such a system was utilised in [11, 12]. However, as reported by Birk

et al. in [28] as well as by Lyding *et al.* in [4] the control unit is a component with a high failure rate. Therefore, such a centralised control would not benefit fault tolerance.

The alternative is the use of a distributed control architecture with multiple processors. This could be achieved using a master/slave or hierarchial configuration where one controller is designated the master as described in [48–52]. Such a distributed architecture may also be realised using a heterarchial control structure where each distributed controller operates as synchronised peers running identical programs with shared sensor information [33, 34, 53, 54]. Such a distributed control structure would allow operation under failure of control modules as well.

The use of three phase modules, i.e. distributed or concentrated windings along with the converter that are grouped together in three phase modules, presents the opportunity of using independent control modules that use sensor-less control to develop a heterarchial structure does does not even require the sharing of sensor information. This system could be built on a system with conventional position sensors to create a more robust and fault tolerant control architecture. However, a factor to consider is the need of updating the control power curve when a fault occurs and is isolated. With each module that is removed from operation, the power curve would need to be updated with a de-rating factor.

6.2.4 Thermal Design and Performance

Most failure mechanisms in wind turbine generator systems are driven by temperature [55], therefore, the thermal performance of a generator system is important to ensure reliability. The use of functional modularity with the integration of modular power electronic converter modules with a large direct drive generators would first benefit from the spatial distribution which would allow a larger surface for heat removal, however, this benefit is balanced by the fact that the generator would also be removing heat through the stator surface and prove to be an added heat source. A possible improvement is proposed by Wolmarans *et al.* as an integrated thermal management system for a 50kW integrated drive, where an inner heat exchanger ring is responsible for the stator cooling and an outer ring is for the converter cooling and an intermediate air channel is use to circulate forced air [12].

6.3 Physical Modularity

The aim of modularity in the physical layer is to break up the system into physically independent modules to ease field maintenance. With physical modularity the modules are replaceable in case of failure.

Modular converters can be designed to be physically separate with ease. Further, with a high level of modularity, such as with modular stator windings with independent H-bridge converters for each coil, there is an opportunity to design compact converters that would reduce replacement costs. With smart design, it may be possible to design converters that can be replaced by a single

worker without heavy lifting equipment. Such developments could reduce costs of maintenance considerably.

Furthering this concept of physical modularity is adding segmentation in the stator core. This is represented in fig 6.3. Segmentation introduces the ability of a core module of the generator being replaced in case of any winding failure apart from facilitating higher slot fill factors. This would mean that the replacement would be quicker and cheaper, which is especially attractive for offshore wind turbines. However, such a topology would introduce additional air-gaps in the machine flux path.

Spooner *et al.* proposed such a system for direct drive PM generators, demonstrated a laboratory machine made-up of such segments and identified additional loss mechanisms of such machine types [14]. References [47, 56–58] investigate the effect of the additional flux gaps on the performance of permanent magnet machines. It was found that the working harmonics of air-gap flux densities decrease with the increase of the flux gap widths, however, these gaps reduce the mutual inductance between phases thus improving fault tolerance capabilities. It was also found that stator flux gaps increase cogging torque amplitudes. A production concept for segmented stator BLDC machines was presented in [59] demonstrating the advantages of increased fill factors of segmented machines while in [60] the manufacturing of a segmented stator PM synchronous machine for hybrid machines was presented that shows the advantages in manufacturability of such segmented stators.

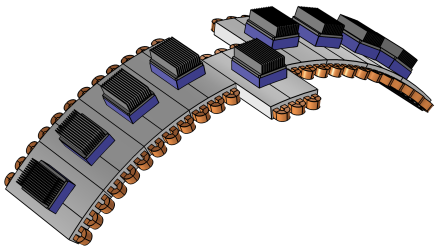

Figure 6.3 Segmented stator core with modular windings and converters. Each set of three-phase winding sets being fed by a modular power electronic converter represented by the blue blocks.

The inclusion of segmentation allows for replacing faulty windings as well. As per [61], stator winding failures account for about 20-30% of all generator failures. These failures are expensive to fix and take considerable time. According to [3], a generator failure averages about 150 hours of downtime. The use of segmentation would reduce the time and cost of faulty winding replacement. Physical modularity in the form of segmentation could therefore be especially attractive for offshore wind turbines.

The rotor, just like the stator, could benefit from segmentation. In a patent, Keim *et al.* proposed a carrier assembly with a releasable attachment to the rotor so that the permanent magnets could be easily removed for repair or replaced [62]. A rotor with segmentation was also included in the design by Spooner *et al.* in [14]. Apart from the advantages in manufacturing, this would make it easier to replace magnets in case they are demagnetised or replace rotor windings in case they suffer from a failure. These failures in wind turbines are rare [5, 61], and so the segmented rotor is

not an attractive solution for wind turbines.

The following sections discuss some important considerations that become important with the addition of modularity in the physical layer. First, the different ways that physical modularity can be achieved in machines is discussed in section 6.3.1, then the challenges involved in supporting such physically separated modules in large wind turbines is discussed in section 6.3.2.

6.3.1 Segment Topologies

Adding segmentation to the stator core results in physically separate stator modules which can be replaced in the event of a winding failure. This physical modularity concept for the stator core is achieved by building the complete machine out of a number of separate core segments, this generally results in the addition of air-gaps in the stator core when the machine is put together. When selecting the segment topology two important factors should be considered - the reduction in the electrical performance due to the additional air-gaps, and the weight of each segment which has a bearing on the ease of field maintenance.

The segment topologies described here are from the point of view of radial flux machines. The first topology described in fig. 6.4a is built up of stator E-core blocks with concentrated tooth wound windings. This is the design proposed by Spooner *et al.* in [13–15]. Li *et al.* have carried out further investigations on such a configuration (with small machines) including the effect of different winding and tooth designs [47, 63].

(a) Topology 1 **(b)** Topology 2

Figure 6.4 E-core and Tooth-cored segment with single concentrated tooth wound windings

Studies performed on linear PM machines gave rise to similar results [58, 64]. While many of these studies considered the additional flux gaps as the unwanted but inevitable, by-products of the manufacture of segmented motors, this chapter proposes these flux gaps as a way to create generators with replaceable stator core modules leading to more maintainable machines.

As the replaceability of the winding is the principal factor for going in for segmentation, this can be enhanced by the use of tooth segments as shown in fig. 6.4b. Here, as the tooth and winding alone form the replaceable part, such systems allow the smallest segments which mean they are the easiest to replace. However, the addition of an air-gap directly in the flux path would mean that the performance of the machine is significantly affected,

Since the segmentation discussed in this section aims to ease the process of removal of faulty

segments, the size of the stator air-gaps should be chosen taking into account this removal process. For the E-core structure larger air-gaps would facilitate easy removal and as the added air-gaps are not directly in the flux paths, this would not have a considerable effect on the electrical performance. For the tooth core structures the tooth has to be mechanically supported by the core. These supporting structures (for example bolting systems) would on one hand reduce the air-gap lengths, improving the electrical performance, but on the other hand would reduce the ease of removal of these segments. Further, the forces on the tooth would make the structural system very challenging. For these reasons the tooth core topology is a poor choice.

Another possible topology is to have segments built-up of a set of three phase windings as shown in fig. 6.5a and fig. 6.5b. The use of three phase segments gives the freedom to choose between distributed winding and modular winding designs. In such systems fault tolerance requirements, like magnetic isolation and physical isolation, are maintained between the three phase segments and not between the individual windings.

(a) Topology 3 **(b)** Topology 4

Figure 6.5 Three phase segmented stator cores.

The use of segments built-up of three phase windings give rise to another winding possibility. While topologies 3 and 4 utilised single layer windings, there is the possibility of using double layer windings as well. However, for a replaceable core the tooth wound winding cannot be wound around a tooth with a segmentation gap, this would lead to a configuration where certain slot positions would remain empty leading to a degraded performance.

Another possibility is the placement of these gaps in the yoke. Although the use of these 'T-cores' may not be optimal from the magnetic circuit point of view (as in the case of the tooth segments), they could aid in the ease of manufacture and increasing the fill factor of the slots as reported in [65] where fill factors of 78% were achieved. Fig. 6.6a and fig. 6.6b give examples of such configurations. The performance parameters, such as cogging torque, for a similar configuration was investigated in [56] and [57] which showed the increase in the cogging torque with the introduction of these additional gaps.

It has already been discussed that the electrical performance is an important consideration when a topology is being selected. To illustrate the effect that different segment topologies may have on the performance of a machine, the E-core and tooth-core topology was compared with a non segmented machine. The compared machines are based on the design proposed by Polinder *et al.* for direct drive wind turbines [66] with permanent magnets. The given design is used to create a machine with a modular winding (q=0.4) by only changing the number of slots in the design. In this machine additional air-gaps are added to create E-cored and tooth-cored machines and

(a) Topology 6 **(b)** Topology 7

Figure 6.6 Segmentation with flux gaps in the stator yoke.

their rated air-gap power is compared. For the E-core machine a stator air-gap length equal to the air-gap is used, while for the tooth core machine the stator air-gap is one-fifth of the air-gap. For tooth cored machines it was found that the rated air-gap power was reduced to 87% of the non-segmented machine under identical conditions while this was only reduced to 96% for the E-core machine. These results show that the modular tooth-core topology would require larger generator sizing for the same rated power which brings into question their usefulness.

Second, the logistics of replacing segments must be considered. Here, the weight of each segment would be an important factor. Table 6.1 compares the weight of a single stator segment for a 3MW wind turbine without considering any structural mass. Here too the design is based on the paper by Polinder *et al.* [66] and is modified for the chapter as described above.

Table 6.1 Active weight of each stator segment

Modular E-core	Modular Tooth-core	Modular E-core 3-Ph Seg	Distributed E-core 3-Ph Seg
200 kg	110 kg	600 kg	250 kg

Even though the tooth-core machines have the possibility of the lightest segments, the issues with such a design that have already been discussed in this section make the modular E-core and the distributed three phase E-core the more viable designs.

6.3.2 Support Structures

For large wind turbines the inactive structural elements become dominant [67, 68], therefore, the support structure is an import factor for generator design. This becomes especially challenging for segmented machines as the increase in the number of separate parts adds to the complexity of the structural design.

The structure in the generator is required to be stiff and robust to maintain the small air-gap clearances. This has to be done against the force of gravity and the forces of attraction between the stator and rotor [69]. There are two major forces to be considered - the shear stress and

normal stress. In generators with large air-gap flux density (greater than 0.8T), the normal stress is approximately ten times that of the shear stress [70]. In machines constructed with a view to make these segments easily replaceable, these stresses would mean that each segment would need to be supported by structure independently as proposed by Spooner *et al.* in [13–15] described in fig. 6.7a.

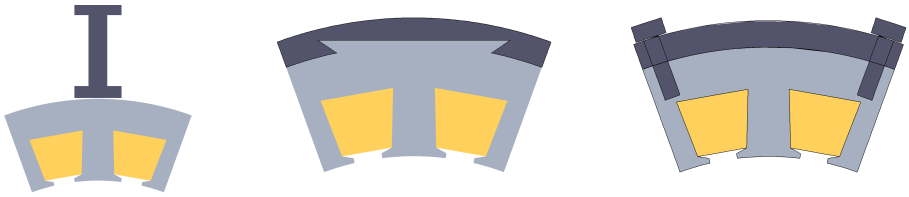

(a) **(b)** **(c)**

Figure 6.7 Support Structures for Segmented Machines.

Another possibility is to use an outer housing as has been used for smaller machines [47,59,63,71]. In such a structure the segment may be attached by a groove type structure as shown in fig. 6.7b, by a number of bolts as shown in fig. 6.7c, and using adhesives as is commonly used to attach the rotor magnets to the rotor iron structure. However, the use of an adhesive may not be ideal when replaceability is an aim of segmentation.

One of the ways to reduce the dominant normal stress, which may be beneficial for segmented generators, is the use of iron-less stators [72, 73]. With the elimination of iron in the stator the direct magnetic attraction between the stator and rotor iron is eliminated and the lighter structures are still capable of carrying the shear stresses in the machine. Such designs have a much lower working flux density and hence need to be much larger. Spooner *et al.* in a comparison showed that even though the air-gap diameters of such iron-less machines may be approximately three times the diameter of a conventional direct drive machine, they are lighter as they do not have to stand the normal stresses [72]. However, this large increase in size raises questions about the ease of replacing segments in case of a failure as well as the feasibility of such designs for large direct drive wind turbines.

Other concepts have been proposed in literature, such as the NewGen configuration [74] and the use of magnetic bearings [75], where the bearings are placed adjacent to the air-gap leading to lower stiffness requirements and in turn saving in structural mass. The development of such concepts could also be used to make the design of segmented direct drive machines lighter and simpler.

6.4 Extreme Modularity in Converters

This section investigates modularity in the power electronic converter of wind turbines. The previous chapters investigated temperature driven failure mechanisms. The following analysis takes a step back and looks at failure mechanisms that may not be addressed in the design. Therefore, it takes a constant failure rate without considering the source or mechanism of failure.

It starts by making a number of simplifying assumptions and then adding the required complexity in steps. The converter system is assumed to be built-up of independent and identical parallel modules, such that the failure in one has no effect on the performance of the other. The failure rate is denoted by λ, which is identical for each module and is assumed to be constant (this may be thought of as the continuous failure region of the bathtub curve [76]). To begin with, it is also assumed that the failure rate is independent of the rating of the module. As an example, if λ is the failure rate with a single module, the failure rate with N modules will be $N \times \lambda$. Furthermore, the rate of repair is denoted by μ.

Although Markov chains can be used to calculate probabilities of a system being in each state, it is easier to compare systems if they are defined by a single performance index. One such index used in this thesis is the equivalent availability, given by

$$A_{eq} = \frac{\sum_{k=0}^{k=N} P_k p_k}{P}, \tag{6.1}$$

where N is the total number of modules, P_k is the power output of $State-k$ with a probability of p_k, and P is the rated power of the complete converter system. As an illustration, consider a case of a system with N identical modules with a combined power rating of P such that each module has a rating of $\frac{P}{N}$. The system has states from 0 to N, with $State-0$ representing no failure (power production of P) and having a probability of occurrence of p_0 and $State-k$ representing failures in k modules (resulting in a power production of $\frac{N-k}{N}P$) with a probability of occurrence given by p_k. The effective availability of this system would be given by

$$\begin{aligned} A_{eq} = (P \cdot p_0 + \frac{N-1}{N} P \cdot p_1 + \cdots + \frac{N-k}{N} P \cdot p_k + \cdots \\ \cdots + \frac{1}{N} P \cdot p_{N-1}) / P, \end{aligned} \tag{6.2}$$

or in a vectorised form

$$A_{eq} = \mathbf{P^T} \cdot \mathbf{p}, \tag{6.3}$$

with the power fraction vector ($\mathbf{P}$) and the state probability vector ($\mathbf{p}$).

6.4.1 System with Continuous Repair

The simplest case is the case where the system is repaired once there is a failure with a repair rate of μ. The Markov state space model with reduced states is given in Fig. 6.8.

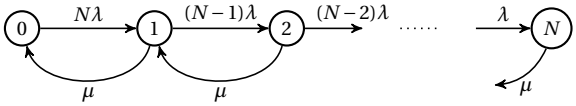

Figure 6.8 Reduced state Markov chain with continuous repair.

It can be shown that in this case the equivalent availability is independent of the number of modules [24], and is given by

$$A_{eq} = \frac{\mu}{\mu + \lambda}. \tag{6.4}$$

While there is no improvement in the equivalent availability of the converter system by adding modularity, the actual cost of repair would be higher because of an increased failure rate. This, however, is an impractical case as the basis of the introduction of modularity is to make the system fault tolerant and reduce the necessity of immediate repair.

6.4.2 System with Periodic Repair

One method to reduce the operating cost of a wind turbine is to eliminate unscheduled visits and only allow periodic scheduled maintenance. This would require the fault modules to go 'off-line'while the healthy modules continue operation. All failed modules would be replaced in the periodic maintenance visit. Fig. 6.9a shows the expected availability of this system in time. The Markov state space representation of such a system is shown schematically in Fig. 6.9b with the system being reset to state 0 when $t = T_m$. Here the time taken for the maintenance is neglected. This is based on the assumption that the time for replacing the converters are much smaller than the maintenance period, due to which it is also assumed that the time for replacement is independent of the number of modules to be replaced. In this case too the effective availability remains independent of the number of modules.

The effective availability used to this point has only considered rated power conditions in its calculations and disregarded partial loading. Such a method is equivalent to derating the power curve in the event of module failure. However, wind turbines regularly operate at partial loads. This fact can be used to improve performance by allowing healthy modules to take a larger load in such partial loading conditions, while still remaining below the rated power of each module. The difference between these two approaches is highlighted using power curves in Fig. 6.10.

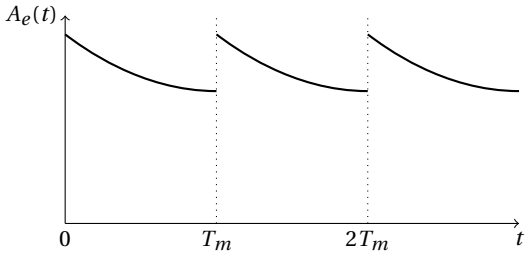

(a) Plot of Availability with time. T_m represents the occurance of the periodic maintenance event.

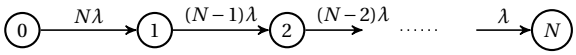

(b) Complete Markov chain

Figure 6.9 System with periodic repair.

Fig. 6.10b shows that the operating region of the system at any $State-k$ (i.e. a condition where k modules have failed) has three regions:

- $v < v_{corner}$, where the net power output is equal to the unfaulted condition (this is achieved by allowing the healthy modules to take a larger share of the power while keeping this value lower than the rating of each module). This v_{corner} is defined as the wind speed where the module processes a current equal to its rated current, and is the 'corner' wind speed between two regions. In this region, the turbine generates a torque equal to a condition with no faults. At $v = v_{corner}$, the turbine generates rated torque.

- $v_{corner} < v < v_{rated}$, where the torque is maintained at the rated value. The power increases linearly with the rotational speed.

- $v > v_{rated}$, where the torque and speed are maintained at the rated value. The power output in this region is given by $\frac{N-k}{N} P_{rated}$.

As $T \propto v_{wind}^2$, v_{corner} for $State-k$ can be given by,

$$v_{corner}(k) = \left(\frac{N-k}{N}\right)^{\frac{1}{2}} \cdot v_{rated} \tag{6.5}$$

Given that the wind velocity is characterised by a Weibull distribution with a shape factor a, and

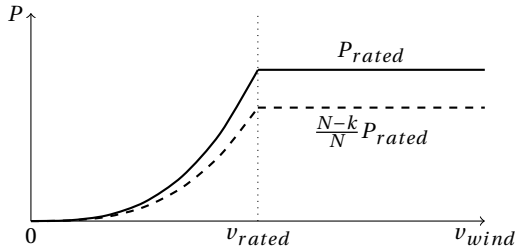

(a) Power curve of a turbine with derating in case of module failure. The dashed line describes a turbine operating with failures in k modules with each module processing a power of $\frac{P}{N}$ resulting in a net turbine power of $\frac{N-k}{N}P$.

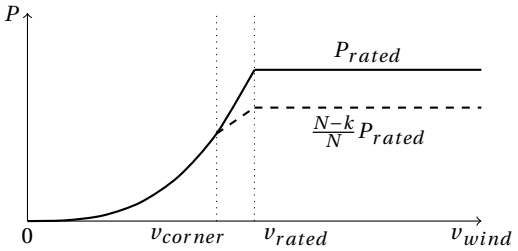

(b) Power curve of a turbine considering partial loading. The dashed line describes a turbine operating with failures in k modules with each modules processing a power of $\frac{P}{N-k}$ till v_{corner} and $\frac{P_{rated}}{N}$ after v_{rated}.

Figure 6.10 System with periodic repair.

scale factor b, the power fraction vector can be updated using (6.6)–(6.7):

$$P(k) = \frac{\int_0^{v_c} P_g(v) f(v,a,b)\,dv + \int_{v_c}^{v_r} P_l(v) f(v,a,b)\,dv}{\int_0^{v_r} P_g(v) f(v,a,b)\,dv + \int_{v_r}^{\infty} P_r f(v,a,b)\,dv}$$
$$\cdots + \frac{\int_{v_r}^{\infty} \frac{N-k}{N} P_r f(v,a,b)\,dv}{\int_0^{v_r} P_g(v) f(v,a,b)\,dv + \int_{v_r}^{\infty} P_r f(v,a,b)\,dv},$$
$$P(k) = \frac{g(v_c, v_r, a, b, k)}{h(v_r, a, b)}, \tag{6.6}$$

with

$$g(v, v_r, a, b, k) = \left(\frac{b}{v_r}\right)^3 \left\{\frac{3}{a}\Gamma\left(\frac{3}{a}\right)\gamma\left(\left(\frac{v}{b}\right)^a, \frac{3}{a}\right)\right\} + \frac{N-k}{N} \cdot$$
$$\frac{b}{v_r a}\Gamma\left(\frac{1}{a}\right)\left\{\gamma\left(\left(\frac{v_r}{b}\right)^a, \frac{3}{a}\right) - \gamma\left(\left(\frac{v}{b}\right)^a, \frac{3}{a}\right)\right)\right\},$$
$$h(v, a, b) = \left(\frac{b}{v_r}\right)^3 \left\{\frac{3}{a}\Gamma\left(\frac{3}{a}\right)\gamma\left(\left(\frac{v}{b}\right)^a, \frac{3}{a}\right)\right\}, \tag{6.7}$$

where $P_g(v)$ is the power curve of the generator system as a function of wind velocity, P_l is the linear power curve when $v_{corner} < v < v_{rated}$, $f(v,a,b)$ is the Weibull probability function with parameters a and b. $\Gamma(x)$ is the Gamma function and $\gamma(x,y)$ is the Incomplete Gamma function. The appendix explains the method used to obtain these results in more detail. No cut-out wind velocity is considered to simplify the expressions and the error due to this assumption is minimised by the use of the Weibull distribution which has an almost zero occurrence for higher wind speeds.

This power fraction vector depends on the number of modules. The increase in the power fraction vector for an increase in the number of modules is estimated using $\frac{dP(k)}{dN}$. From (6.5)–(6.7), this can be calculated to be

$$\begin{aligned}\frac{dP(k)}{dN} &\propto \frac{d}{dN}\gamma\left(\left(\frac{v_c}{b}\right)^a, \frac{3}{a}\right),\\ \frac{dP(k)}{dN} &\propto \frac{k}{N^2}\left\{\gamma\left(\left(\frac{v_c}{b}\right)^a, \frac{3}{a}\right) + \left(\frac{N-k}{N}\right)^{\frac{1}{3}} \cdots \right.\\ &\qquad \left.\left(ln\left(\frac{3}{a}\right)\cdot\gamma\left(\left(\frac{v_c}{b}\right)^a, \frac{3}{a}\right) + \frac{3}{a}\cdot T\left(3, \left(\frac{v_c}{a}\right)^a, \frac{3}{a}\right)\right)\right\},\end{aligned} \tag{6.8}$$

where T is the Meijer G-function [77]. This expression advances two important conclusions; $P(k)$ is monotonically increasing, and the magnitude of this increase decreases with an increase in N. These conclusions can be extended to the equivalent availability, as the equivalent availability is a function of the power fraction and the state probability.

This model is now used to quantify the effect of the number of modules on the effective availability. The parameters used in the model are given in Table 6.2.

Table 6.2 Modeling Parameters

Wind Speed Weibull Distribution		
Shape Parameter	a	2.1
Scale Parameter	b	11.29 m/s
Average Wind Speed	v_{avg}	10 m/s
Maintenance Parameters		
Failure Rate	λ	0.2 turbine^{-1}year^{-1}
Maintenance Period	T_m	1 year
Turbine Parameters		
Rated Wind Speed	v_{rated}	12 m/s

The variation of the effective availability (A_e) in time is shown in Fig. 6.11 with two different number of modules. This shows that an increase in the number of modules (N) leads to an increase in effective availability.

If this effective availability is averaged over one maintenance period (T_m), the resulting 'averaged effective availability' ($A_{e,avg}$) for different modular configurations can be compared. This is shown in Fig. 6.12. The figure shows that the expected improvement in the availability in the converter system is small for successive increments in the number of modules once $N > 20$ for the simplified model considered here, as can be expected based on (6.8).

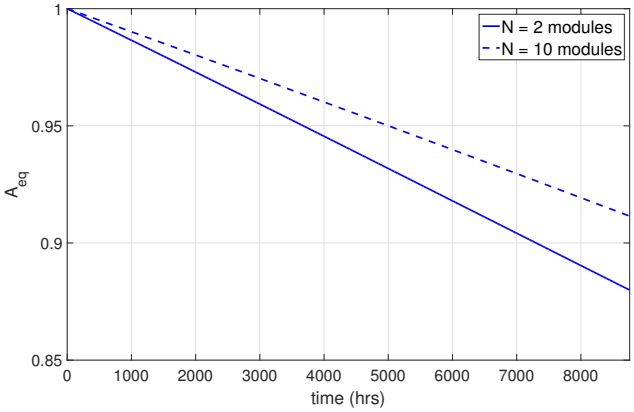

Figure 6.11 The effective availability of the converter system with time over one maintenance period T_m. An increase in the number of modules leads to a greater effective availability.

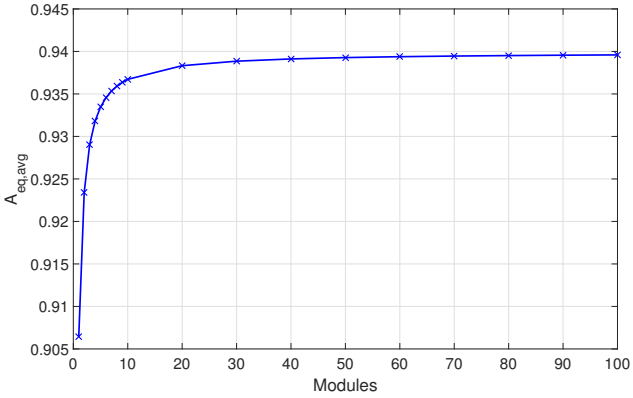

Figure 6.12 The effect of the number of modules on the effective availability averaged over one maintenance period.

Effect of Failure Rates (λ)

The failure rates of the converter modules impacts the availability of the turbine. There have been a number of studies that have studied the failure rates of wind turbine converters. *Spinato et al.* propose a failure rate of 0.2 turbine^{-1}year^{-1} based on the data from the LWK study in [3] while noting that the failure rates of converters from industrial experience are between 0.045-0.2 item^{-1}year^{-1} [3, 78]. Fig. 6.13 plots the effect of module numbers on effective availability for a few failure rates within this range.

It is logical that a higher failure rate results in a reduced effective availability. However, it is also

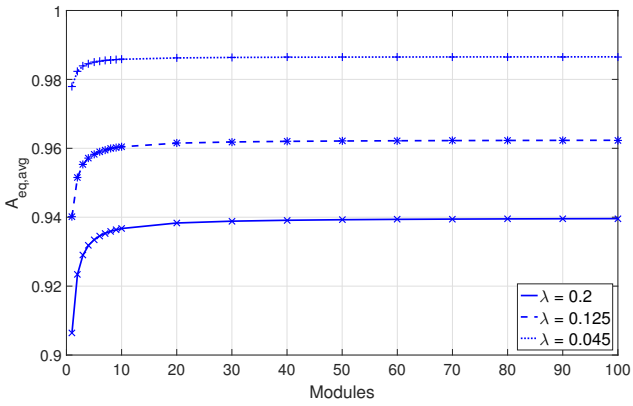

Figure 6.13 The effect of the number of modules on the effective availability averaged over one maintenance period for different failure rates and T_m = 1 year.

seen here that the improvement due to the addition of modules is larger for larger failure rates. Therefore, modularity is more important when the higher failure rates are considered. This too is an intuitive result. Table 6.3 shows the improvements achieved when increasing the number of modules from 20 to 100 for different failure rates. It also shows the absolute values for availability with 20 modules. As the probability of the system being in a failed state is strongly proportional to the failure rate (λ), the variation of $A_{N=20}$ with λ is linear as well.

Table 6.3 Improvement in Availability for extensive modularity (wrt λ)

	T_m = 1 year		
Failure Rate λ	$A_{N=20}$	ΔA_{eq}	$A_{N=100}$ - $A_{N=20}$
λ = 0.045	0.9862	0.0087	0.0004
λ = 0.125	0.9615	0.0222	0.0008
λ = 0.200	0.9383	0.0331	0.0013

ΔA_{eq} is the net increase in the average equivalent availability ($A_{e,avg}$) when the number of modules are changed from $N = 1$ to $N = 100$.

Effect of Maintenance Periods (T_m)

The maintenance period (T_m) is an important consideration for the cost of energy of wind turbines. Enforcing periodic scheduled maintenance is a way of reducing maintenance costs. With this constraint, modular design can play a role in increasing the availability of the converter system.

Fig. 6.14 plots the availability over number of modules for three different periodic maintenance strategies.

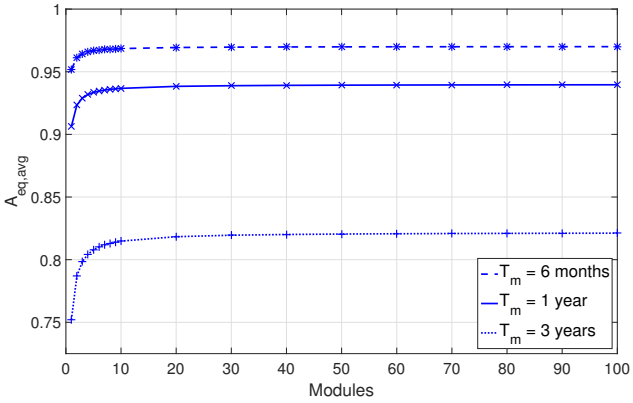

Figure 6.14 The effect of the number of modules on the effective availability averaged over one maintenance period for different maintenance periods and $\lambda = 0.2$ turbine^{-1}year^{-1}.

Table 6.4 Improvement in Availability for extensive modularity (wrt T_m)

	$\lambda = 0.2$		
Failure Rate T_m	$A_{N=20}$	ΔA_{eq}	$A_{N=100}$ - $A_{N=20}$
T_m = 6 months	0.9693	0.0182	0.0007
T_m = 1 year	0.9383	0.0331	0.0013
T_m = 3 years	0.8183	0.0692	0.0049

Again, modularity is more important when the higher periods for maintenance (T_m) are considered. Table 6.4 shows the small improvements achieved when increasing the number of modules from 20 to 100 for different failure rates. As with the previous case, the variation of $A_{N=20}$ with T_m is almost linear.

Effect of Wind Speed Distribution

It has been discussed that under partial loading conditions, the modular system of converters can process a larger amount of power with failures (compared to a non modular system). Fig. 6.10b shows that this improvement is dependant on the corner wind velocity (also seen from (6.7)). Therefore, a wind speed distribution with a concentration on the lower wind speeds will have a higher improvement with the inclusion of modularity. The shape factor will have a similar effect on availability improvement. Fig. 6.15 shows the effect of modularity with three different wind speed distributions.

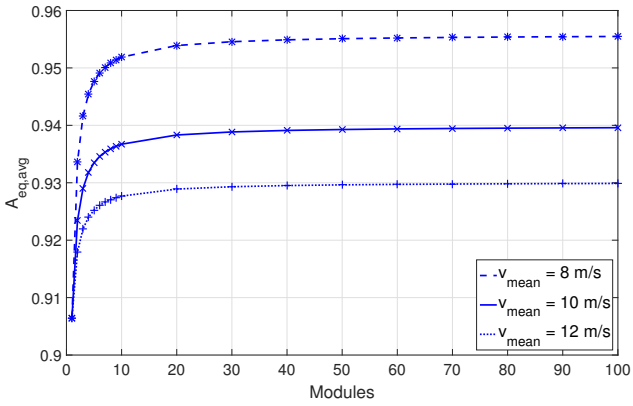

Figure 6.15 The effect of the number of modules on the effective availability averaged over one maintenance period for different wind speed profiles with different mean wind speeds. The rated wind speed of the turbine is maintained at 12m/s and $\lambda = 0.2$ turbine^{-1}year^{-1}.

Table 6.5 Improvement in Availability for extensive modularity (wrt $\bar{v}$)

	$T_m = 1$ year $\lambda = 0.2$		
Mean Wind Speed $\bar{v}$	$A_{N=20}$	ΔA_{eq}	$A_{N=100}$ - $A_{N=20}$
$\bar{v} = 8$ m/s	0.9539	0.0490	0.0016
$\bar{v} = 10$ m/s	0.9383	0.0331	0.0013
$\bar{v} = 12$ m/s	0.9289	0.0234	0.0010

Discussion on Systems with Periodic Repair

The study in the previous sections gives rise to a number of properties that are important to consider for the design of such systems.

- An improvement in equivalent availability for modular systems requires some form of over-rating or redundancy. This results in a system that can handle a larger fraction of power than the fraction of modules that are healthy.
- As a significant portion of the operation of a wind turbines is with partial loading, the above requirement is met without the need of either over-rating or additional redundant modules.
- The improvement in equivalent availability reduces with the addition of each additional module. This improvement varies inversely with the number of modules.
- With the number of modules exceeding 10-20, the improvements become such a small fraction of the availability that extreme modularity grants no significant benefit.

- Wind speed distributions with lower mean speeds experience a larger improvement in availability with modularity. This is as such distributions favour partial loading conditions, allowing effective exploitation of modularity.

6.4.3 Systems with Modularity Dependant Failure Rates

The previous analysis considered constant failure rates. This section builds on the analysis by considering failure rates that depend on the extent of modularity. The first case considered, is where the failure rates reduce as a continuous function with the number of modules as shown in Fig. 6.16. A reason for such a variation could be the reduced power rating of each module as the number of modules is increased. As an example, the failure rate of industrial converters was found to have a lower failure rate (of 0.045 converter^{-1}year^{-1}) when relatively small converters were considered in [3]

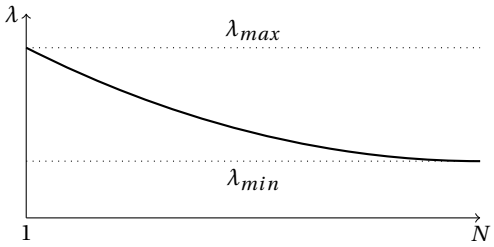

Figure 6.16 Failure rates as a continuous function of the extent of modularity

Another possibility is that the change in failure rates occur due to a change in technology. Examples of this could be the cooling system where as the power rating of the converter module reduces, the cooling system can be changed from a liquid cooled system to a air cooled system and finally to a passively cooled system. Each of these technology change steps could reduce the failure rates. Another example of this could be the use of PCB based converters when the power rating of the module is small enough which reduces the probability of connection failures. Such a case is shown in Fig. 6.17.

First, the failure rate is assumed to be a continuous function of the number of modules of the converter system. The analysis considers two curves; a linear, and an exponential function. These are limited between $\lambda = 0.2$ and $\lambda = 0.045$ which are the outer limits for converter failures in the study of wind turbine reliability in [3]. Second, the case of step changes in failure rates is considered. For this illustration, the step is considered at the point when ($N > 50$). The variation of the considered failure rates are shown in Fig. 6.18.

Fig. 6.19 shows the performance of modularity with the linear and exponential variable failure rate curves shown in the Fig. 6.18. The effect of extreme modularity is now notable. As the failure rate is dependant on the number of modules, and reduces with increasing modularity, the resulting

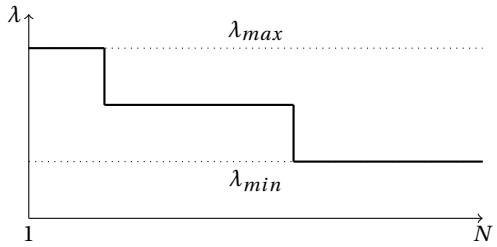

Figure 6.17 Failure rates as a step function of the extent of modularity

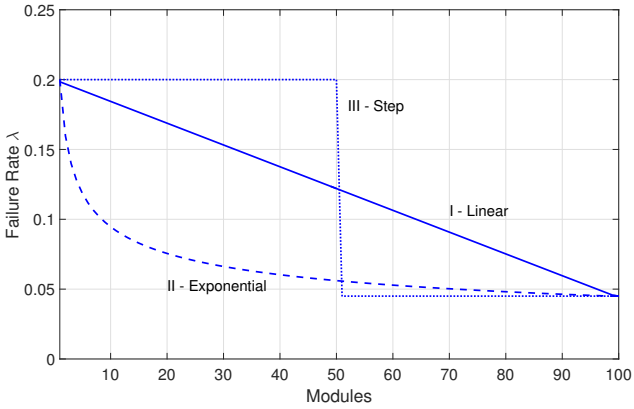

Figure 6.18 The failure rate curves

equivalent availability too improves with increasing modularity. The availability curve (Fig. 6.19) closely follows the failure rate curves ((Fig. 6.18)).

Fig. 6.20 shows the availability response to modularity for a system with a step change in failure rates. Here, the change is considered between a failure rate of 0.2 to 0.045 as shown in Fig. 6.18. turbine^{-1}year^{-1}.

The analysis in this section highlights the following considerations for systems with modularity dependant failure rates,

- The equivalent availability of such a system is strongly dependant on the failure rate curve.
- Extreme modularity is now an option that merits consideration as it can lead to larger improvements in the equivalent availability.

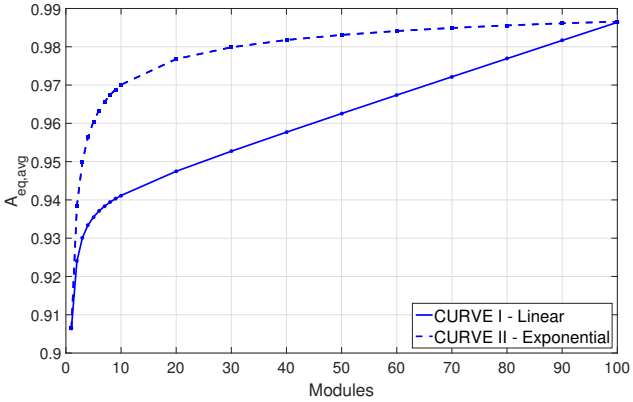

Figure 6.19 Equivalent Avialability with continuous function failure rates that depend on the number of modules.

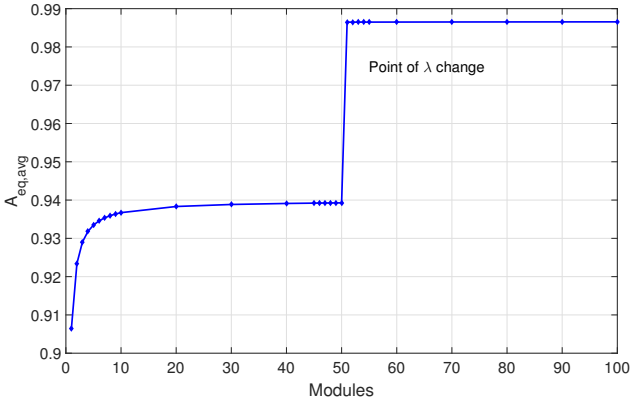

Figure 6.20 Equivalent Avialability with step function-like failure rates that depend on the number of modules. For this illustrative example, the step is considered at the point when $N > 50$

6.4.4 Case Study of 10MW turbine

In this section, a case study is analysed to quantify the influence of modularity. These case studies only consider periodic scheduled maintenance because such systems are desirable, as they reduce logistic costs of maintenance.

A 10MW wind turbine as designed in [79] with an annual energy yield of 48.4 GWh (for a wind speed distribution with $\bar{v}$= 10 m/s) is utilised for the study. Furthermore, a failure rate of $\lambda = 0.593$ failures turbine^{-1}year^{-1} are considered. This value from [5] is for liquid cooled full scale converters. Fig. 6.21 plots the annual energy yield for different maintenance periods (T_m) and number of

modules (N). In this case the availability of the rest of the turbine is assumed to be 1 and the variations in converter efficiency with modularity is ignored.

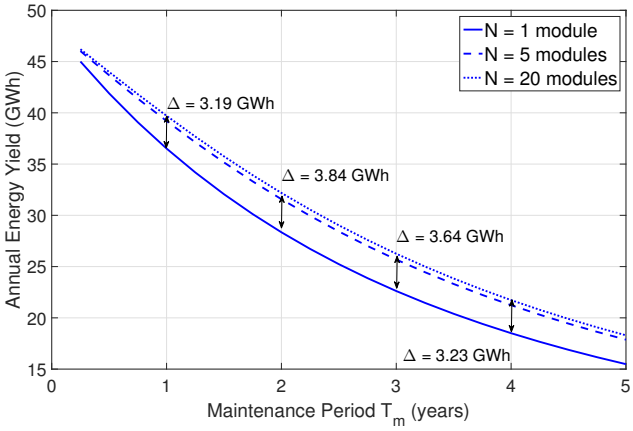

Figure 6.21 Annual energy yield for 1, 5, and 20 modules.

It was seen in Fig. 6.21 that the smaller the maintenance period, the better was the net energy yield, however, there will be a lower limit to this when the cost of maintenance trips and the cost of modularity are considered. Further, from the figure it is evident that modularity can be used to allow an increase in the maintenance period when compared to a case with no modularity. Table 6.6 marks the improvement possible in the maintenance period with the use of a converter system with 20 modules, while maintaining the same annual energy yield for the case studied above.

Table 6.6 Increased Maintenance periods with constant Annual Energy Yield

	Maintenance Period T_m (years)		
Annual Yield (GWh)	1 module	20 modules	Gain
45	0.24	0.39	62.5%
40	0.67	0.96	43.3%
35	1.16	1.60	37.9%

According to the study in [5], approximately 44% of the failures in the fully rated converters are due to the cooling system. With the introduction of extreme modularity, it is possible to implement thermal management for the converter using passive cooling. It can be hypothesised that this change would result in a reduction of the failure rate by approximately 44% as it eliminates a failure mode. A comparison of the annual energy yield when the number of modules are sufficient to allow passive cooling ($N = N_{passive}$) is presented in Fig. 6.22. $N_{passive}$ depends on a large

number of factors such as – device technology, modulation technique, switching frequency, placement in the nacelle, etc.

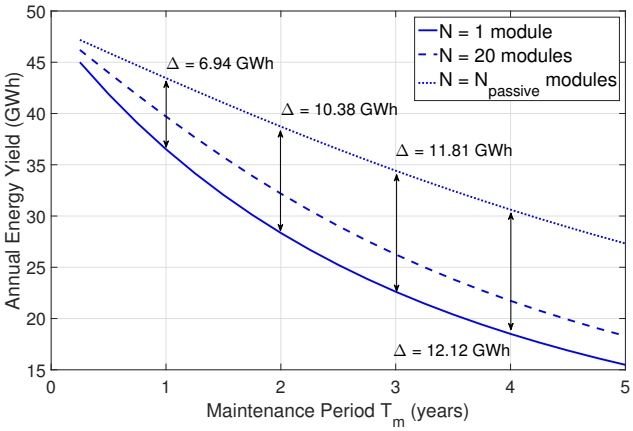

Figure 6.22 Annual energy yield with extreme modularity.

Furthermore, the possible increase in the maintenance period with the use of a converter system with $N_{passive}$ modules, while maintaining the same annual energy yield for the case studied above is presented in Table 6.7. The results show that extreme modularity, if it brings about a reduction in failure rates, can have a significant impact on the cost of energy.

Table 6.7 Increased Maintenance periods with constant Annual Energy Yield with the inclusion of extreme modularity

	Maintenance Period T_m (years)		
Annual Yield (GWh)	1 module	$N_{passive}$ modules	Gain
45	0.24	0.68	183.3%
40	0.67	1.72	156.7%
35	1.16	2.86	145.9%

The use of modular converters also has a number of consequences that are difficult to quantify for the range of modularity considered in this chapter. One such example is the cost of converters, which is affected by a large number of factors that can vary with the number of modules considered. These aspects are briefly addressed here:

- Harmonics — parallel modular converters can be used to eliminate PWM-harmonics [28]. This can result in reduced filter sizing [80, 81].

- Efficiency — this also gives rise to the possibility of choosing converters to operate close to rated power, thereby increasing efficiency [28]. Efficiency improvement can also be achieved when modularity allows a transition in the technology used. An example of this is depicted in [82] for a DC-DC converter, where an increase in modules allows a transition from IGBT to MOSFETS leading to an increase in the efficiency.
- Cost — this is a factor that is difficult to accurately estimate across the large range of modules considered in this chapter. Increased modularity generally results in an increase in costs. However, some consequences of modularity can reduce this cost burden. For example, the reduced filter sizing as well as a transition in technology as illustrated above can reduce the magnitude of the cost burden. Finally, increased modularity can also cause changes in manufacturing techniques (for example going from hand assembly to automation) which also has a bearing on the final cost of the converters.

6.5 Extreme Modularity in Generators

The generator is built up of independant and identical modules, so that the failure in one has no effect on the performance of the other. The failure rate is denoted by λ, which is identical for each module and is assumed constant (this may be thought of as the continuous failure region of the bathtub curve [76]). This type of modularity does not change the total number of windings in the generator. Therefore, the net failure rate remains constant. This means that the sum of failure rate of each module must add up to the net failure rate, leading the failure rate of each module to be λ / N, where λ is the net failure rate of the stator windings.

6.5.1 System with No Repair

Stator windings have a much lower rate of failure when compared to other components in a wind turbine but cause long downtimes. Therefore, this chapter first studies a case where functional modularity of stator windings is considered and no repair is performed on them.

The equivalent availability of the generator over a lifetime of 20 years is calculated considering downtimes due to failure rate - 0.0216 failures turbine^{-1}year^{-1}, or 0.432 downtimes per lifetime.

This is compared to the equivalent availability for a generator with extreme modularity and without repair. This system is represented with a Markov State Space model with reduced states in Figure 6.23.

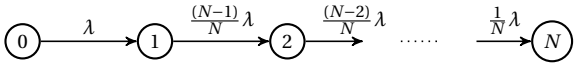

Figure 6.23 Reduced state Markov model for generator windings.

Further, there are two ways modularity can be utilised in this system. The first method derates the power curve when modules fail. However, wind turbines regularly operate at partial loads. This can be used to improve performance by allowing healthy modules, in such partial loading conditions, to take a larger load while still remaining below the rated power of each module. This is the second possible way in which modularity can be operated in the system. The difference between these two approaches is highlighted using power curves in Figure 6.10.

Figure 6.10b shows that the operating region of the system at any $State-k$ (i.e. a condition where k modules have failed) has three regions: one, with $v < v_{corner}$, where the net power output is equal to the unfaulted condition (this is achieved by allowing the healthy modules to take a larger share of the power while keeping this value lower than the rating of each module); the second, with $v_{corner} < v < v_{rated}$, where rated torque is maintained; the third, with $v > v_{rated}$, is the derated power curve region. As $T \propto v_{wind}^2$, the corner wind velocity for $State-k$ can be given by

$$v_{corner}(k) = \left(\frac{N-k}{N}\right)^{\frac{1}{2}} v_{rated}. \tag{6.9}$$

Figure 6.24, shows the comparison of equivalent availability with the two approaches discussed above. The results show that adding modularity to the generator results in an improved equivalent

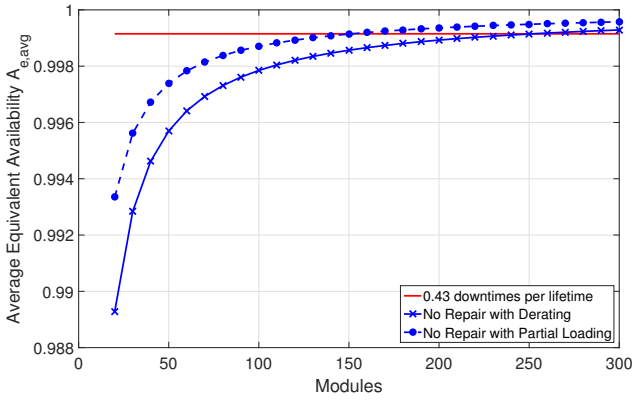

Figure 6.24 The effect of the number of modules on a - no repair - strategy. The solid blue line considers derating of the power converter with failures, depicted in Figure 6.10a, while the dashed blue line considers modules with partial loading leading to full power production upto corner wind speed as seen in Figure 6.10b, this is compared to the average availability when 0.43 downtimes of 345 hours per lifetime are considered. The equivalent availability is averaged over a lifetime of 20 years.

availability for cases when no repair is considered. When partial loading is considered, the equivalent availability of a generator with more than 150 modules and no-repair is better than that of a system with repair and no modularity (0.432 downtimes per lifetime with 345 hours per downtime). Therefore, the use of extreme modularity could make the no repair strategy

a feasible option for the generator, more so when repair costs are included into the analysis. Furthermore, the feasibility of this strategy increases with an increase in the downtime due to stator winding failures or an increase in repair costs, therefore, for offshore turbines and large direct-drive generators this strategy may be more meaningful.

6.6 Conclusions

This chapter has introduced some of the opportunities and challenges in the use of modular and segmented generator systems for large wind turbine generator systems. Though further investigation is required to make a firm conclusion on their suitability, such systems do seem to be promising with a view towards increasing turbine availability through fault tolerant operation as well as reduced downtimes.

The addition of modularity in the functional layer is a useful design concept for all large wind turbines. This step has fewer challenges to be overcome in its implementation and many wind turbines already use this to some extent. Functional modularity has a number of areas that provide opportunities for further investigation,

- The development of independent control modules that employ sensor-less control algorithms that would bring a higher tolerance to controller component failures as described in section 6.2.3
- The use and design of integrated thermal management systems to improve thermal performance of the system as described in section 6.2.4.
- The investigation of post-fault performance of modular winding and converter systems and the possibilities of the mitigation of any deleterious phenomenon as described in section 6.2.2.

The addition of modularity in the physical layer has to overcome a number of challenges. Physical modularity may be more suitable for offshore wind turbines where the cost of repair can be very high. Here too there are a number of opportunities for further investigation,

- The design of compact converters that can be replaced by a single worker without heavy lifting equipment as described in section 6.3.
- Section 6.3.1 describes a number of different topologies for segmentation in the generator, a detailed investigation comparing these topologies and reviewing their suitability for use in wind turbine generators is required.
- The support structure for a segmented generator is a big challenge. Further investigation into the requirements of these support structures and their design is needed.

Next, this chapter investigated the use of extreme modularity in a wind turbine converter system from the point of view of its availability. Based on the analysis a number of conclusions have been drawn for systems with failure rates that are constant and independent of module rating:

- For systems with continuous repair, modularity does not improve availability. In fact, modularity would increase the cost of repair as it would involve a higher number of maintenance visits.
- For systems with periodic repair, improvement in availability comes with some form of over-rating and modularity.
- As wind turbine systems often run at partial loading conditions, they are well suited to take advantage of this to improve availability without the need for either over-rating or redundancy.
- The improvement in availability reduces with each increment in the number of modules. The improvement after the number of modules exceeds 10-20 becomes insignificant.
- Therefore, extreme modularity does not offer any benefits when the failure rates are constant.

Further, the chapter analysed systems where the failure rates are dependant on the extent of modularity. This analysis concludes that:

- Extreme modularity may now be a viable option as it can lead to a reduction in failure rates and hence an improvement in the availability of the system.

In conclusion, extreme modularity for converter systems where failure rates are constant do not hold merit as they do not offer significant improvements in availability unless the failure rates can be reduced by introducing extreme modularity. Therefore, extreme modularity can be a powerful tool, but only when it is accompanied by a reduction in failure rates for converters. Also, the use of extreme modularity could make the no repair strategy a feasible option for the generator, more so when repair costs are included into the analysis.

Appendix

The power fraction vector gives the ratio of power produced in a $State-k$ to the power produced with no failures (or $State-0$). As discussed in Section 6.4.2, a modular wind turbine can produce power as per the origional power curve upto a corner wind speed v_c and uses a derated power for larger wind speeds. Therefore, the power fraction vector is defined by (6.6) where P_g is the power curve of the generator system as a function of wind velocity, P_l is the power curve when $v_{corner} < v < v_{rated}$, $f(v,a,b)$ is the Weibull probability function with parameters a and b and are given in (6.10).

$$\begin{aligned} P_g(v) &= P_r \cdot \left(\frac{v}{v_r}\right)^3 \\ P_l(v) &= P_g(v_c) + \frac{P_g(v_r) - P_g(v_c)}{v_r - v_c} \cdot v \\ f(v,a,b) &= \frac{a}{b} \cdot \left(\frac{v}{b}\right)^{a-1} \cdot exp\left(-\left(\frac{v}{b}\right)^a\right) \end{aligned} \tag{6.10}$$

where P_r and v_r are rated power and wind speed. Therefore,

$$g_1(v_c,a,b)=\int_0^{v_c} P_r\cdot\Big(\frac{v}{v_r}\Big)^3\cdot\frac{a}{b}\cdot\Big(\frac{v}{b}\Big)^{a-1}\cdot exp\Big(-\Big(\frac{v}{b}\Big)^a\Big)\,dv$$

using $x=(v/b)^a$ resulting in $dx=(a/b)\cdot(v/b)^{a-1}$, this simplifies to,

$$g_1(v_c,a,b)=\int_0^{(\frac{v_c}{b})^a}\frac{P_r\cdot b^3}{v_r^3}\cdot x^{\frac{3}{a}}\cdot exp(-x)\,dx \tag{6.11}$$

Using integration by parts, this results in,

$$\begin{aligned}g_1(v_c,a,b)=\frac{P_r\cdot b^3}{v_r^3}\cdot\Big\{&-x^{\frac{3}{a}}\cdot exp(-x)\Big]_0^{(\frac{v_c}{b})^a}\\&+\frac{3}{a}\cdot\int_0^{(\frac{v_c}{b})^a} exp(-x)\cdot x^{\frac{3}{a}-1}\,dx\Big\}\end{aligned} \tag{6.12}$$

which simplifies to,

$$\begin{aligned}g_1(v_c,a,b)=\frac{P_r\cdot b^3}{v_r^3}\cdot\Big\{&-\Big(\frac{v_c}{b}\Big)^3\cdot exp\Big(-\Big(\frac{v_c}{b}\Big)^a\Big)\\&+\frac{3}{a}\cdot\Gamma\Big(\frac{3}{a}\Big)\cdot\gamma\Big(\Big(\frac{v}{b}\Big)^a,\frac{3}{a}\Big)\Big\}\end{aligned} \tag{6.13}$$

where $\Gamma(x)$ is the Gamma functions, and $\gamma(x,y)$ is the Incomplete Gamma function, given by,

$$\gamma(x,y)=\frac{1}{\Gamma(y)}\int_0^x t^{y-1}\cdot exp(-t)\,dt \tag{6.14}$$

Similarly, g_2, and g_3 simplify to,

$$\begin{aligned}g_2=&\frac{N-k}{N}\frac{P_r}{v_r}\Big\{v_c exp\Big(-\Big(\frac{v_c}{b}\Big)^a\Big)-v_r exp\Big(-\Big(\frac{v_r}{b}\Big)^a\Big)\Big\}\cdots\\&+\frac{N-k}{k}\frac{P_r b}{v_r a}\Gamma\Big(\frac{1}{a}\Big)\Big\{\gamma\Big(\Big(\frac{v_r}{b}\Big)^a,\frac{1}{a}\Big)-\gamma\Big(\Big(\frac{v_c}{b}\Big)^a,\frac{1}{a}\Big)\Big\}\\g_3=&\frac{N-k}{N}\cdot P_r\cdot exp\Big(\Big(\frac{v_r}{b}\Big)^a\Big).\end{aligned} \tag{6.15}$$

The addition of these functions, g_1, g_2, and g_3, results in,

$$\begin{aligned}g=\Big(\frac{b}{v_r}\Big)^3\Big\{\frac{3}{a}\Gamma\Big(\frac{3}{a}\Big)\gamma\Big(\Big(\frac{v}{b}\Big)^a,\frac{3}{a}\Big)\Big\}+\frac{N-k}{N}\cdot\\\frac{b}{v_r a}\Gamma\Big(\frac{1}{a}\Big)\Big\{\gamma\Big(\Big(\frac{v_r}{b}\Big)^a,\frac{3}{a}\Big)-\gamma\Big(\Big(\frac{v}{b}\Big)^a,\frac{3}{a}\Big)\Big)\Big\}.\end{aligned} \tag{6.16}$$

When the power fraction vector is put together, it can be seen that it is independent of P_r but a function of a, b, k, and N.

Bibliography

[1] P. J. Tavner, G. J. W. V. Bussel, and F. Spinato, "Machine and converter reliabilities in wind turbines," in *2006 3rd IET International Conference on Power Electronics, Machines and Drives (PEMD 2006)*, April 2006, pp. 127–130.

[2] E. Echavarria, B. Hahn, G. J. W. van Bussel, and T. Tomiyama, "Reliability of wind turbine technology through time," *Journal of Solar Energy Engineering*, vol. 130, no. 3, p. 031005, 2008.

[3] F. Spinato, P. Tavner, G. van Bussel, and E. Koutoulakos, "Reliability of wind turbine subassemblies," *IET Renewable Power Generation*, vol. 3, no. 4, p. 387, 2009.

[4] P. Lyding, S. Faulstich, B. Hahn, and P. Tavner, "Reliability of the electrical parts of wind energy systems-a statistical evaluation of practical experiences," in *3rd EPE Wind Energy Chapter Symposium*, 2010, pp. 1–8.

[5] J. Carroll, A. McDonald, and D. McMillan, "Reliability comparison of wind turbines with DFIG and PMG drive trains," *IEEE Transactions on Energy Conversion*, vol. 30, no. 2, pp. 663–670, 2015.

[6] ——, "Failure rate, repair time and unscheduled O&M cost analysis of offshore wind turbines," *Wind Energy*, vol. 19, no. 6, 2015.

[7] ORE Catapult, "System Performance, Availability and Reliability Trend Analysis: Portfolio Review 2016," SPARTA Project, Tech. Rep., March 2017.

[8] U. Shipurkar, H. Polinder, and J. A. Ferreira, "Modularity in wind turbine generator systems – opportunities and challenges," in *2016 18th European Conference on Power Electronics and Applications (EPE'16 ECCE Europe)*, Sept 2016, pp. 1–10.

[9] T. Hjort, "Modular converter system with interchangeable converter modules," 2009, Patent WO/2009/027520.

[10] B. Andresen and J. Birk, "A high power density converter system for the Gamesa G10x 4.5 MW wind turbine," in *2007 European Conference on Power Electronics and Applications*, Sept 2007, pp. 1–8.

[11] N. R. Brown, T. M. Jahns, and R. D. Lorenz, "Power converter design for an integrated modular motor drive," in *2007 IEEE Industry Applications Annual Meeting*, Sept 2007, pp. 1322–1328.

[12] J. J. Wolmarans, M. B. Gerber, H. Polinder, S. W. H. de Haan, J. A. Ferreira, and D. Clarenbach, "A 50kw integrated fault tolerant permanent magnet machine and motor drive," pp. 345–351, June 2008.

[13] Z. Chen and E. Spooner, "A modular, permanent-magnet generator for variable speed wind turbines," in *1995 Seventh International Conference on Electrical Machines and Drives*, Sep 1995, pp. 453–457.

[14] E. Spooner and A. Williamson, "Modular, permanent-magnet wind-turbine generators," in *Thirty-First IAS Annual Meeting, Industry Applications Conference*, vol. 1. IEEE, 1996, pp. 497–502.

[15] E. Spooner, A. C. Williamson, and G. Catto, "Modular design of permanent-magnet generators for wind turbines," *IEE Proceedings - Electric Power Applications*, vol. 143, no. 5, pp. 388–395, Sep 1996.

[16] R. W. Butler and S. C. Johnson, "Techniques for modeling the reliability of fault-tolerant systems with the markov state-space approach," *NASA Reference Publication*, 1995.

[17] Y. Song and B. Wang, "Survey on reliability of power electronic systems," *IEEE Transactions on Power Electronics*, vol. 28, no. 1, pp. 591–604, 2013.

[18] S. Lee, L. Li, and J. Ni, "Markov-based maintenance planning considering repair time and periodic inspection," *Journal of Manufacturing Science and Engineering*, vol. 135, no. 3, p. 031013, 2013.

[19] G. Chan and S. Asgarpoor, "Optimum maintenance policy with markov processes," *Electric Power Systems Research*, vol. 76, no. 6, pp. 452–456, 2006.

[20] D. McMillan and G. W. Ault, "Techno-economic comparison of operational aspects for direct drive and gearbox-driven wind turbines," *IEEE Transactions on Energy Conversion*, vol. 25, no. 1, pp. 191–198, 2010.

[21] G. Wilson and D. McMillan, "Assessing wind farm reliability using weather dependent failure rates," in *Journal of Physics: Conference Series*, vol. 524, no. 1, 2014, p. 012181.

[22] C. W. Zhang, T. Zhang, N. Chen, and T. Jin, "Reliability modeling and analysis for a novel design of modular converter system of wind turbines," *Reliability Engineering & System Safety*, vol. 111, pp. 86–94, 2013.

[23] V. Najmi, J. Wang, R. Burgos, and D. Boroyevich, "Reliability modeling of capacitor bank for modular multilevel converter based on markov state-space model," in *2015 IEEE Applied Power Electronics Conference and Exposition (APEC)*, March 2015, pp. 2703–2709.

[24] A. McDonald and G. Jimmy, "Parallel wind turbine powertrains and their design for high availability," *IEEE Transactions on Sustainable Energy*, vol. 8, no. 2, pp. 880–890, 2017.

[25] C. Kim and S. Lee, "Redundancy determination of hvdc mmc modules," *Electronics*, vol. 4, no. 3, pp. 526–537, 2015.

[26] X. Yu and A. M. Khambadkone, "Reliability analysis and cost optimization of parallel-inverter system," *IEEE Transactions on Industrial Electronics*, vol. 59, no. 10, pp. 3881–3889, 2012.

[27] L. J. Mayor and R. C. Girones, "Electric power converter system with parallel units and fault tolerance," 2011, US Patent US/2014/0312704.

[28] J. Birk and B. Andresen, "Parallel-connected converters for optimizing efficiency, reliability and grid harmonics in a wind turbine," in *2007 European Conference on Power Electronics and Applications*, Sept 2007, pp. 1–7.

[29] T. Zhang and A. Zain, "Modular converter system reliability amp; performance analysis in design," in *The 2nd International Symposium on Power Electronics for Distributed Generation Systems*, June 2010, pp. 252–258.

[30] A. Wobben, "Wind power plant having a power generation redundancy system," 2005, US Patent US6946750.

[31] T. M. Jahns, "Improved reliability in solid-state ac drives by means of multiple independent phase drive units," *IEEE Transactions on Industry Applications*, vol. IA-16, no. 3, pp. 321–331, May 1980.

[32] D. Vizireanu, X. Kestelyn, S. Brisset, P. Brochet, Y. Milet, and D. Laloy, "Polyphased modular direct-drive wind turbine generator," in *2005 European Conference on Power Electronics and Applications*, Sept 2005, pp. P.1–P.9.

[33] A. Shea and T. M. Jahns, "Hardware integration for an integrated modular motor drive including distributed control," in *2014 IEEE Energy Conversion Congress and Exposition (ECCE)*, Sept 2014, pp. 4881–4887.

[34] M. D. Hennen, M. Niessen, C. Heyers, H. J. Brauer, and R. W. De Doncker, "Development and Control of an Integrated and Distributed Inverter for a Fault Tolerant Five-Phase Switched Reluctance Traction Drive," *Power Electronics, IEEE Transactions on*, vol. 27, no. 2, pp. 547–554, 2012.

[35] M. Zulqarnain, D. Xu, and B. Yuwen, "Multi modular converters with automatic interleaving for synchronous generator based wind energy system," in *The 7th International Power Electronics and Motion Control Conference*, vol. 3, June 2012, pp. 2255–2261.

[36] C. Ditmanson, P. Hein, S. Kolb, J. Mölck, and S. Bernet, "A new modular flux-switching permanent-magnet drive for large wind turbines," *IEEE Transactions on Industry Applications*, vol. 50, no. 6, pp. 3787–3794, Nov 2014.

[37] X. Yuan, Y. Li, J. Chai, and M. Ma, "A modular direct-drive permanent magnet wind generator system eliminating the grid-side transformer," in *2009 13th European Conference on Power Electronics and Applications*, Sept 2009, pp. 1–7.

[38] F. Deng and Z. Chen, "A new structure based on cascaded multilevel converter for variable speed wind turbine," in *IECON 2010 - 36th Annual Conference on IEEE Industrial Electronics Society*, Nov 2010, pp. 3167–3172.

[39] X. Yuan, J. Chai, and Y. Li, "A transformer-less high-power converter for large permanent magnet wind generator systems," *IEEE Transactions on Sustainable Energy*, vol. 3, no. 3, pp. 318–329, 2012.

[40] M. A. Parker, C. Ng, and L. Ran, "Fault-tolerant control for a modular generator – converter scheme for direct-drive wind turbines," *IEEE Transactions on Industrial Electronics*, vol. 58, no. 1, pp. 305–315, Jan 2011.

[41] S. S. Gjerde and T. M. Undeland, "Fault tolerance of a 10 MW, 100 kV transformerless offshore wind turbine concept with a modular converter system," in *2012 15th International Power Electronics and Motion Control Conference (EPE/PEMC)*, Sept 2012, pp. LS7c.3–1–LS7c.3–8.

[42] P. C. Loh, D. G. Holmes, and T. A. Lipo, "Implementation and control of distributed PWM cascaded multilevel inverters with minimal harmonic distortion and common-mode voltage," *IEEE Transactions on Power Electronics*, vol. 20, no. 1, pp. 90–99, Jan 2005.

[43] B. C. Mecrow, A. G. Jack, J. A. Haylock, and J. Coles, "Fault-tolerant permanent magnet machine drives," *IEE Proceedings - Electric Power Applications*, vol. 143, no. 6, pp. 437–442, Nov 1996.

[44] B. C. McCrow, A. G. Jack, D. J. Atkinson, and J. A. Haylock, "Fault tolerant drives for safety critical applications," in *IEE Colloquium on New Topologies for Permanent Magnet Machines*, Jun 1997, pp. 5/1–5/7.

[45] C. Noel, N. Takorabet, and F. Meibody-Tabar, "Short-circuit current reduction technique for surface mounted pm machines high torque-low speed applications," in *2004 39th IAS Annual Meeting Industry Applications Conference*, vol. 3, Oct 2004, pp. 1427–1433.

[46] B. Vaseghi, N. Takorabet, and F. Meibody-Tabar, "Short-circuit current reduction of pm motors by magnet segmentation technique," in *2010 14th Biennial IEEE Conference on Electromagnetic Field Computation*, May 2010, pp. 1–1.

[47] G. Li, Z. Zhu, W. Chu, M. Foster, and D. Stone, "Influence of flux gaps on electromagnetic performance of novel modular PM machines," *IEEE Transactions on Energy Conversion*, vol. 29, no. 3, pp. 716–726, 2014.

[48] T. Laakkonen, V. Naumanen, J. Luukko, and J. Ahola, "Universal control scheme for power electronics building-block-based cascaded multilevel inverters," in *2009 35th Annual Conference of IEEE Industrial Electronics*, Nov 2009, pp. 931–936.

[49] T. Laakkonen, "Distributed control architecture of power electronics building-block-based frequency converters," Ph.D. dissertation, Lappeenranta University of Technology, 2010.

[50] W. Liu, R. Jayakar, W. Song, and A. Q. Huang, "A modular digital controller architecture for multi-node high power converter applications," in *2005 31st Annual Conference of IEEE Industrial Electronics Society (IECON)*, Nov 2005, pp. 715–720.

[51] W. Song, Z. Yang, Y. Liu, A. Huang, and B. Chen, "A layered modular controller structure for multilevel converters," in *2007 IEEE Power Electronics Specialists Conference*, June 2007, pp. 1448–1452.

[52] C. Lv, M. K. Muhammad, Z. Lv, and C. Li, "Hierarchical structure of multi-modular converter system and modularized design scheme," in *2014 International Power Electronics and Application Conference and Exposition*, Nov 2014, pp. 800–804.

[53] M. A. Parker, L. Ran, and S. J. Finney, "Distributed control of a fault-tolerant modular multilevel inverter for direct-drive wind turbine grid interfacing," *IEEE Transactions on Industrial Electronics*, vol. 60, no. 2, pp. 509–522, 2013.

[54] G. Choi, Z. Xu, M. Li, S. Gupta, T. Jahns, F. Wang, N. A. Duffie, and L. Marlino, "Development of Integrated Modular Motor Drive for Traction Applications," *SAE Int. Journal of Engines*, vol. 4, no. 1, pp. 286–300, 2011.

[55] U. Shipurkar, K. Ma, H. Polinder, F. Blaabjerg, and J. A. Ferreira, "A review of failure mechanisms in wind turbine generator systems," in *2015 17th European Conference on Power Electronics and Applications (EPE'15 ECCE-Europe)*, Sept 2015, pp. 1–10.

[56] Z. Q. Zhu, Z. Azar, and G. Ombach, "Influence of additional air gaps between stator segments on cogging torque of permanent-magnet machines having modular stators," *IEEE Transactions on Magnetics*, vol. 48, no. 6, pp. 2049–2055, 2012.

[57] J. Yuan, C. W. Shi, and J. X. Shen, "Analysis of cogging torque in surface-mounted permanent magnet machines with segmented stators," in *2014 17th International Conference on Electrical Machines and Systems (ICEMS)*, Oct 2014, pp. 2513–2516.

[58] J. Shi, H. Kong, L. Huang, Q. Lu, and Y. Ye, "Influence of flux gaps on the performance of modular pm linear synchronous motors," in *2014 17th International Conference on Electrical Machines and Systems (ICEMS)*, Oct 2014, pp. 1566–1571.

[59] J. Brettschneider, R. Spitzner, and R. Boehm, "Flexible mass production concept for segmented bldc stators," in *2013 3rd International Electric Drives Production Conference (EDPC)*, Oct 2013, pp. 1–8.

[60] B. Bickel, J. Franke, and T. Albrecht, "Manufacturing cell for winding and assembling a segmented stator of pm-synchronous machines for hybrid vehicles," in *2012 2nd International Electric Drives Production Conference (EDPC)*, Oct 2012, pp. 1–5.

[61] K. Alewine and W. Chen, "A review of electrical winding failures in wind turbine generators," *IEEE Electrical Insulation Magazine*, vol. 28, no. 4, pp. 8–13, July 2012.

[62] T. A. Keim, P. Mongeau, and T. Dade, "Detachable magnet carrier for permanent magnet motor," 1998, US Patent US5831365.

[63] G. J. Li, Z. Q. Zhu, M. P. Foster, D. A. Stone, and H. L. Zhan, "Modular Permanent-Magnet Machines with Alternate Teeth Having Tooth Tips," *IEEE Transactions on Industrial Electronics*, vol. 62, no. 10, pp. 6120–6130, 2015.

[64] M. J. Jin, C. F. Wang, J. X. Shen, and B. Xia, "A modular permanent-magnet flux-switching linear machine with fault-tolerant capability," *IEEE Transactions on Magnetics*, vol. 45, no. 8, pp. 3179–3186, 2009.

[65] A. G. Jack, B. C. Mecrow, P. G. Dickinson, D. Stephenson, J. S. Burdess, N. Fawcett, and J. T. Evans, "Permanent-magnet machines with powdered iron cores and prepressed windings," *IEEE Transactions on Industry Applications*, vol. 36, no. 4, pp. 1077–1084, 2000.

[66] H. Polinder, F. F. A. Van Der Pijl, G. J. De Vilder, and P. J. Tavner, "Comparison of direct-drive and geared generator concepts for wind turbines," *IEEE Transactions on Energy Conversion*, vol. 21, no. 3, pp. 725–733, 2006.

[67] D. Bang, H. Polinder, G. Shrestha, and J. A. Ferreira, "Review of generator systems for direct-drive wind turbines," in *European Wind Energy Conference and Exhibition*, 2008, pp. 1–11.

[68] A. McDonald, "Structural analysis of low speed, high torque electrical generatos for direct-drive renewable energy converters," PhD Thesis, University of Edinburgh, 2008.

[69] A. Zavvos, A. S. McDonald, M. Mueller, D. J. Bang, and H. Polinder, "Structural comparison of permanent magnet direct drive generator topologies for 5mw wind turbines," in *6th IET International Conference on Power Electronics, Machines and Drives (PEMD 2012)*, March 2012, pp. 1–6.

[70] A. McDonald, M. Mueller, and H. Polinder, "Structural mass in direct-drive permanent magnet electrical generators," *IET Renewable Power Generation*, vol. 2, no. 1, p. 3, 2008.

[71] R. L. Owen, Z. Q. Zhu, A. S. Thomas, G. W. Jewell, and D. Howe, "Fault-tolerant flux-switching permanent magnet brushless ac machines," in *2008 IEEE Industry Applications Society Annual Meeting*, Oct 2008, pp. 1–8.

[72] E. Spooner, P. Gordon, J. Bumby, and C. D. French, "Lightweight ironless-stator PM generators for direct-drive wind turbines," *IEE Proceedings-Electric Power Applications*, pp. 17–26, 2005.

[73] D. J. Bang, H. Polinder, G. Shrestha, and J. A. Ferreira, "Promising direct-drive generator system for large wind turbines," *EPE Journal (European Power Electronics and Drives Journal)*, vol. 18, no. 3, pp. 7–13, 2008.

[74] S. Engstrom and S. Lindgren, "Design of NewGen direct drive generator for demonstration in a 3.5 MW Wind Turbine," in *EWEC - European Wind Energy Conference & Exhibition*, no. 1, 2007, pp. 1–7.

[75] G. Shrestha, H. Polinder, D.-J. Bang, and J. A. Ferreira, "Direct drive wind turbine generator with magnetic bearing," in *European Offshore Wind Conference*, 2007, pp. 1–10.

[76] P. Tavner, J. Xiang, and F. Spinato, "Reliability analysis for wind turbines," *Wind Energy*, vol. 10, no. 1, pp. 1–18, 2007.

[77] K. O. Geddes, M. L. Glasser, R. A. Moore, and T. C. Scott, "Evaluation of classes of definite integrals involving elementary functions via differentiation of special functions," *Applicable Algebra in Engineering, Communication and Computing*, vol. 1, no. 2, pp. 149–165, 1990.

[78] F. Spinato, "The reliability of wind turbines," Ph.D. dissertation, Durham University, 2008.

[79] H. Polinder, D. Bang, R. P. J. O. M. van Rooij, A. S. McDonald, and M. A. Mueller, "10 MW wind turbine direct-drive generator design with pitch or active speed stall control," in *2007 IEEE International Electric Machines Drives Conference*, vol. 2, May 2007, pp. 1390–1395.

[80] D. Zhang, F. Wang, R. Burgos, R. Lai, and D. Boroyevich, "Impact of interleaving on ac passive components of paralleled three-phase voltage-source converters," *IEEE Transactions on Industry Applications*, vol. 46, no. 3, pp. 1042–1054, 2010.

[81] G. Gohil, L. Bede, R. Teodorescu, T. Kerekes, and F. Blaabjerg, "Line filter design of parallel interleaved vscs for high-power wind energy conversion systems," *IEEE Transactions on Power Electronics*, vol. 30, no. 12, pp. 6775–6790, 2015.

[82] T. Yang, C. O'Loughlin, R. Meere, T. O'Donnell, N. Wang, and Z. Pavlovic, "Investigation of modularity in dc-dc converters for solid state transformers," in *2014 IEEE 5th International Symposium on Power Electronics for Distributed Generation Systems (PEDG)*, June 2014, pp. 1–8.

CHAPTER 7

Conclusions

With wind energy playing a significant role in the transition to renewable-based energy consumption, there is a demand for solutions to lower costs of energy especially in offshore wind turbines. The motivation behind this thesis was to improve the availability of turbines as this directly affects the cost of wind energy. The thesis has targeted availability rather than reliability because this is a comprehensive approach that incorporates reliability, fault tolerance, and maintainability. The importance of this objective is further strengthened when the future scenario for offshore wind is considered, where the estimated installed capacity in Europe alone would be between 45—100 GW by 2030. The primary objective of this thesis is – to improve the equivalent availability of wind turbine generator systems. To achieve this, it poses a number of research questions which are addressed in this chapter.

What are the methods that can be used to improve the equivalent availability of wind turbine generator systems?

To address this question, the first step is to develop an understanding of failures and failure mechanisms occurring in the generator system. Chapter 2 uses a review of existing studies to analyse failures in wind turbine generators and power electronic converters, their probabilities and their failure mechanisms.

Next, Chapter 3 performs a review of approaches to improve the availability of wind turbine generator systems. It asserts that the availability is based on five pillars or approaches – the design for component reliability, active control for reliability, design for fault tolerance, prognostics, and design for maintainability. This thesis focusses on the first three, i.e., component reliability, active control, and fault tolerance. It further highlights promising approaches for investigation that are analysed in the rest of the thesis.

How does over-rating – with over-rated topologies and over-rated components – compare in regard to the lifetime of the power semiconductors?

In Chapter 4, multilevel converters were investigated from the viewpoint of reliability. The approach followed used stress and strength modelling to map the loads that drive the failure mechanisms in the considered components. The assessment was based on the power losses of each converter, the distribution of these losses, and their impact on the thermal behaviour of the power electronic components.

With a focus on developing converters with extended reliability which would result in increased energy yields and reduced costs, the current practice is to use over-rated components. However, another solution could be the use of over-rating in terms of topology - i.e., the designing of more complex topologies or control strategies that offer a more evenly distributed loading of the power converter or even topologies that can sustain faults and preserve their functioning ability. This chapter examined such over-rated topologies, as well the use of over-rated components.

It found that the ANPC and T2C topologies were effective in increasing semiconductor lifetimes. They resulted in an increase by a factor of ≈8 and ≈21 for the grid side converter compared to the NPC topology. Further, the use of over-rated components also enhanced semiconductor lifetimes. The use of 1.25 and 1.5 times overrated NPC converters increased lifetimes by a factor of ≈5.3 and ≈18 for the grid side converter.

In conclusion that the use of over-rating – be it in the form of overrated topologies (like the ANPC and the T2C), or the use of over-rated components – is successful in improving the lifetime performance of power semiconductors in converters. However, the improvement offered by overrated topologies over and above the use of over-rated components is not significant and it is unlikely to replace the current practice of using over-rated components.

Can power semiconductor lifetime be extended by controlling the thermal management of the converter?

Chapter 5 investigated the use of adaptive cooling to improve lifetimes of power semiconductors in converters by reducing the junction temperature cycling. It compared two control structures based on the measured (or estimated) junction temperature of the semiconductor to adapt the cooling system resulting in reduced temperature cycling. Simulations have shown that both methods show significant improvement in temperature cycling. In the simulation involving a yearly wind profile, the gradient based control showed an increase in lifetime by a factor of ≈10.

Further, the chapter demonstrated the effectiveness of adaptive cooling system using a scaled-down experimental setup where the possible improvements in temperature cycling were evident. Through the setup, the use of current as an alternative control input was also investigated (which is easier to measure than the junction temperature). However, as the control is based on a quantity other than the target, the results are poor for some operating ranges.

In conclusion, adaptive cooling is a promising method to reduce stresses and increase lifetimes in power semiconductors, especially as most wind turbine converters today use liquid cooling for the converter.

How can modularity improve the availability of a wind turbine generator system? What are the limits of increasing modularity?

This thesis discussed modularity in two layers - the functional layer and the physical layer. Functional modularity is where the modules operate as separate functional blocks. Physical modularity builds on this layer by adding a physical separation, leading to a possibility to remove/replace such modules. First, Chapter 6 used a review of existing literature to examine the use of these different layers of modularity in wind turbine generator systems and introduced some of the opportunities and challenges in the use of modular and segmented generator systems for large wind turbine generator systems.

The addition of modularity in the functional layer is a useful design concept for all large wind turbines. This step has fewer challenges to be overcome in its implementation and many wind turbines already use this to some extent. The addition of modularity in the physical layer has to overcome a number of challenges and may be more suitable for offshore wind turbines where the cost of repair can be very high.

Next, the chapter analysed the effect of functional and physical modularity on the availability of the converter in a wind turbine. Furthermore, it focussed on extreme modularity - i.e., designs where the number of modules is much larger than what is used at present (in the industry). It concluded that extreme modularity for converter systems where failure rates are constant do not hold merit as they do not offer significant improvements in availability. However, if the failure rates can be reduced by introducing extreme modularity, the increase in availability can be significant. Therefore, extreme modularity can be a powerful tool, but only when it is accompanied by a reduction in failure rates.

Recommendations for Future Research

While this thesis has focussed on the wind turbine generator system, this work remains a drop in the proverbial ocean. One of the biggest challenges behind this study has been the availability of data on sub-component level failures and mechanisms for wind turbines. Therefore, studies that analyse failed components and build-up a database of what are the predominant failure mechanisms in wind turbines would be very beneficial for the wind community as a whole. Another clear avenue of future research is focussing on other components of a wind turbine that fail. The statistics discussed in this thesis point towards the pitch system, the gearbox, and the rotor/blades as notable candidates.

Most of the approaches discussed in this thesis centred around the power semiconductors. The use of over-rated components is an easy way to enhance power semiconductor lifetimes by increasing the strength of the component. The use of adaptive thermal management reduces the stress imposed on the power semiconductor and thus extends lifetime. Both these have shown to increase the lifetime by an order of magnitude. As these methods act on temperature cycling

based failure mechanisms it is possible that the extension in lifetime would be limited by other failure mechanisms. Further research on these mechanisms and their solution is required.

The next direction of research would be focussing on the other sub-components in the generator systems. For example, while bearings have been ignored in this work, the concept of fault tolerance through modularity lends itself well to the use of magnetic bearings. The use of magnetic bearings with modular design could be one way of increasing the availability of the bearing system. Physically modular magnetic bearings could introduce fault tolerance in the bearing system, as well as reduce the time and cost of repair. However, this concept requires more investigation before its suitability can be ascertained.

Finally, despite attempts at complete case study analyses, these are aspects that have not been considered here. Therefore, these aspects form the final recommended direction of investigation:

- Active Control – Previous studies have concentrated on the control of electrical parameters instead. This thesis investigated the use of adaptive cooling to achieve the same objective. A detailed comparative analysis of these methods – control of electrical parameters, and control of thermal parameters – is required. Also, the use of phase change materials could be a passive way to achieve variable cooling based on power loss. This should be investigated as an alternative to active control for junction temperature cycling reduction.
- Modularity – The use of modularity in the system is interesting from the viewpoint of availability. Apart from introducing fault tolerance, modularity could be used to make the turbine easier and cheaper to maintain. Modularity is especially attractive when the growth of offshore wind is considered. With large offshore turbine populations, the logistics of maintenance become of prime importance. In this scenario, the use of modularity to allow periodic maintenance strategies could be vital to the cost of energy. Physically modular generators could reduce maintenance time and cost, as well as make transportation and installation easier. However, a major hurdle in realising such a physically modular generator is the support structure. Further investigation of the design and implementation of the support structure of a modular generator design is required. Furthermore, a design and investigation of extremely modular converters that allow passive cooling is required to fully understand their suitability.

List of publications

Thesis related publications

Journal papers:

- U. Shipurkar, F. Wani, Z. Qin, J. Dong, H. Polinder and J. A. Ferreira, "Adaptive Cooling for Improved Power Semiconductor Lifetime in Wind Turbine Converters," submitted to *IEEE Journal of Emerging and Selected Topics in Power Electronics*, 2018.
- U. Shipurkar, J. Dong, H. Polinder and J. A. Ferreira, "Availability of Wind Turbine Converters with Extreme Modularity," in *IEEE Transactions on Sustainable Energy*, vol. 9, no. 4, pp. 1772–1782, Oct. 2018.
- U. Shipurkar, E. Lyrakis, K. Ma, H. Polinder and J. A. Ferreira, "Lifetime Comparison of Power Semiconductors in Three-Level Converters for 10MW Wind Turbine Systems," in *IEEE Journal of Emerging and Selected Topics in Power Electronics*, vol. 6, no. 3, pp. 1366–1377, Sept. 2018.
- U. Shipurkar, H. Polinder and J. A. Ferreira, "A review of methods to increase the availability of wind turbine generator systems," in *CPSS Transactions on Power Electronics and Applications*, vol. 1, no. 1, pp. 66–82, Dec. 2016.

Conference papers:

- U. Shipurkar, F. Wani, J. Dong, G. Alpogiannis, H. Polinder P. Bauer, and J. A. Ferreira, "Comparison of modular wind turbine generators considering structural aspects," *IECON 2017 - 43rd Annual Conference of the IEEE Industrial Electronics Society*, Beijing, 2017, pp. 3707–3712.
- U. Shipurkar, H. Polinder and J. A. Ferreira, "Modularity in wind turbine generator systems – Opportunities and challenges," *2016 18th European Conference on Power Electronics and Applications (EPE'16 ECCE Europe)*, Karlsruhe, 2016, pp. 1–10.
- U. Shipurkar, K. Ma, H. Polinder, F. Blaabjerg and J. A. Ferreira, "A review of failure mechanisms in wind turbine generator systems," in *2015 17th European Conference on Power Electronics and Applications (EPE'15 ECCE-Europe)*, Geneva, 2015, pp. 1–10.

Other publications

- F. Wani, U. Shipurkar, J. Dong and H. Polinder, "A Study on Passive Cooling in Subsea Power Electronics," in *IEEE Access*, vol. 6, pp. 67543–67554, 2018.
- U. Shipurkar, T. D. Strous, H. Polinder, J. A. Ferreira and A. Veltman, "Achieving sensorless control for the brushless doubly fed induction machine," in *IEEE Transactions on Energy Conversion*, vol. 32, no. 4, pp. 1611–1619, 2017.
- T. D. Strous, U. Shipurkar, H. Polinder and J. A. Ferreira, "Comparing the Brushless DFIM to other generator systems for wind turbine drive-trains" in *Journal of Physics: Conference Series*, vol. 753, no. 11, 2016.
- U. Shipurkar, T. D. Strous, H. Polinder, J. A. Ferreira, "LVRT performance of brushless doubly fed induction machines – A comparison," *2015 IEEE International Electric Machines & Drives Conference (IEMDC)*, Coeur d'Alene, ID, 2015, pp. 362–368.

Acknowledgements

This thesis marks the end of an enjoyable and eventful PhD journey. While it is my name on this document, the contributions of many people have been invaluable and have played a significant role in shaping it. I want to thank and acknowledge their support.

First, I would like to thank my promotors Dr. Henk Polinder and Prof. J.A. Ferreira for giving me the opportunity to pursue a PhD at TU Delft and their guidance during its course. Henk has been a great supervisor – allowing a lot of research freedom, fostering independence, but at the same time asking critical questions that only improved this thesis. Most importantly, I have really enjoyed working with him. I have also received a lot of support from Prof. Ferreira. The regular meetings we had always left me with new questions and ideas. I also thank all the participants in the D4REL project, although our topics were quite different, I learned a lot about wind turbines during our project meetings. I would especially like to thank Stoyan Kanev, who was very supportive of our work.

I would also like to thank Dr. Ke Ma for his support and guidance while I was visiting Aalborg University. My collaboration with him taught me a lot about the subject of my thesis, and I am very grateful to him for that. Dr. Jianning Dong has been a great colleague and a great friend. Collaborating with him has always been fun and productive. He has also introduced me to Chinese science fiction - and I owe him for that! Dr. Zian Qin has also been a great help, especially when dealing with power electronics, and our paper on adaptive cooling really benefited from his insight and experience. When my PhD was at a very nascent stage, I had some constructive discussions with Dr. Jelena Popovic on power electronics packaging and reliability. All the work in the lab would not have been possible without the support of Dr. Bart Roodenburg, Joris Koeners, Harrie Olsthoorn, and Chris Swanink. Their inputs have been invaluable in making and running the laboratory setups I have been involved in. With me gone, I hope they have fewer 'Frankenstein-setups' in their future. I'm also very grateful to Sharmila Rattansingh who has always been very helpful and eased our administrative woes!

I have also been lucky to collaborate with a number of Master students at TU Delft. All of them, in some way or the other, have contributed to this thesis. Tjerk Sluimer worked on insulation diagnosis for low-voltage machines. Emmanouil Lyrakis worked on a reliability comparison of multilevel converters, and we co-authored a paper on this topic. George Alpogiannis worked on the analytical modelling of modular machines, and the models he developed were later used in a paper where he is a co-author. Chetan Kumar worked on sensor-less FOC in a six-phase PM machine and demonstrated it in the laboratory. Shaochuan Zhang worked on the LVRT control of the BDFIG. Shihang Yin worked on an analysis of active control methods for improving reliability with some interesting results.

I also want to thank my colleagues. When I first started the PhD, Tim Strous and Martin van der

Geest were my introduction to the group. I learned a lot about the field of electrical engineering and research in general from them. I first shared an office with Dong Liu, and I appreciate his advice on the PhD process. I also appreciate Xuezhou Wang's insight on electrical machines and our short collaboration on the BDFIG. I also thank Ilija Peceij for the discussions in the lab. Prasanth Venugopal and his 'philosophical' discourses on compassion have always been entertaining. Tsegay Hailu has been a great friend and our discussions on world politics will be missed. I enjoyed beating Minos Kontos in basketball and listening to why he supported the '23rd best team in south-Athens'. It was always fun talking to Laurens Mackay. Incidentally, he was our ski instructor on a ski-trip, and that's when I realised why all master students want to do projects with him. Soumya Bandyopadhyay has shared an office with me for the last part of my PhD, I have enjoyed his company and the office has been fun thanks to him. I also thank him for reminding me every day how little I care about the 'EPL'. I must also warn future PhD students about allowing him to select movies for group outings – he has not been successful in the past (to put it mildly). Nils van der Blij has been great company, I have enjoyed our many coffee breaks and discussions. He has also been more motivated about me going to the gym than I have, so I thank him for that! Pavel Purgat is another key participant in our 'coffee meetings'. I think we have all benefited from this calm and analytical approach. I also enjoyed the trip we took to a conference in China and the ski trip he organised to Slovakia. Lucia Larumbe, as head of the Party Planning Committee, has done a great job and is credited for introducing us to escape rooms! Aditya Shekhar has made the group quite entertaining, I appreciate his willingness to take a joke. Gautham Ram has always been helpful, especially during the end of my PhD where I looked to him for advice on many aspects of finishing. I enjoyed discussions with Nishant Narayan and Victor Garita, on topics ranging from history to politics. I also enjoyed the company of Mladen Gagic, he taught us about the 'other wikipedia'. I have had a very successful and enjoyable collaboration with Faisal Wani, and I appreciate his friendship. I have learned a lot from the post-lunch discussions with Dr. Thiago Batista Soeiro, talks with him are always enlightening. Dr. Babak Gholizad has also been great comapny during lunch and the post-lunch discussions. I also thank Yunhe Yu and Shubhagi Bhadoria, the latest additions to our office. I have enjoyed your company!

My friends, in and around Delft, were invaluable in this process. Siddhartha has been a great friends and housemate. I think all evening meals and entertainment were a welcome respite from the workday. Also, Satyaki for being a great friend. Lucia for all the entertaining dinners and trying to teach us the art of the tiramisu. Kanta, for remembering to send us a message once in two bluemoons! Daniel for all the fun we have had over many years. Many other people have made my stay in the Netherlands enjoyable: Ralino, Aniket, Foivos, Nikolas, Einar, Joost, Aneil, KC, Adarsha, Daniella, Kaveri, Siddharth, Kai, and Shu-Meng. Thank you all!

Last, but definitely not least, I would like to thank my family. This acknowledgement is insignificant compared to what they mean to me, but I bash on regardless. My parents are the reason I am who I am, and their support has been very important to me. My grandparents and aunts for all their love, my sister for always being there, and Mani mama for being a rock.

So long, and thanks for all the fish!

Biography

Udai Shipurkar was born in New Delhi, India, in 1987. He pursued his Bachelors in Electrical and Electronics Engineering and went on to work as a Project Executive at ITC Limited, India, from 2009 to 2012.

He received the MSc degree in Electrical Power Engineering in 2014 and from August 2014 he pursued a PhD degree on the availability of wind turbine generator systems at the Delft University of Technology, Delft, The Netherlands. His research interests include wind energy conversion systems and electrical systems for maritime applications.